NASA TECHNICAL NOTE

NASA TN D-2382

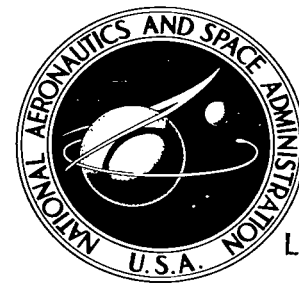

NASA TN D-2382

FORCE-TEST INVESTIGATION OF A 1/4-SCALE MODEL OF THE MODIFIED VZ-2 AIRCRAFT

by Robert H. Kirby, Robert O. Schade, and Louis P. Tosti

Langley Research Center
Langley Station, Hampton, Va.

NATIONAL AERONAUTICS AND SPACE ADMINISTRATION • WASHINGTON, D. C. • AUGUST 1964

FORCE-TEST INVESTIGATION OF A 1/4-SCALE MODEL OF THE MODIFIED VZ-2 AIRCRAFT

By Robert H. Kirby, Robert O. Schade, and Louis P. Tosti

Langley Research Center
Langley Station, Hampton, Va.

NATIONAL AERONAUTICS AND SPACE ADMINISTRATION

For sale by the Office of Technical Services, Department of Commerce,
Washington, D.C. 20230 -- Price $2.00

FORCE-TEST INVESTIGATION OF A 1/4-SCALE MODEL OF THE MODIFIED VZ-2 AIRCRAFT

By Robert H. Kirby, Robert O. Schade,
and Louis P. Tosti
Langley Research Center

SUMMARY

A force-test investigation has been conducted to determine the longitudinal aerodynamic characteristics and the aileron control effectiveness of a 1/4-scale model of the modified VZ-2 tilt-wing vertical-take-off-and-landing aircraft equipped with a full-span slotted flap. The model was also tested over the transition range with a leading-edge droop modification.

The results of the force tests indicated that the use of full-span slotted flaps produced sizable increases in lift which resulted in considerable reductions in the wing incidence angles required throughout the transition range; and these reductions in wing incidence were very beneficial in reducing wing stalling in the transition range. The use of leading-edge droop had no appreciable effect on the static longitudinal characteristics. The use of full-span ailerons as a yaw control for hovering and low-speed transition flight appears to offer considerable promise; however, the phasing in of some roll producing control is necessary fairly early in the transition to eliminate the adverse roll that is encountered.

INTRODUCTION

Flight tests of the original VZ-2 tilt-wing vertical-take-off-and-landing (VTOL) aircraft, described in reference 1, showed that the aircraft had unacceptable lateral stability and control characteristics in the transition flight conditions in a speed range of approximately 40 to 70 knots which corresponded to a range of wing incidence from approximately 45° to 25°. The difficulties resulted from wing stalling and were more severe for descent conditions than for level-flight or climb conditions. The use of a wing-section modification consisting of a modest amount of leading-edge droop and an increase in nose radius was found to relieve the lateral stability and control troubles to a considerable extent.

The tendency toward wing stall in the transition range had been recognized from wind-tunnel tests as pointed out in references 2 to 4. The effect of this stalling on the lift, drag, and power required, and, consequently, on short-take-off-and-landing (STOL) and engine-out performance had been appreciated for

some time. The use of high-lift devices, both trailing-edge flaps and leading-edge devices, had been recommended to relieve the wing stalling by increasing the lift capability of the wing. With the use of these high lift devices the wing can produce more of the lift required of the wing-propeller system and thereby reduce the angle of attack of the wing-propeller combination as explained in detail in reference 4. As a result of this wind-tunnel work, the aircraft was modified by the addition of a large flap to determine the effect of such a flap on the lateral handling qualities in the transition range.

As a result of the foregoing experience, an investigation has been made with the 1/4-scale free-flight model of the VZ-2 used in the previous investigations of references 5 to 10 to determine: first, if upon close examination of the range of flight conditions in which the lateral stability and control difficulties associated with stalling had been observed in flight, the same objectionable characteristics could be observed with a free-flight model; and, second, if the difficulties could be recognized, whether the characteristics would be improved by the use of the wing flaps that were to be installed on the full-scale aircraft as a modification.

One phase of this investigation, reported in reference 11, dealt with results of flight tests of the model with a full-span slotted flap and with and without a full-span Krueger type nose flap. These flight tests included both level and simulated descent flights over a range of airspeeds where wing stalling might be expected to occur. The other phase of this investigation, which is discussed in the present paper, consisted of force tests to determine the aerodynamic characteristics of the model with a full-span slotted flap and leading-edge droop. Tests were also made to determine the effectiveness of full-span ailerons when used as yaw control for hover and low-speed flight. Most of the tests were made in the wing incidence range between 20° and 40° where wing stalling was expected to be most objectionable, but a few additional tests were made to cover the complete range of wing incidence angle from 9° to 87°.

SYMBOLS

The forces and moments are based on the stability-axis system, which is an orthogonal system with the origin at the aircraft center of gravity. The Z-axis is in the plane of symmetry and perdendicular to the relative wind, the X-axis is in the plane of symmetry and perpendicular to the Z-axis, and the Y-axis is perpendicular to the plane of symmetry.

b wing span, ft

C_D drag coefficient, F_D'/qS

C_L lift coefficient, F_L/qS

C_Y side-force coefficient, F_Y/qS

C_m pitching-moment coefficient, M_Y/qSc

C_n yawing-moment coefficient, M_Z/qSb

C_l rolling-moment coefficient, M_X/qSb

c wing chord, ft

F_D' drag, lb

F_L lift, lb

F_Y side force, lb

i_w wing incidence, deg

M_X rolling moment, ft-lb

M_Y pitching moment, ft-lb

M_Z yawing moment, ft-lb

q free-stream dynamic pressure, lb/sq ft

S wing area, sq ft

V scaled-up aircraft velocity, knots

α angle of attack of fuselage, deg

β angle of sideslip, deg

δ_a deflection of aileron, deg

$\delta_{a,R}$ deflection of right aileron, positive trailing edge down, deg

δ_f flap deflection, deg

APPARATUS AND MODEL

A photograph of the 1/4-scale model of the VZ-2 tilt-wing VTOL aircraft with full-span flap is shown as figure 1, a three-view drawing of the model is presented as figure 2, and pertinent geometric characteristics are given in table I. The model had two 3-blade propellers with flapping hinges and was powered by a pneumatic motor which drove the propellers through interconnecting shafting and right-angle gear boxes. The speed of the motor was changed to vary the thrust of the propellers and the propeller blade angle was set at 12° at the 75-percent-radius station. Blade-form curves of the propellers are presented in reference 8.

Details of the wing, full-span aileron, and sliding flap are shown in figure 3. The geometric changes which have been made to the model to simulate the full-scale aircraft in its modified configuration can be readily seen by comparing figure 2 and table I of the present paper with figure 1 and table I of reference 10. For the purpose of this paper, the main change was the installation of the full-span slotted flap which resulted in a 10-percent increase in the wing chord when the flap was in the retracted position. The wing was pivoted at the 33.7-percent mean-aerodynamic-chord station and was tilted to provide incidences from 9° to 87°.

TESTS

The tests were made in the Langley full-scale tunnel with the model support strut mounted near the lower edge of the entrance cone and about 5 feet above a ground board. Electric strain-gage balances were used to measure the forces and moments on the model, and an electric tachometer was used to determine the model propeller speeds. Blockage and interference effects in the tunnel were believed to be very small and, therefore, no wind-tunnel corrections were applied to the data.

Force tests were made to determine the longitudinal characteristics of the model for the flap-retracted condition and for flap deflections from 0° to 40° at angles of wing incidence from 9° to 87° through an angle-of-attack range from -10° to 20°. The flap conditions from 0° to 40° are with the flap fully extended and pivoted at the leading edge of the flap which, when extended, is located at station 12.80 as shown in figure 3. Force tests to determine the lateral stability characteristics of the flap-retracted configuration were made at wing incidences of 9° and 40°. A few longitudinal tests were also made in the flap-retracted configuration with a leading-edge-droop fairing added to the wing for wing incidences of 20°, 30°, and 40°. A section showing the shape of the leading-edge droop is shown in figure 3. The spanwise extent of the droop was between the nacelles for one group of tests and full span for another group of tests.

Full-span aileron-control-effectiveness tests were made at angles of wing incidence from 9° to 87° for the flap-retracted condition and for the extended-flap condition with flap deflections from 0° to 40°.

Tuft tests were made on the model in the flap-retracted and in the flap-deflected 40° conditions. These tests were made through an angle-of-attack range from -4° to 16° at wing incidences from 25° to 45° for the flap-retracted condition and at wing incidences from 5° to 25° for the flap-deflected condition. These wing incidences represented a velocity range from approximately 61 knots to 39 knots for both the flaps-retracted and flaps-deflected conditions.

All the force tests were made with power settings which, with the fuselage at zero angle of attack and the controls neutral, gave zero forward acceleration. In each test the angle of attack, angle of sideslip, or right aileron deflection was changed while the model propeller speed was held constant.

The majority of the tests at angles of wing incidence below 40° were made at an airspeed of 22.2 knots which gave an effective Reynolds number based on the wing chord and free-stream velocity of about 310,000. For the tests at higher angles of wing incidence it was necessary to reduce the tunnel airspeed below 22.2 knots to avoid excessive propeller speeds in order to achieve the zero-forward-acceleration condition.

RESULTS AND DISCUSSION

The results of a force-test investigation to determine the aerodynamic characteristics of the VZ-2 tilt-wing VTOL aircraft with a full-span slotted flap, leading-edge droop, and ailerons are presented in scaled-up dimensional form for the convenience of the user in applying directly to the VX-2 aircraft and in nondimensional form for ease in applying to other configurations without rescaling these data. The dimensional forces and moments are scaled up to the full-scale aircraft weight of 3450 pounds for steady level-flight conditions at a fuselage angle of attack of 0°. The moments are based on the center-of-gravity positions shown in table II. The dimensional data may be rescaled if desired to other sizes and weights by use of the simple formulas for scaling data shown in the appendix of reference 12.

Longitudinal

Effect of flaps.- Figures 4 and 5 present the basic longitudinal data in scaled-up dimensional form, and figures 6 and 7 present the same data in terms of conventional nondimensional coefficients based on free-stream velocity.

Summary figures for the longitudinal data are presented in figures 8 to 10 for the condition of zero angle of attack, which is the angle of attack at which the drag was set equal to zero in the tests. The data of figure 8 show that the use of a full-span slotted flap produced sizable increases in lift coefficient for all wing incidences tested. This increased lift results in considerable reductions in the angle of wing incidence required for any given lift throughout the transition range. For example, the use of a flap deflection of 40° results in a reduction in wing incidence of 15° to 20° throughout the transition speed range. Another effect of the flap, as shown by the summary plot of pitching-moment data in figure 10, is to reduce the large nose-up pitching moment in the transition range which was characteristic of the original VZ-2 configuration. It would be expected, however, that the main purpose of the flap would be to relieve wing stalling in order to improve the flying qualities and reduce the power required in the transition range.

An indication of the effectiveness of the flap in reducing wing stalling is shown by the tuft-test results of figure 11. This figure shows the stall patterns for the flap-retracted and 40° flap conditions with the data presented side by side for angles of wing incidence that would give approximately the same airspeed. These data show that the flap had a very marked effect in relieving the wing stall but that this effect became less and less as the

airspeed was reduced. There is always some question as to the applicability of small-scale tuft-test data; therefore, a comparison of the results of tuft tests of the full-scale aircraft and the 1/4-scale model for the original unmodified configuration is presented in figure 12. These data show that the stall patterns of the model were quite similar to those of the full-scale aircraft and, therefore, infer that the effect of the flap on the stall shown in figure 11 is reasonably accurate.

Leading-edge droop modification.- The effect of leading-edge droop on the longitudinal stability characteristics of the model with flap retracted are presented in figures 13 to 16 for wing incidences of 20°, 30°, and 40°. These data indicate that there was no appreciable effect of this small change on the longitudinal characteristics - the result that would be expected on the basis of conventional aerodynamics. The force tests of the full-scale aircraft reported in reference 13, also indicated that the drooped-leading-edge modification had very little effect on the level-flight longitudinal characteristics in this same wing incidence range. However, flight tests of the full-scale aircraft in level flight indicated that the installation of the drooped leading edge on the full-scale aircraft alleviated the wing dropping, buffeting, and yaw disturbances. The model was not flight tested with the leading-edge droop, but the free-flight tests with a different leading-edge droop configuration (a Krueger flap) reported in reference 12 indicated some improvement in flight characteristics. Evidently, on this aircraft the use of leading-edge droop improves the stalling characteristics of the wing in such a way as to be effective in improving the flying qualities without causing a sufficiently major change to show up in the gross lift of the aircraft. This characteristic is discussed in considerable detail in reference 13.

Lateral

Lateral stability.- Lateral stability data are presented in figures 17 and 18 for the flap-retracted condition at wing incidences of 9° and 40°. At both angles of incidence the model was directionally stable at the larger angles of sideslip, but at small angles of sideslip it was about neutrally stable at a wing incidence of 9° and unstable at a wing incidence of 40°. In the flight tests of the configuration without flaps reported in reference 14, the aircraft also experienced directional instability in the low sideslip-angle range.

Aileron control effectiveness.- The results of tests made to determine the effectiveness of full-span ailerons throughout the wing incidence range are presented in figures 19 and 20 for the flaps-retracted condition. Figure 21 presents the basic data for various wing incidences through the transition range with three flap deflections at each wing incidence chosen to roughly bracket a zero-pitching-moment condition with the controls neutral. The data from figures 19 and 21 are summarized in the form of the variation of yaw and roll control effectiveness derivatives M_Z/δ_{aR} and $-M_X/\delta_{aR}$, respectively, with forward speed and are presented in figure 22. The values of the derivatives were obtained by taking the slopes between test points for right aileron control deflections of 10° and -10°. The data show that the yawing moment

produced by the ailerons drops off somewhat between hovering flight and a speed of about 20 knots and then remains fairly constant through the remainder of the transition. The data also show that the various flap deflections used in the test program did not appear to have a systematic effect on the yaw characteristics through the transition range.

The effectiveness of the full-span ailerons as a yaw control in hovering and at low speeds can best be seen by comparing them with the tail-fan yaw control on the VZ-2 aircraft which, according to reference 14, gave a maximum value of ±1358 foot-pounds of yawing moment. The data of figure 22 show that approximately ±11° of aileron deflection would be required in hovering flight and approximately ±14° of aileron deflection would be required in the low speed transition range to give this value of yawing moment. It should be emphasized that reference 14 also stated that this amount of yaw control was definitely considered inadequate for anything but ideal zero wind conditions and the most modest maneuvers in yaw. However, the fact that considerably more yaw control can be obtained over and above this value by further increases in deflection would indicate that full-span ailerons offer some promise as an effective hovering and low-speed yaw control. The adverse roll of the ailerons was practically nil in hovering and increased slowly as the speed was increased to about 20 knots. At speeds above this value, however, the adverse roll increased rapidly at about a constant rate with speed. Extending and deflecting the flaps decreased the adverse roll about 20 foot-pounds per degree at the lower speeds regardless of the flap deflection angle. It appears that because of the adverse roll associated with the aileron control it would be necessary to phase in some roll producing control such as differential propeller pitch with the yaw control fairly early in the transition to eliminate the adverse roll that will be encountered.

CONCLUSIONS

On the basis of static force tests of a 1/4-scale model of the VZ-2 aircraft with a full-span slotted flap, leading-edge droop, and full-span ailerons the following conclusions are drawn:

1. The use of a full-span slotted flap produced sizable increases in lift which resulted in considerable reductions in the wing incidence angle required throughout the transition range. These reductions in wing incidence were very beneficial in reducing the wing stall in transition.

2. The use of leading-edge droop had no appreciable effect on the static longitudinal characteristics.

3. The use of full-span ailerons as a yaw control for hovering and low-speed transition flight conditions appears to offer promise. However, the phasing in of some roll producing control will be necessary fairly early in the

transition to eliminate the adverse roll that results from the use of the ailerons as a yaw control.

Langley Research Center,
National Aeronautics and Space Administration,
Langley Station, Hampton, Va., March 16, 1964.

REFERENCES

1. Reeder, John P.: Handling Qualities Experience With Several VTOL Research Aircraft. NASA TN D-735, 1961.

2. Taylor, Robert T.: Wind-Tunnel Investigation of Effect of Ratio of Wing Chord to Propeller Diameter With Addition of Slats on the Aerodynamic Characteristics of Tilt-Wing VTOL Configurations in the Transition Speed Range. NASA TN D-17, 1959.

3. Kuhn, Richard E., and Hayes, William C., Jr.: Wind-Tunnel Investigation of Longitudinal Aerodynamic Characteristics of Three Propeller-Driven VTOL Configurations in the Transition Speed Range, Including Effects of Ground Proximity. NASA TN D-55, 1960.

4. Kuhn, Richard E.: Take-Off and Landing Distance and Power Requirements of Propeller-Driven STOL Airplanes. Preprint No. 690, S.M.F. Pub. Fund Preprint, Inst. Aero. Sci., Inc., Jan. 1957.

5. Newsom, William A., Jr., and Tosti, Louis P.: Force-Test Investigation of the Stability and Control Characteristics of a 1/4-Scale Model of a Tilt-Wing Vertical-Take-Off-and-Landing Aircraft. NASA MEMO 11-3-58L, 1959.

6. Tosti, Louis P.: Flight Investigation of the Stability and Control Characteristics of a 1/4-Scale Model of a Tilt-Wing Vertical-Take-Off-and-Landing Aircraft. NASA MEMO 11-4-58L, 1959.

7. Tosti, Louis P.: Aerodynamic Characteristics of a 1/4-Scale Model of a Tilt-Wing VTOL Aircraft at High Angles of Wing Incidence. NASA TN D-390, 1960.

8. Tosti, Louis P.: Longitudinal Stability and Control of a Tilt-Wing VTOL Aircraft Model With Rigid and Flapping Propeller Blades. NASA TN D-1365, 1962.

9. Newsom, William A., Jr., and Tosti, Louis P.: Slipstream Flow Around Several Tilt-Wing VTOL Aircraft Models Operating Near the Ground. NASA TN D-1382, 1962.

10. Tosti, Louis P.: Rapid-Transition Tests of a 1/4-Scale Model of the VZ-2 Tilt-Wing Aircraft. NASA TN D-946, 1961.

11. Schade, Robert O., and Kirby, Robert H.: Effect of Wing Stalling in Transition on a 1/4-Scale Model of the VZ-2 Aircraft. NASA TN D-2381, 1964.

12. Tosti, Louis P.: Force-Test Investigation of the Stability and Control Characteristics of a 1/8-Scale Model of a Tilt-Wing Vertical-Take-Off-and-Landing Airplane. NASA TN D-44, 1960.

13. Mitchell, Robert G.: Full-Scale Wind-Tunnel Test of the VZ-2 VTOL Airplane With Particular Reference to the Wing Stall Phenomena. NASA TN D-2013, 1963.

14. Pegg, Robert J.: Summary of Flight-Test Results of the VZ-2 Tilt-Wing Aircraft. NASA TN D-989, 1962.

TABLE I.- GEOMETRIC CHARACTERISTICS OF THE MODEL

Propellers (three blades each):	
Diameter, in.	28
Solidity	0.239
Chord, in.	3.0
Wing:	
Pivot station, percent chord	33.7
Sweepback (leading edge), deg	0
Airfoil section	Modified NACA 4415
Aspect ratio	4.78
Chord, in.	15.63
Taper ratio	1.0
Area, sq in.	1166.5
Span, in.	74.63
Dihedral angle, deg	0
Ailerons (each:	
Full chord, in.	2.95
Span, in.	32.62
Full chord, percent c	0.19
Full area, sq in.	96.23
Chord aft of hinge line, in.	2.65
Area aft of hinge line, sq in.	86.44
Flap:	
Chord, in.	5.21
Chord, percent c	0.33
Span, in.	32.62
Area, sq in.	169.95
Vertical tail:	
Sweepback (leading edge), deg	28.0
Airfoil section	Modified NACA 0012
Aspect ratio	0.85
Root chord (at top of fuselage), in.	23.0
Tip chord (extended to plane of horizontal tail), in.	14.63
Taper ratio	0.64
Area, sq in.	301.0
Span (from top of fuselage to plane of horizontal tail), in.	16
Rudder (hinge line perpendicular to fuselage center line):	
Chord, in.	5.75
Span, in.	14.44
Area, sq in.	75.7
Horizontal tail:	
Sweepback (leading edge), deg	0
Airfoil section	Modified NACA 0012
Aspect ratio	2.91
Chord, in.	10.19
Center-section chord, in.	12.63
Area (including center body), sq in.	323.70
Span, in.	29.70
Dihedral angle, deg	0
Ventral fin*:	
Chord, in.	9.25
Span, in.	4.00
Area, sq in.	37.0

*Aft end located on model 11.0 inches forward of rudder hinge line measured along bottom of fuselage.

TABLE II.- WEIGHT OF FULL-SCALE AIRCRAFT AND CENTER-OF-GRAVITY LOCATIONS FOR VARIOUS WING INCIDENCE ANGLES

[Weight, 3450 lb]

i_w, deg	Center-of-gravity position (from wing pivot), ft	
	Horizontal (forward)	Vertical (below)
9	0.167	1.404
20	.174	1.364
25	.175	1.346
30	.175	1.328
35	.173	1.309
40	.169	1.293
50	.158	1.258
60	.140	1.226
70	.118	1.198
80	.092	1.174
86.7	.071	1.160

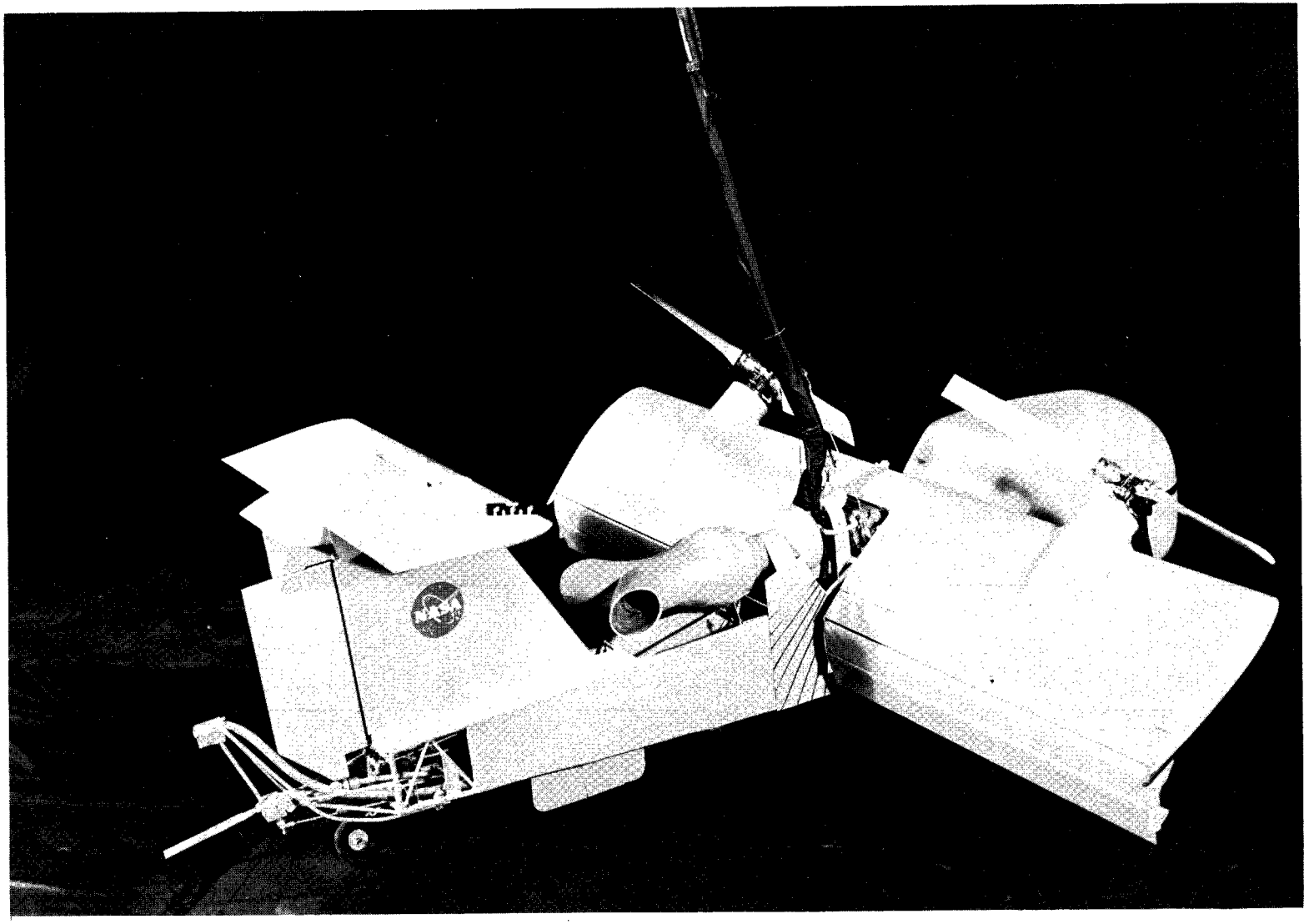

L-61-3172

Figure 1.- Photograph of the 1/4-scale model of the VZ-2 tilt-wing VTOL aircraft with full-span flap and ailerons.

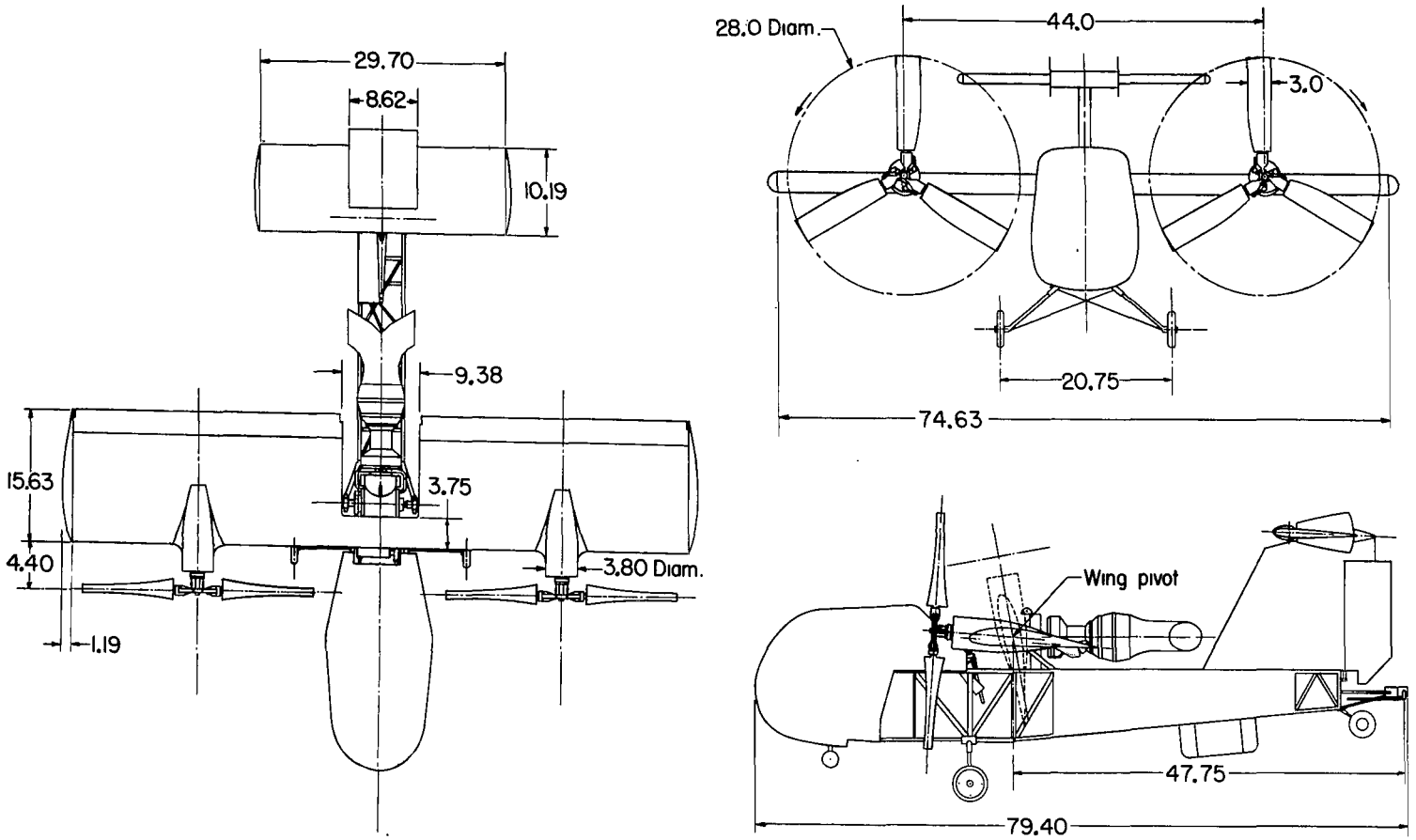

Figure 2.- Three-view sketch of model. All dimensions are in inches.

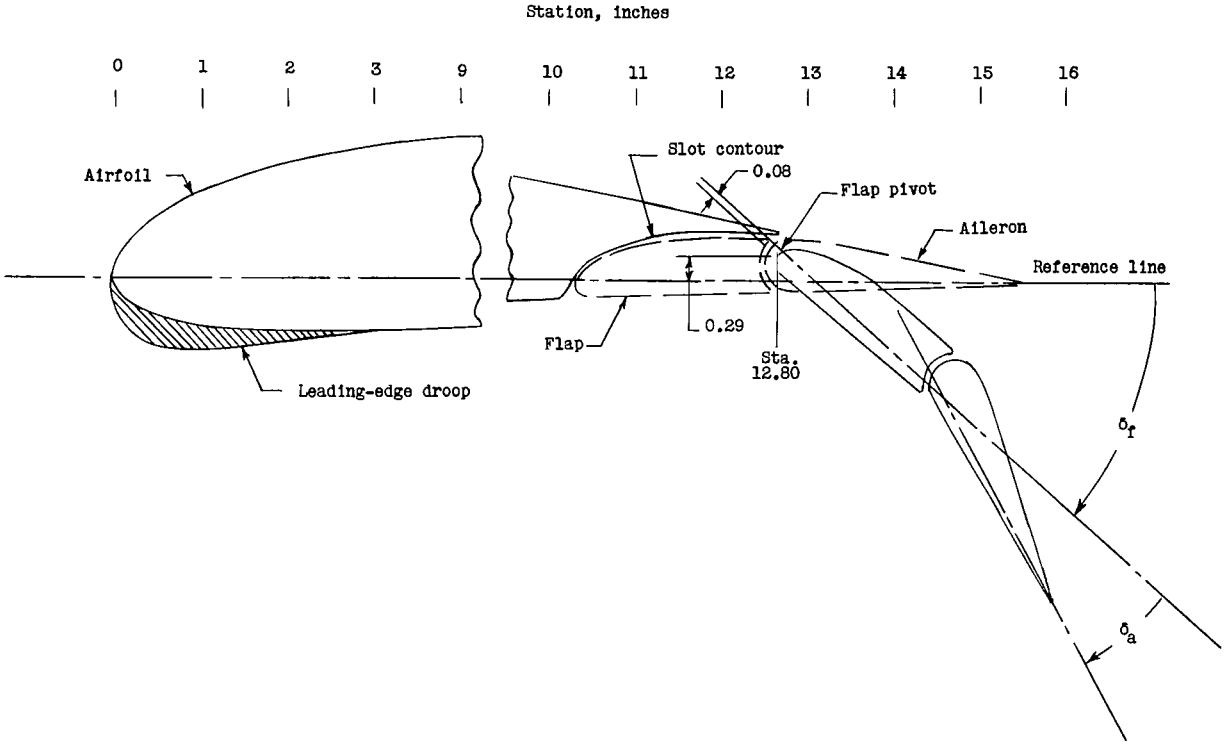

AIRFOIL

NACA 4415 airfoil to Station 9.975

Station	Upper	Lower
0.178	0.437	-0.255
.356	.594	-0.353
.713	.818	-0.466
1.069	.985	-0.529
1.425	1.117	-0.567
2.138	1.321	-0.596
2.850	1.461	-0.591
3.562	1.556	-0.567
4.275	1.603	-0.534
5.700	1.603	-0.463
7.125	1.501	-0.388
8.550	1.325	-0.305
9.975	1.087	-0.221
Straight line fairing to		
15.630	.023	-0.023

LEADING-EDGE DROOP

Radius of L.E. = 0.706 with center at Station 0.672 and coordinate -0.065.

Station	Lower
0.178	-0.570
.356	-0.706
.712	-0.787
1.068	-0.794
1.425	-0.772
1.780	-0.730
2.137	-0.678
2.493	-0.637
2.850	-0.607
3.206	-0.585
3.560	-0.567

FLAP

Station	Upper	Lower
10.420	-.080	-.080
10.460	+.030	-.140
10.500	.080	-.170
10.600	.160	-.195
10.750	.250	Straight line
11.000	.335	given under
11.250	.390	"Airfoil"
11.750	.450	
12.000	.460	
12.400	.480	
12.680	.485	-.125
12.720	.450	-.085
Radius of back end = 0.363" with center at Station 12.980" and coordinate 0.180"		

SLOT CONTOUR

Station	Ordinate
9.970	-.221
10.100	-.215
10.200	-.205
10.300	-.140
10.400	+.020
10.500	.135
10.600	.210
10.800	.320
11.000	.390
11.200	.440
11.500	.500
11.800	.535
12.100	.540
Straight line fairing to	
12.800	.520

AILERON

Radius of L.E. = 0.300 with center at Station 12.980 and coordinate 0.180

Station	Upper	Lower
12.980	.480	-.115
13.100	.470	Straight line
13.300	.450	given under
13.450	.435	"Airfoil"
Straight line given under "Airfoil"		
15.630	.023	-.023

Figure 3.- Geometric characteristics of wing section. All dimensions are in inches.

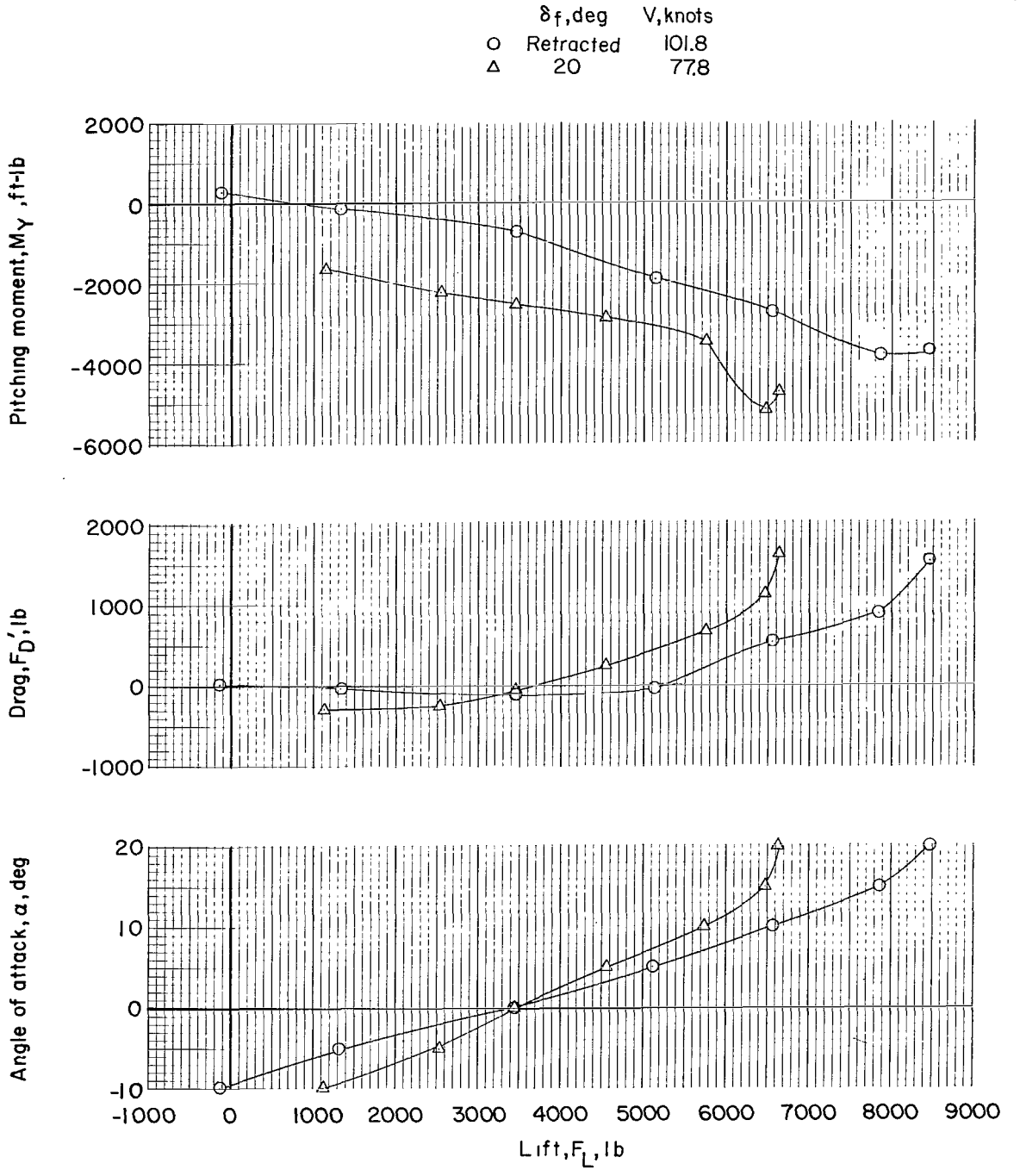

(a) $i_w = 9^\circ$.

Figure 4.- Scaled-up longitudinal stability characteristics at various wing incidences and flap deflections.

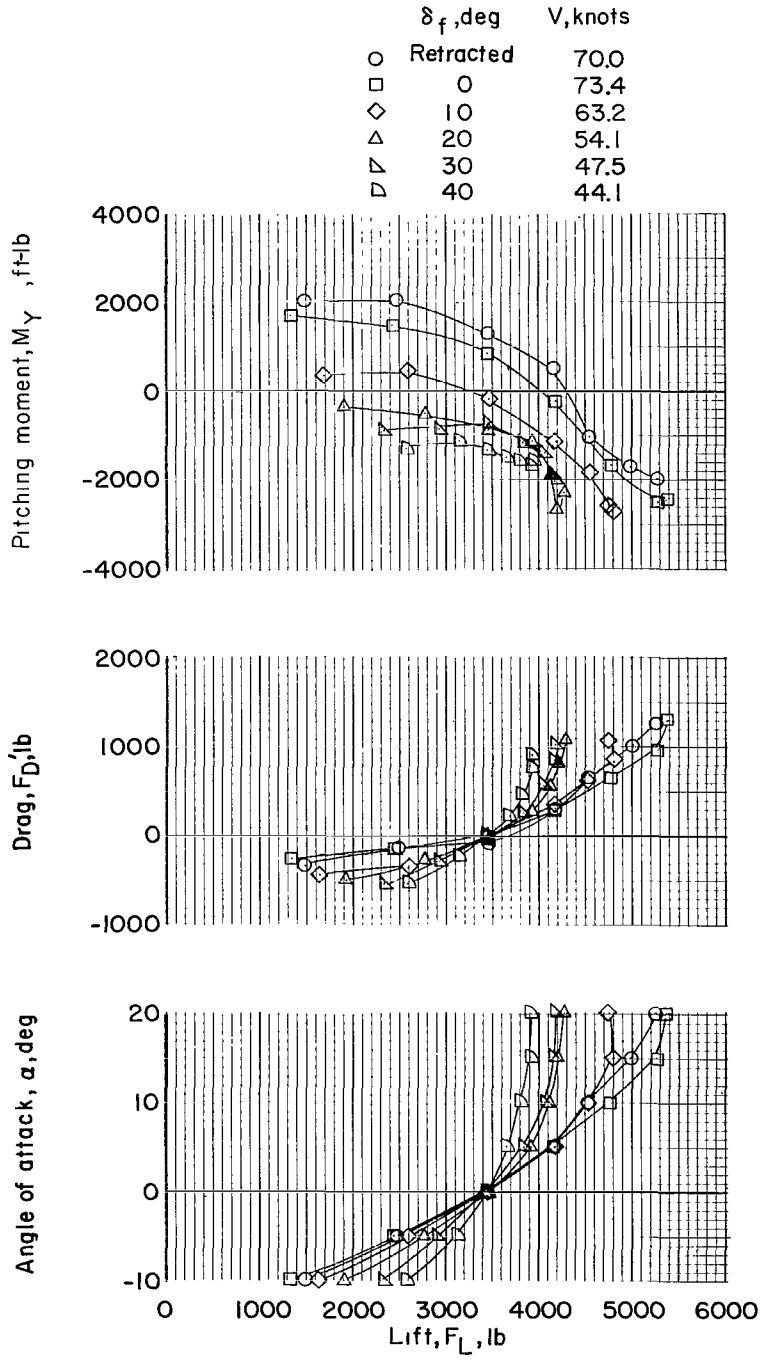

(b) $i_w = 20^\circ$.

Figure 4.- Continued.

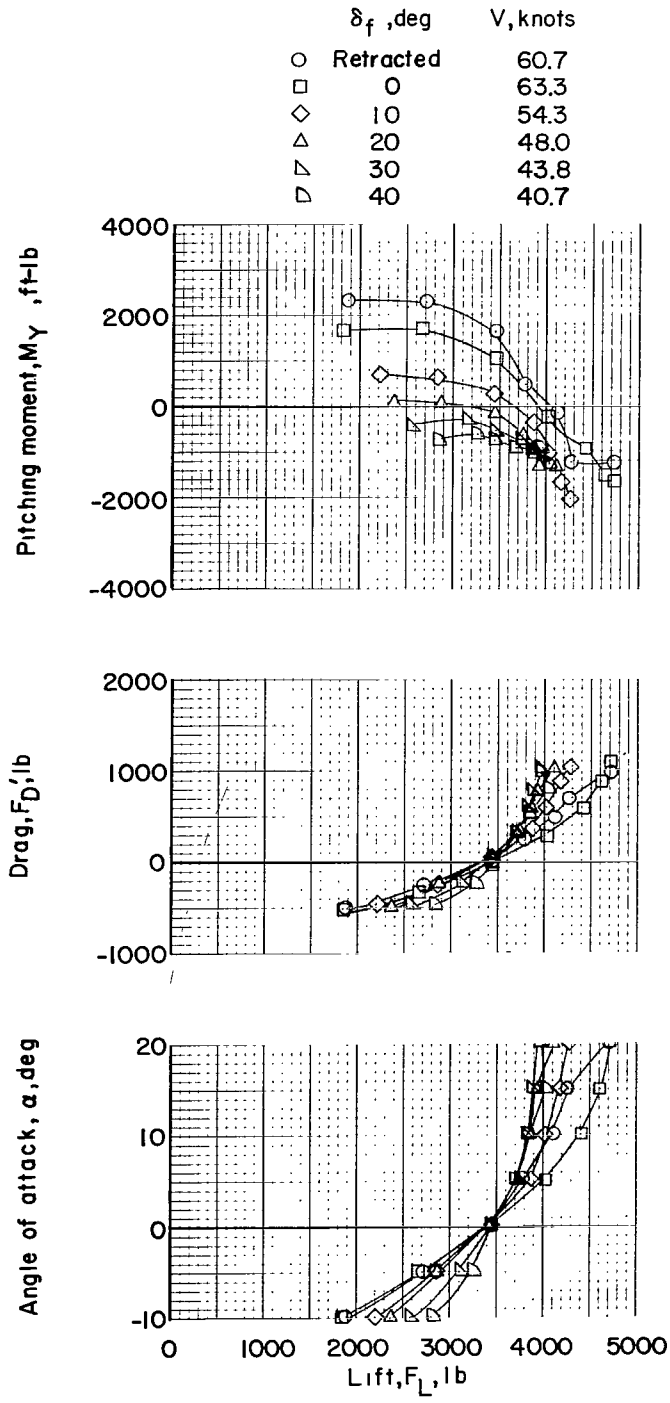

(c) $i_w = 25°$.

Figure 4.- Continued.

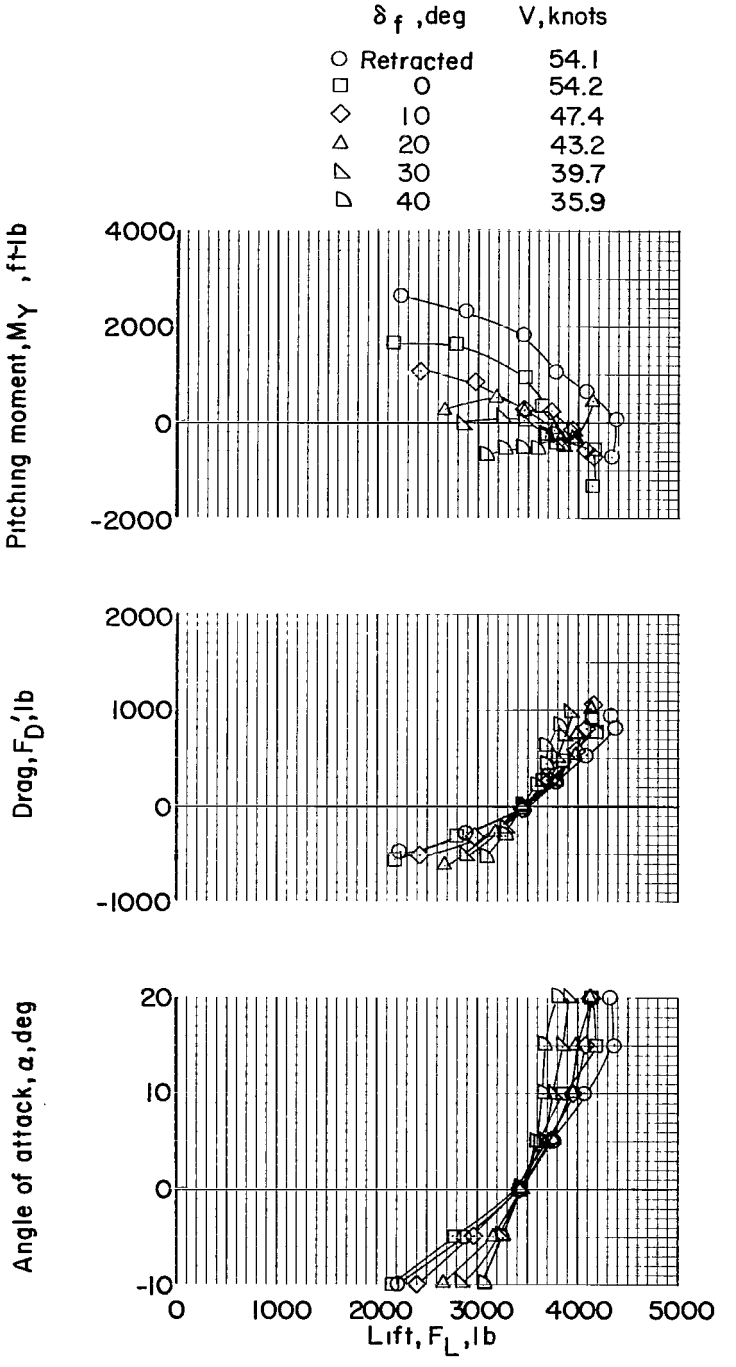

(d) $i_w = 30^\circ$.

Figure 4.- Continued.

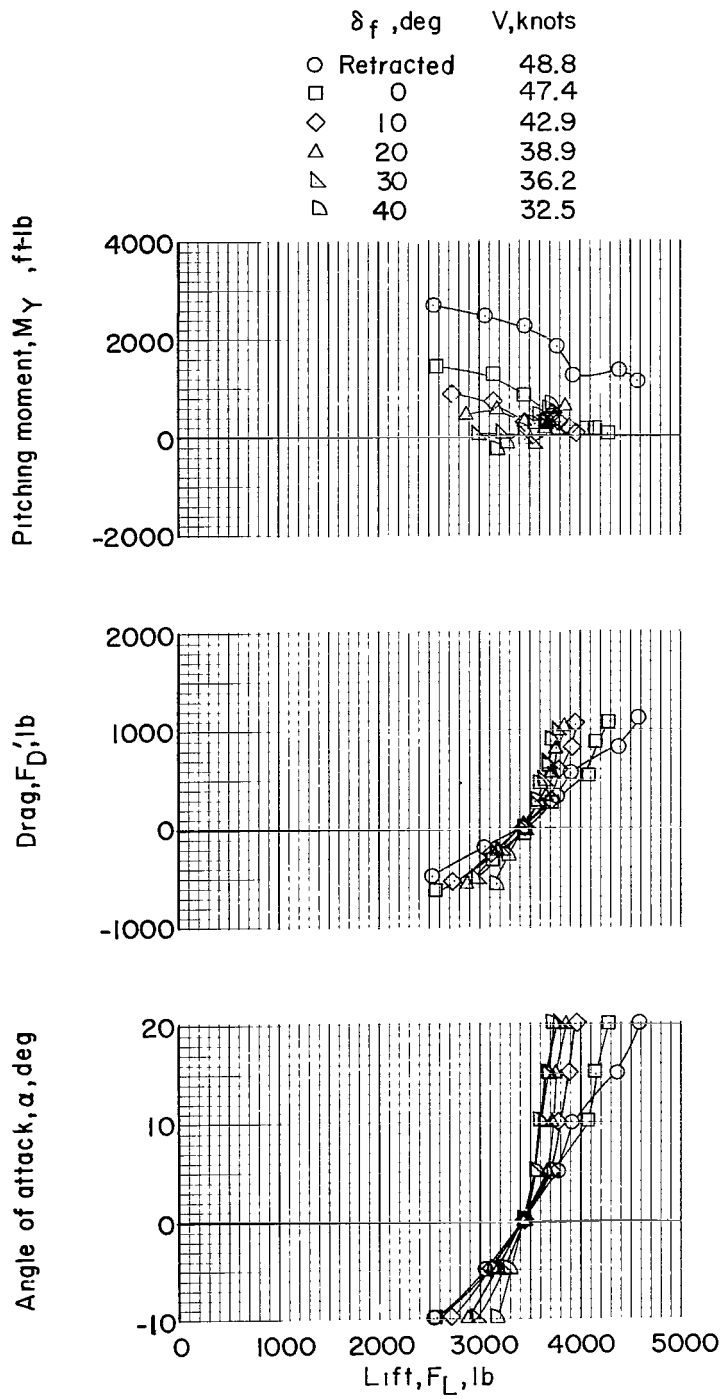

(e) $i_w = 35^\circ$.

Figure 4.- Continued.

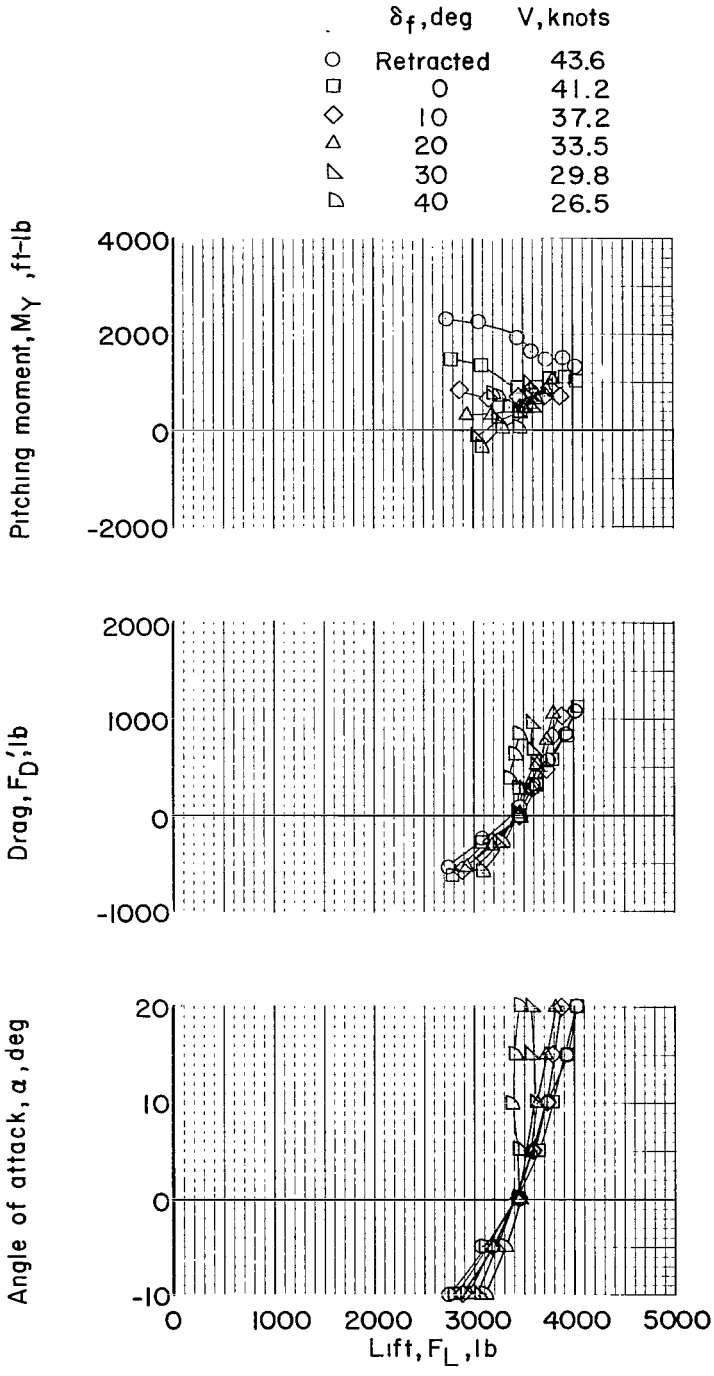

(f) $i_w = 40^\circ$.

Figure 4.- Continued.

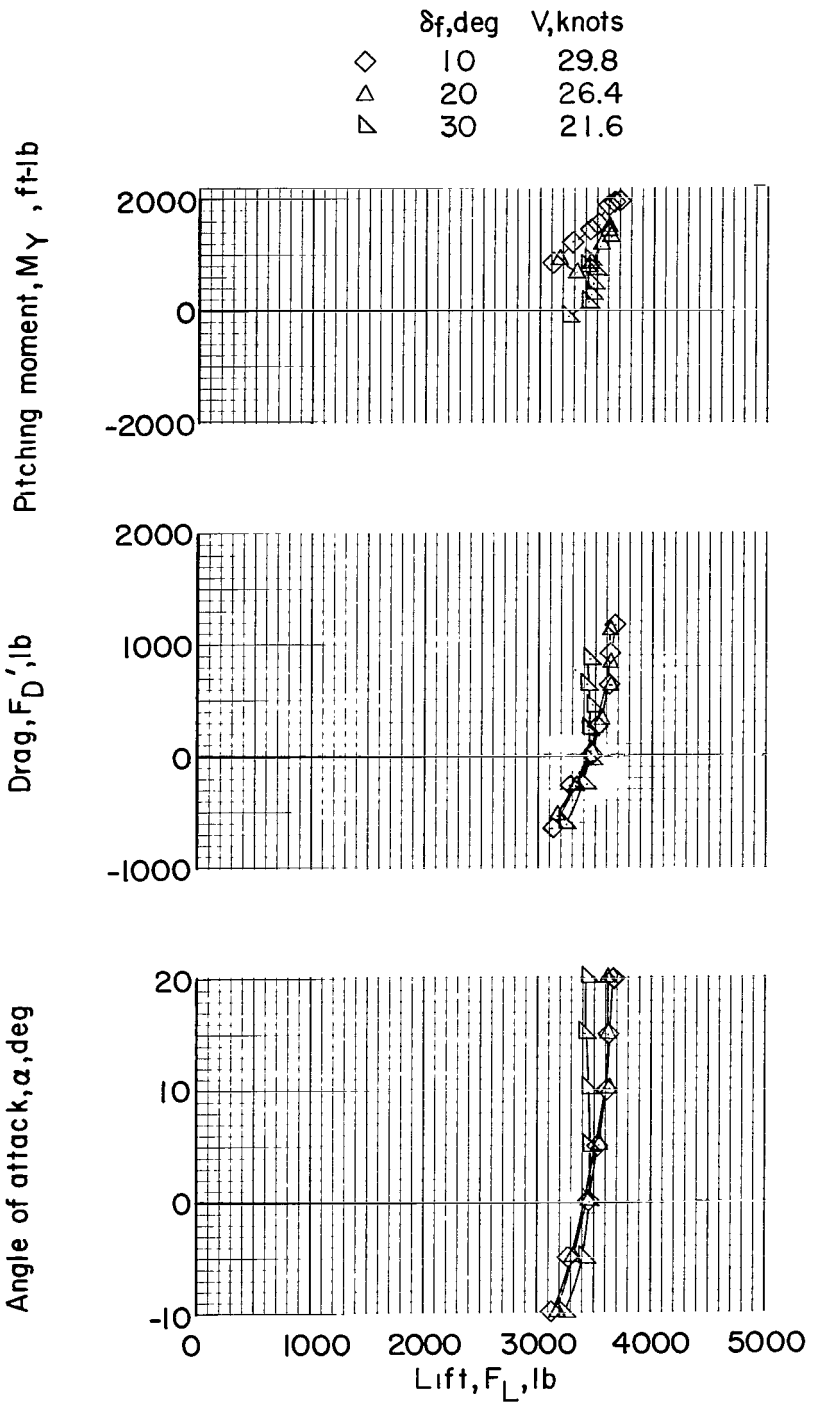

(g) $i_w = 50^\circ$.

Figure 4.- Continued.

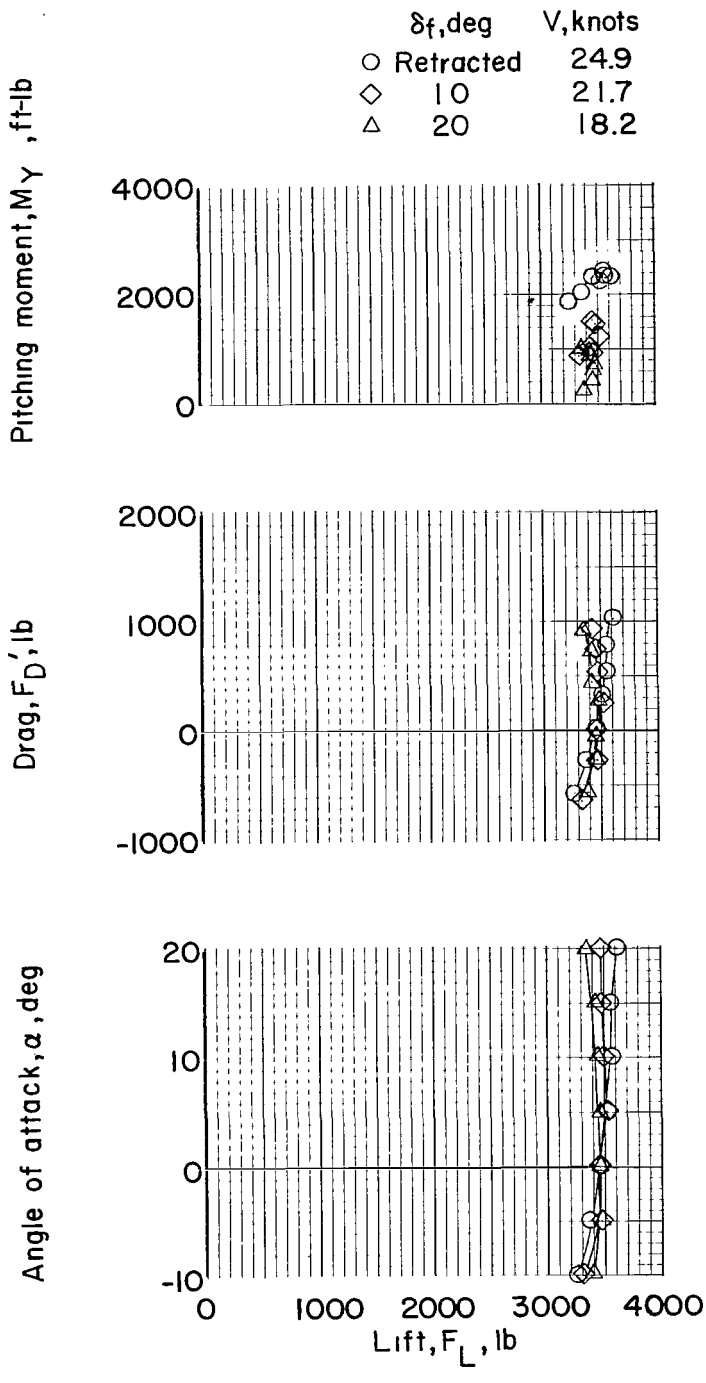

(h) $i_w = 60^\circ$.

Figure 4.- Continued.

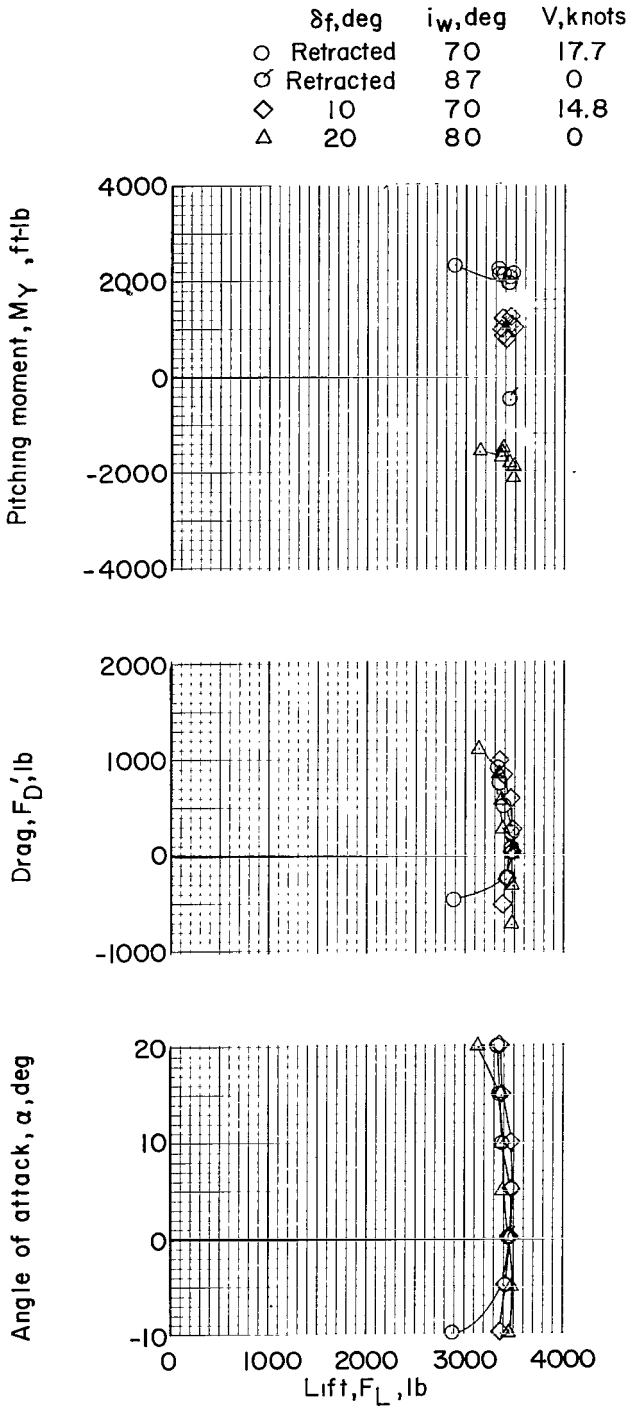

(i) $i_w = 70°$, $80°$, and $87°$.

Figure 4.- Concluded.

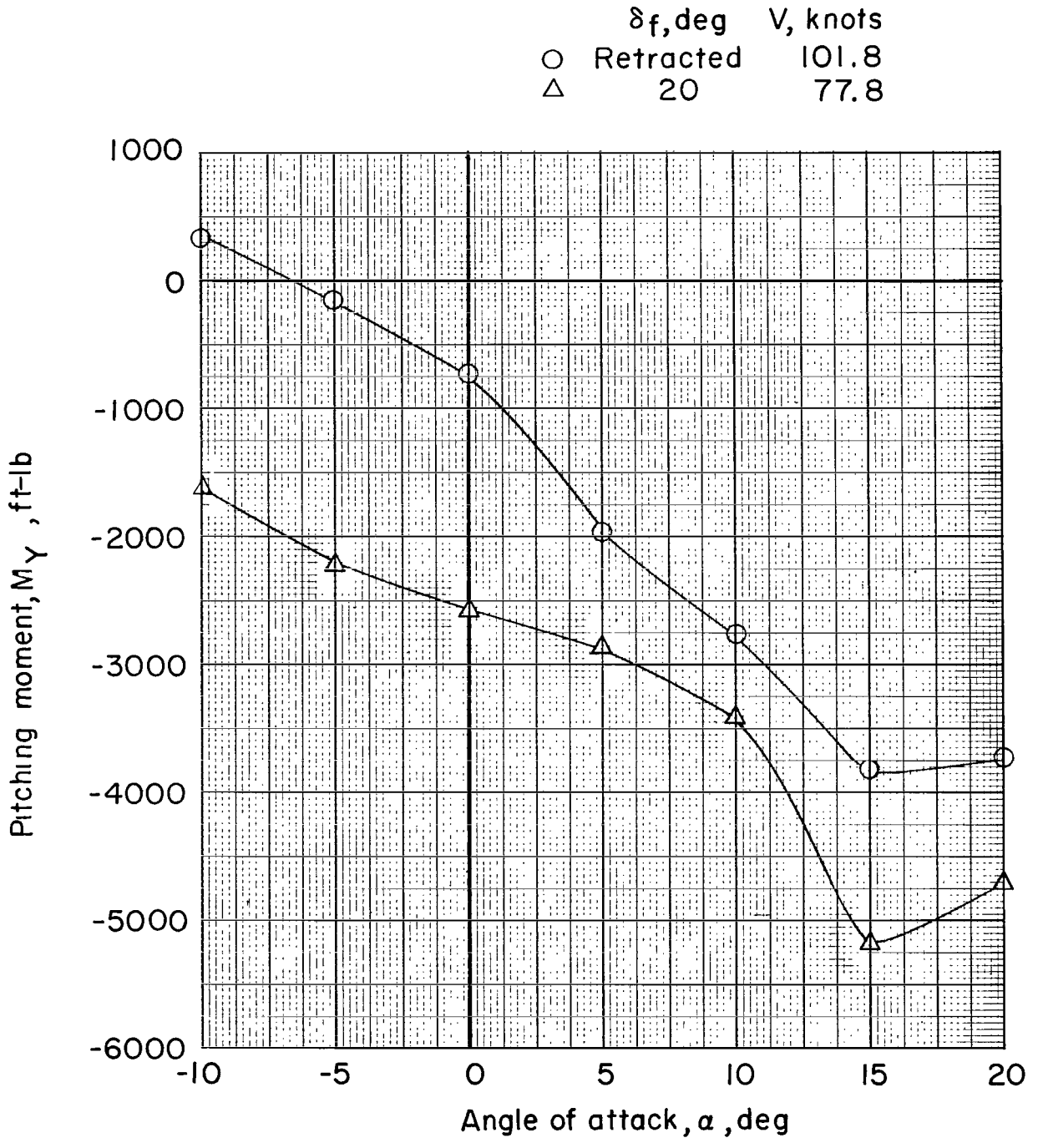

(a) $i_w = 9^\circ$.

Figure 5.- Variation of scaled-up pitching moment with angle of attack.

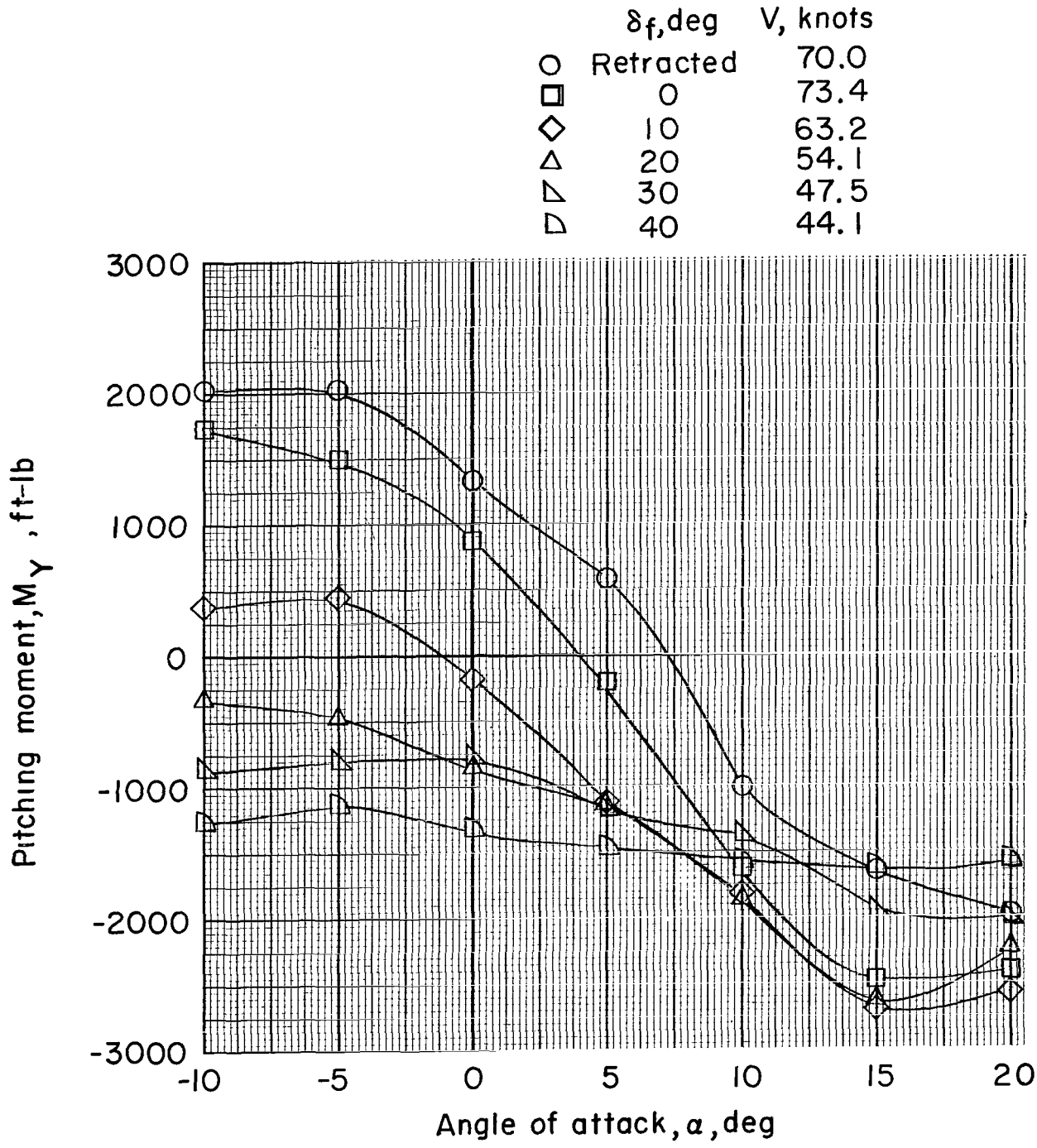

(b) $i_w = 20^\circ$.

Figure 5.- Continued.

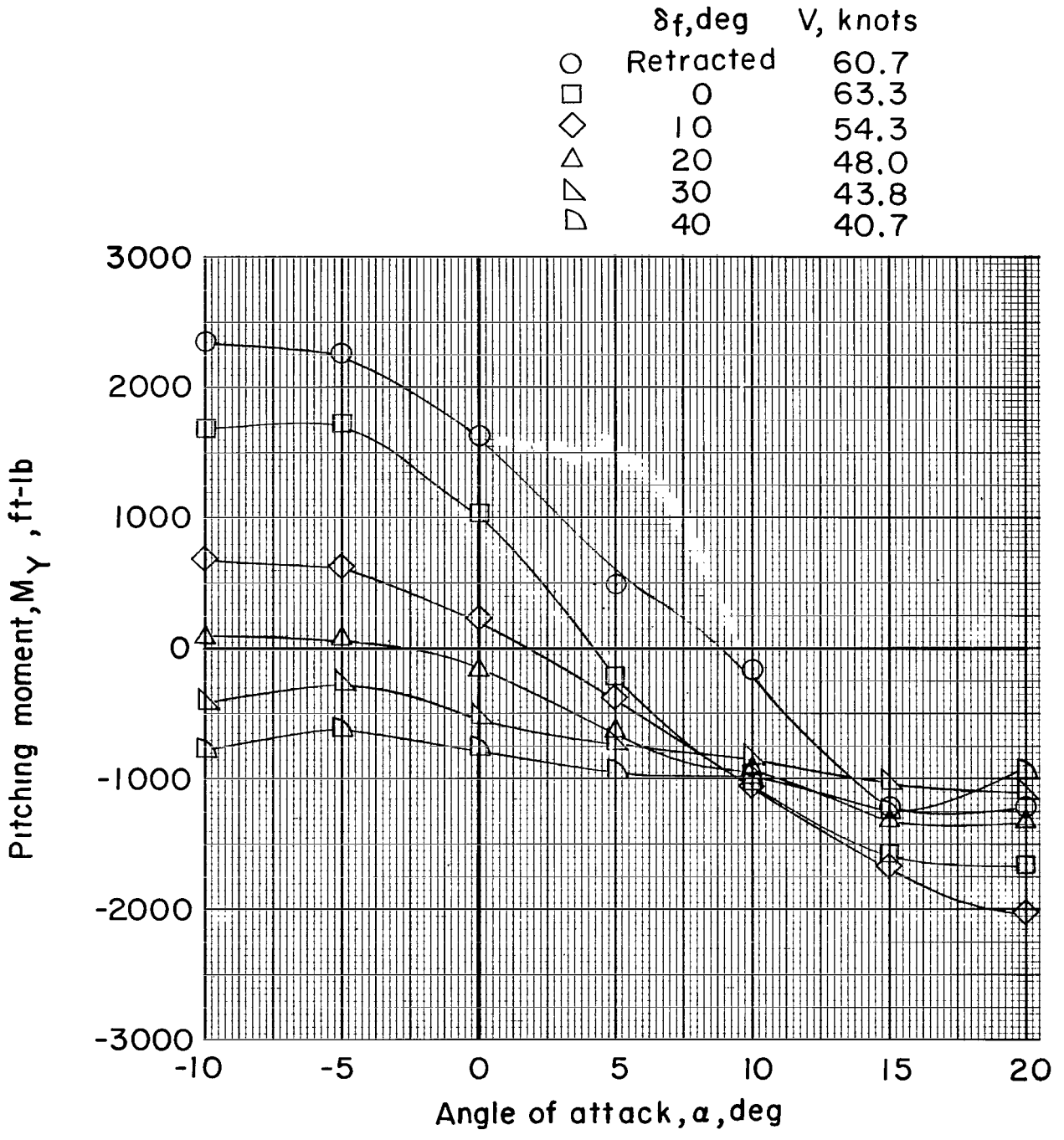

(c) $i_w = 25°$.

Figure 5.- Continued.

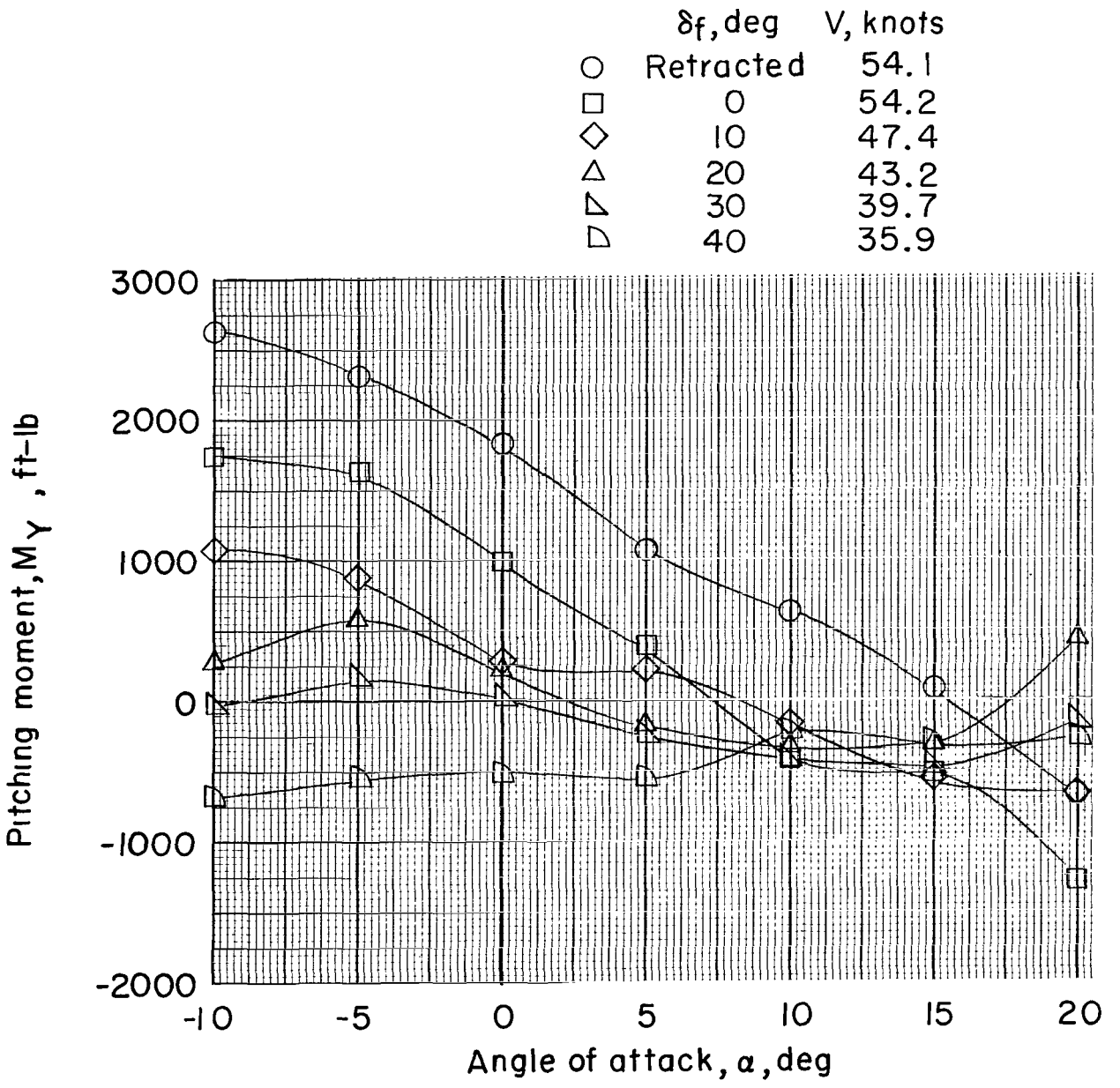

(d) $i_w = 30^\circ$.

Figure 5.- Continued.

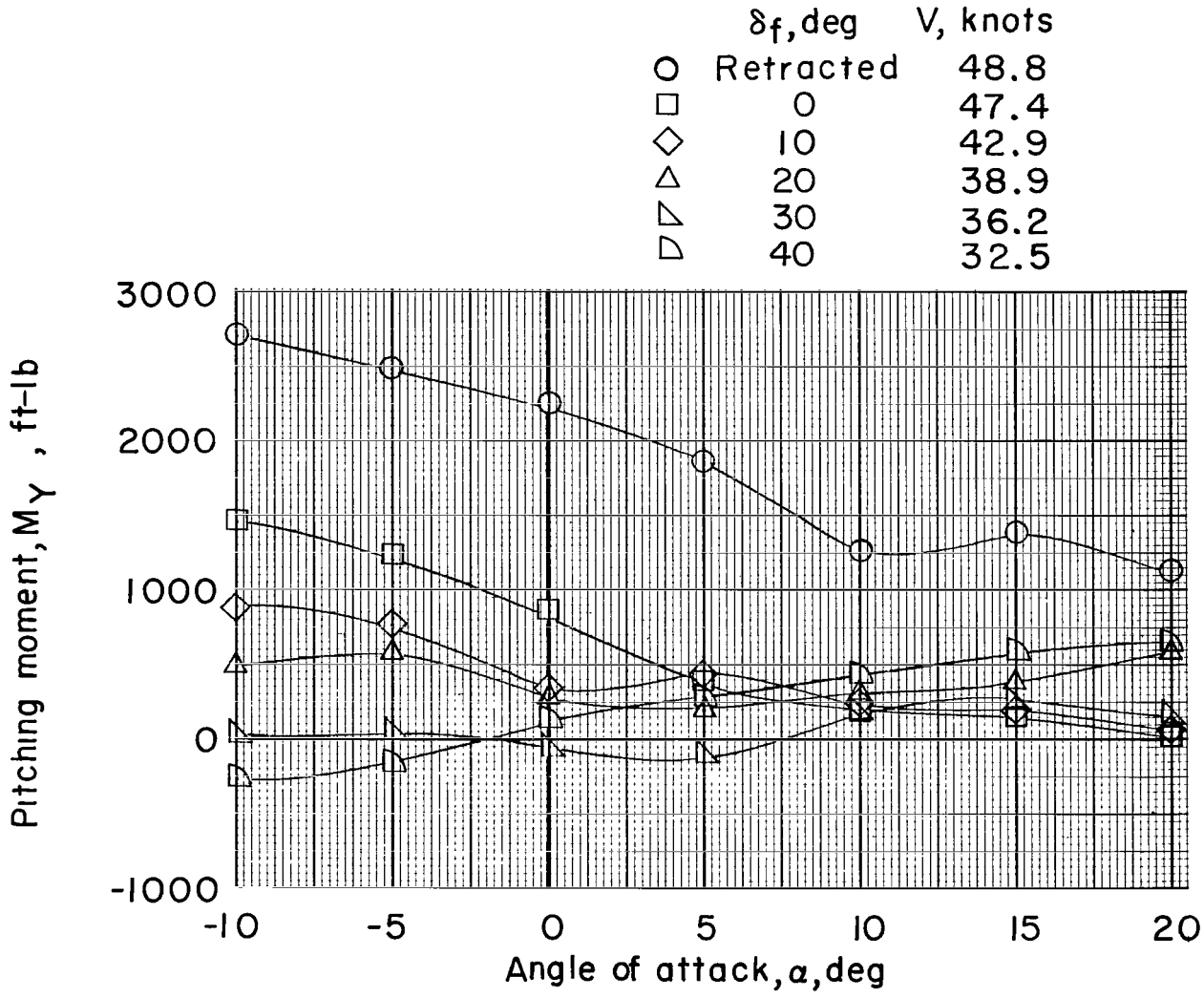

(e) $i_w = 35^\circ$.

Figure 5.- Continued.

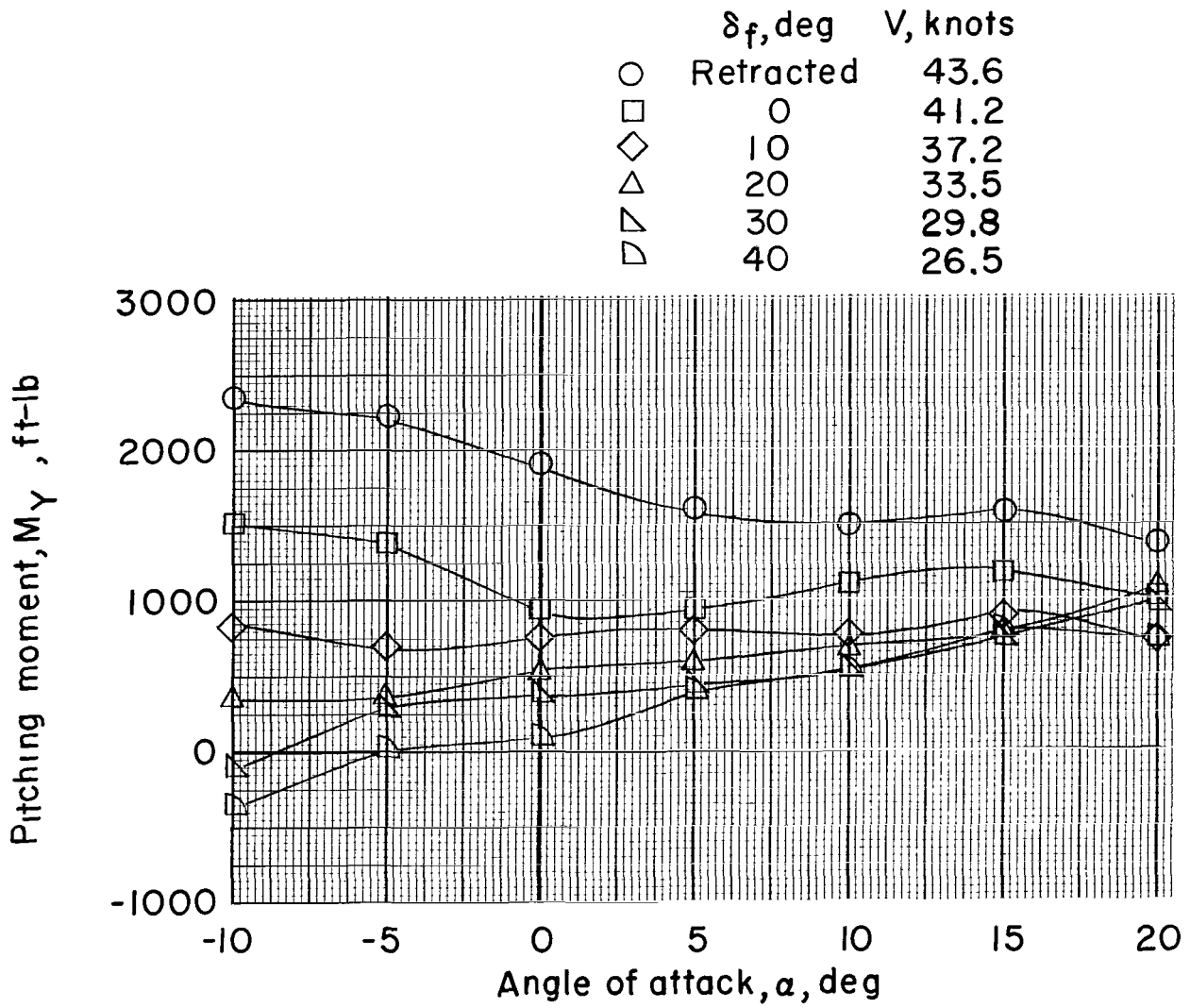

(f) $i_w = 40^\circ$.

Figure 5.- Continued.

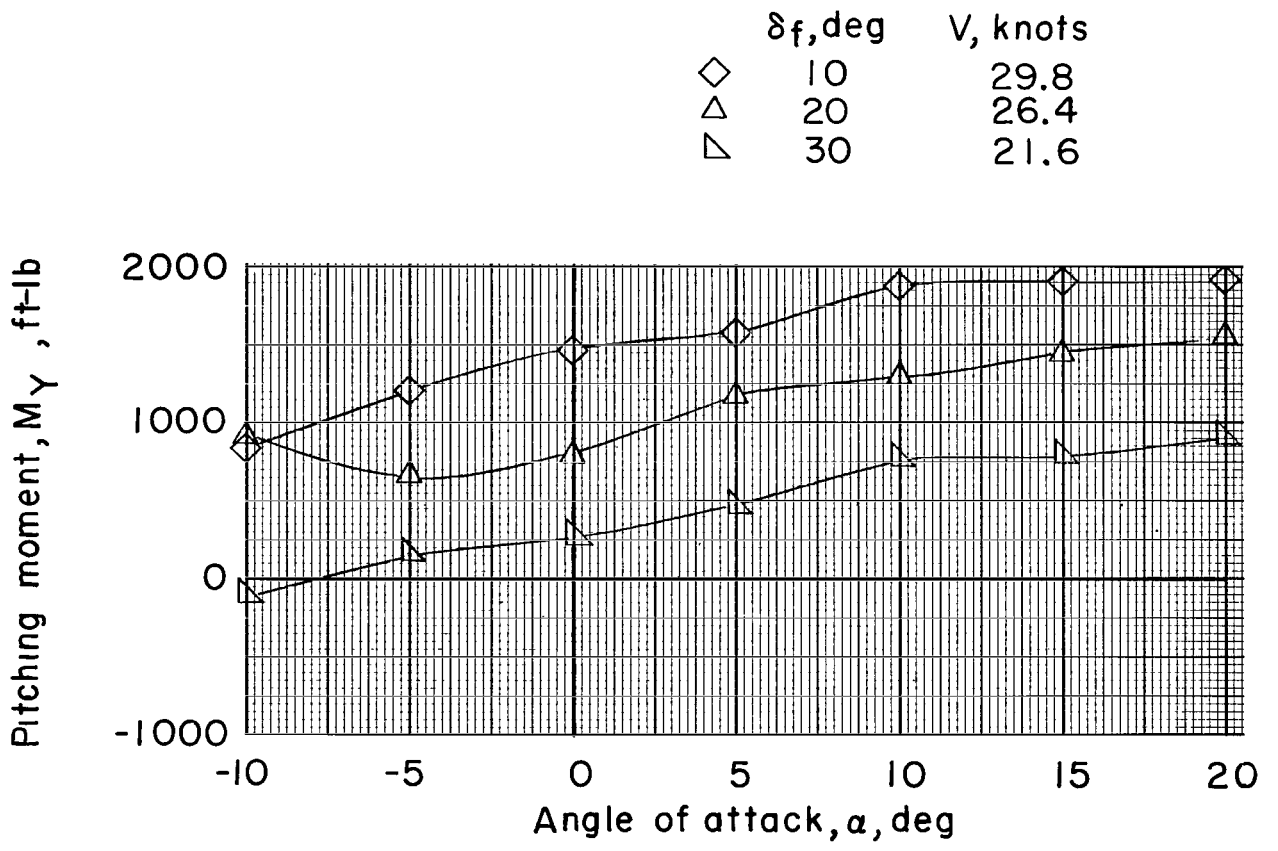

(g) $i_w = 50^\circ$.

Figure 5.- Continued.

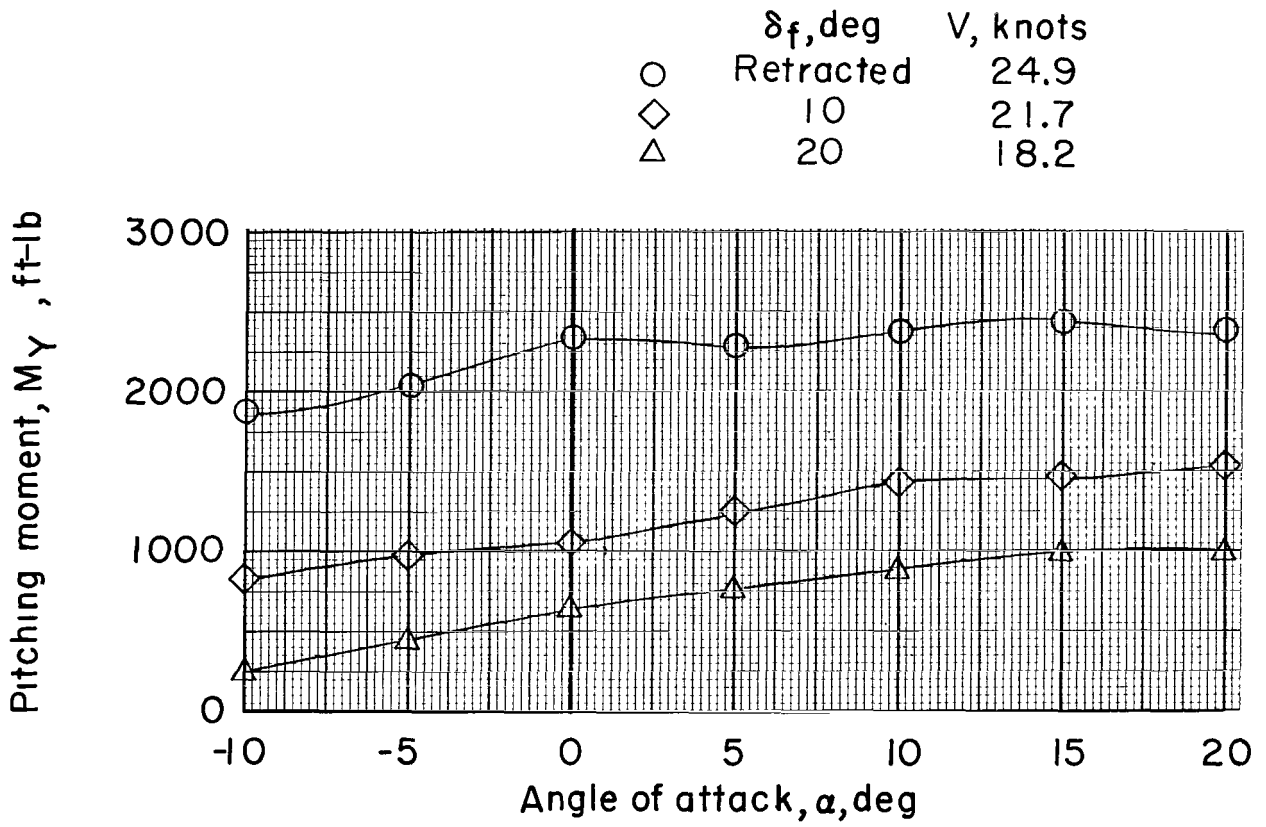

(h) $i_w = 60^\circ$.

Figure 5.- Continued.

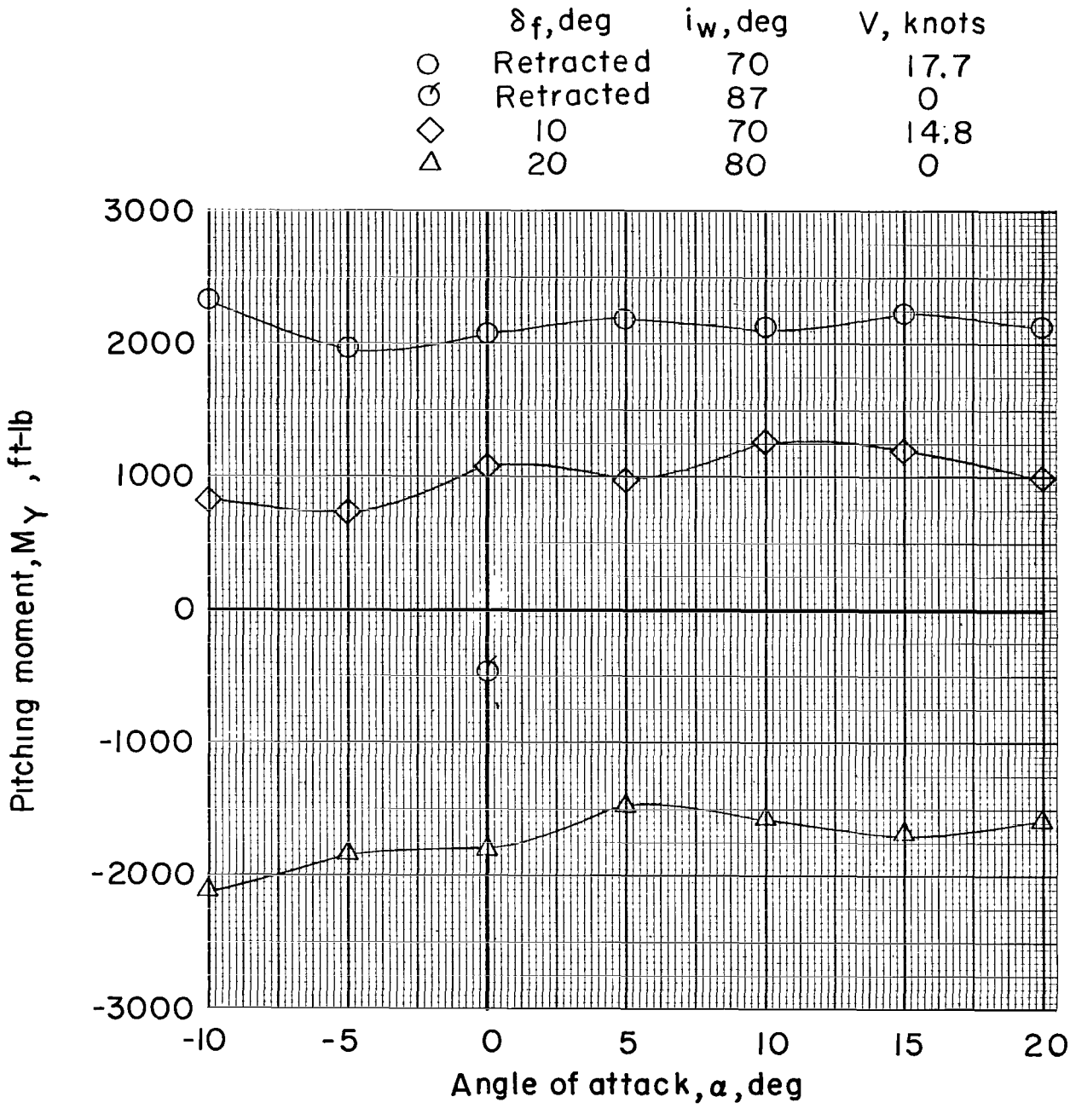

(i) $i_w = 70^\circ$, 80°, and 87°.

Figure 5.- Concluded.

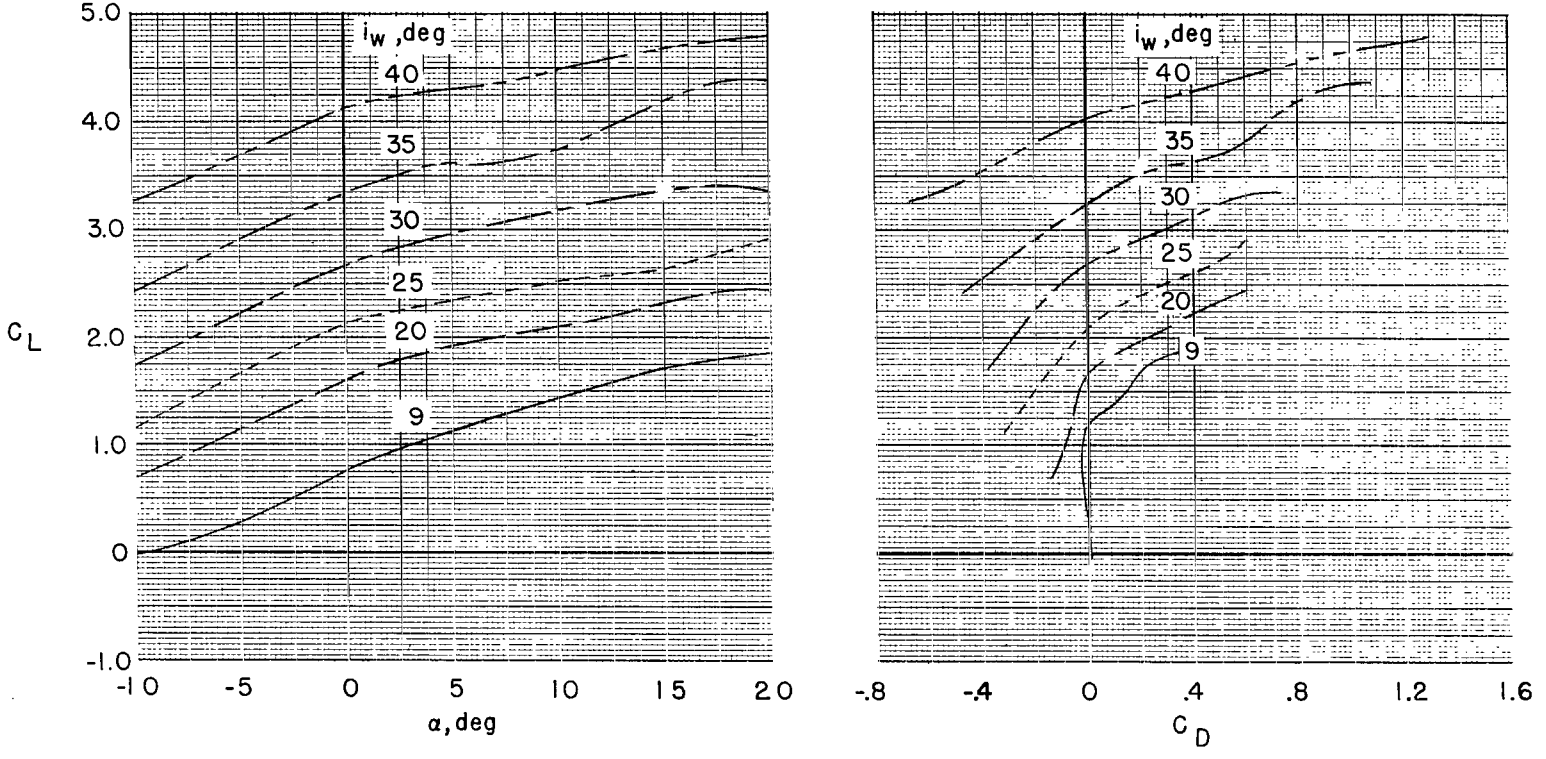

(a) Flap retracted.

Figure 6.- Variation of lift coefficient with angle of attack and drag coefficient.

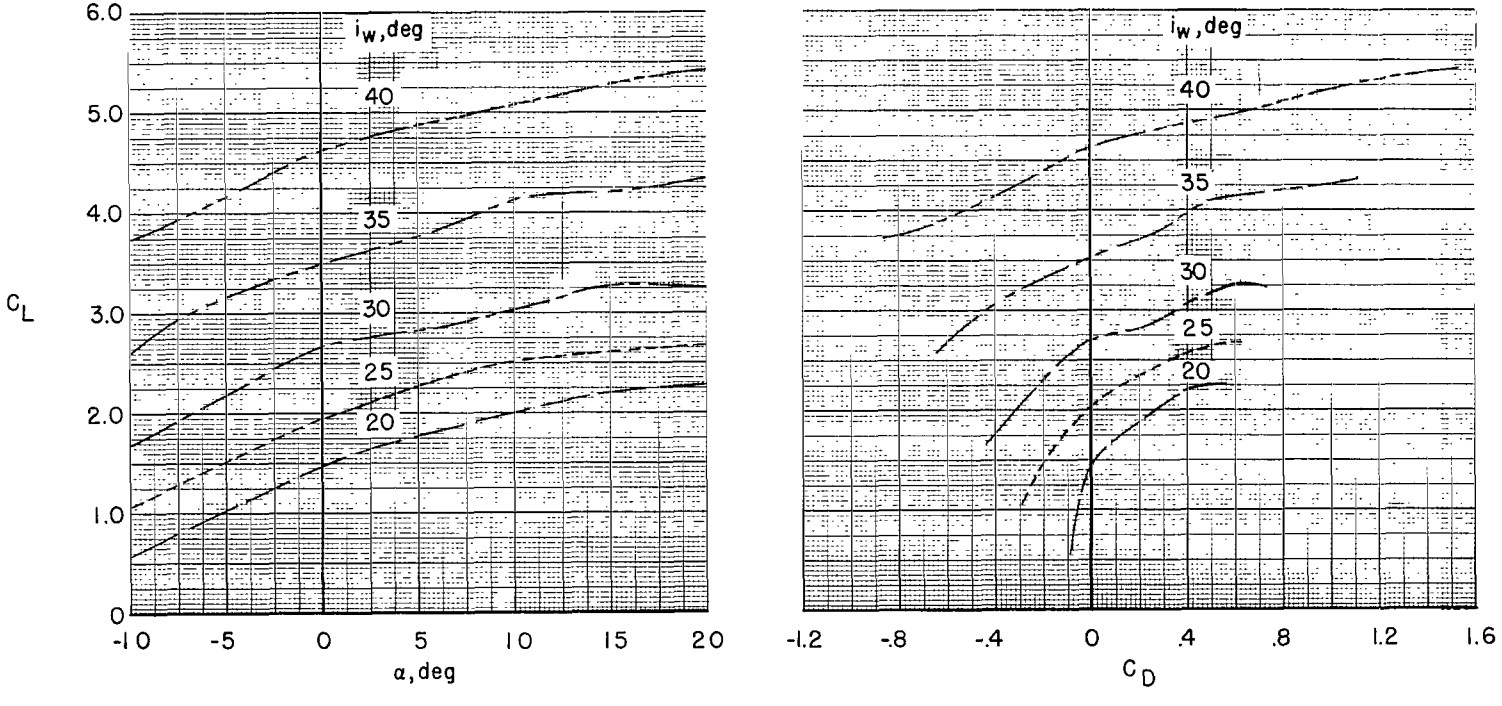

(b) $\delta_f = 0^\circ$ (flap extended).

Figure 6.- Continued.

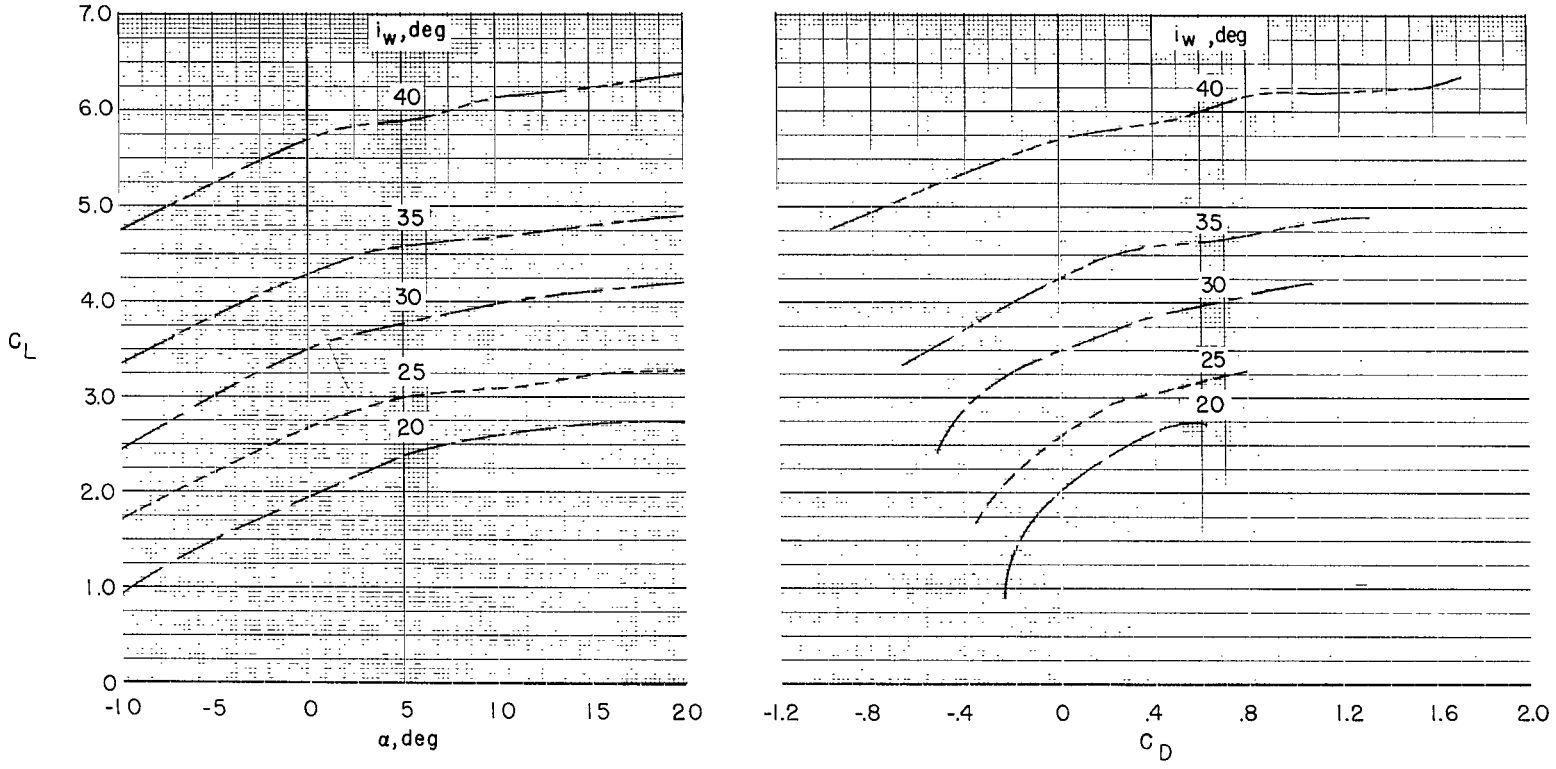

(c) $\delta_f = 10^\circ$.

Figure 6.- Continued.

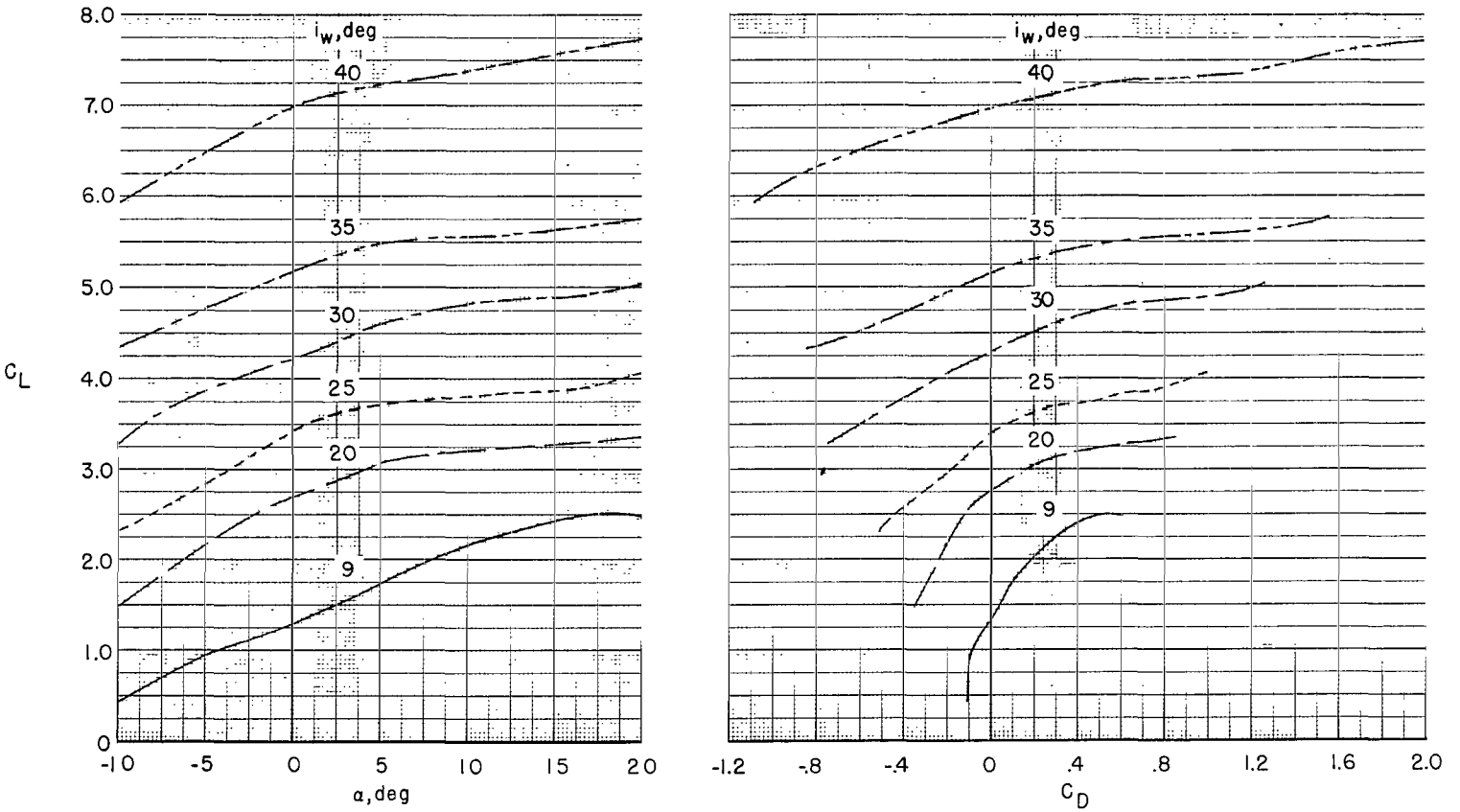

(d) $\delta_f = 20^\circ$.

Figure 6.- Continued.

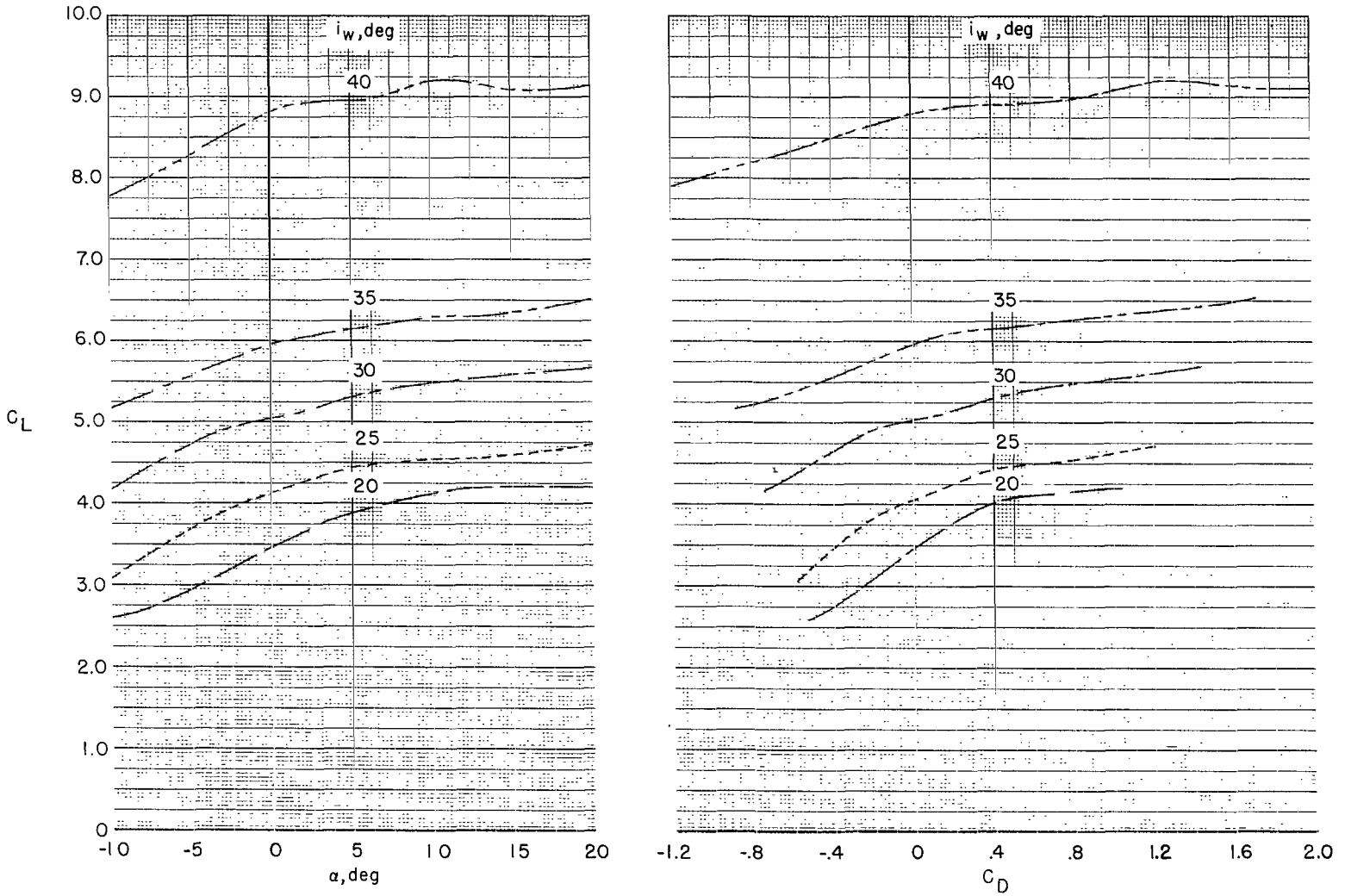

(e) $\delta_f = 30^\circ$.

Figure 6.- Continued.

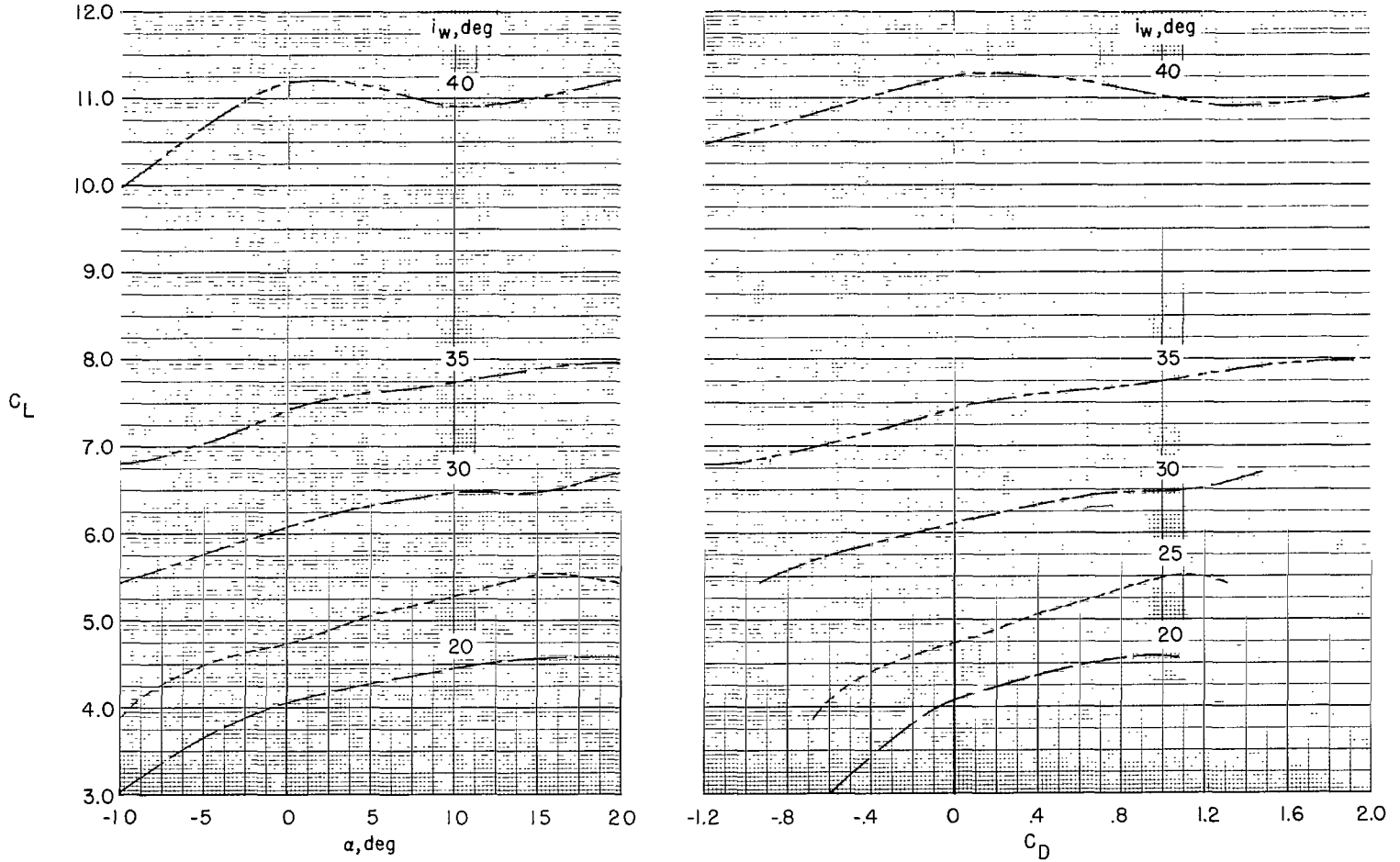

(f) $\delta_f = 40^\circ$.

Figure 6.- Concluded.

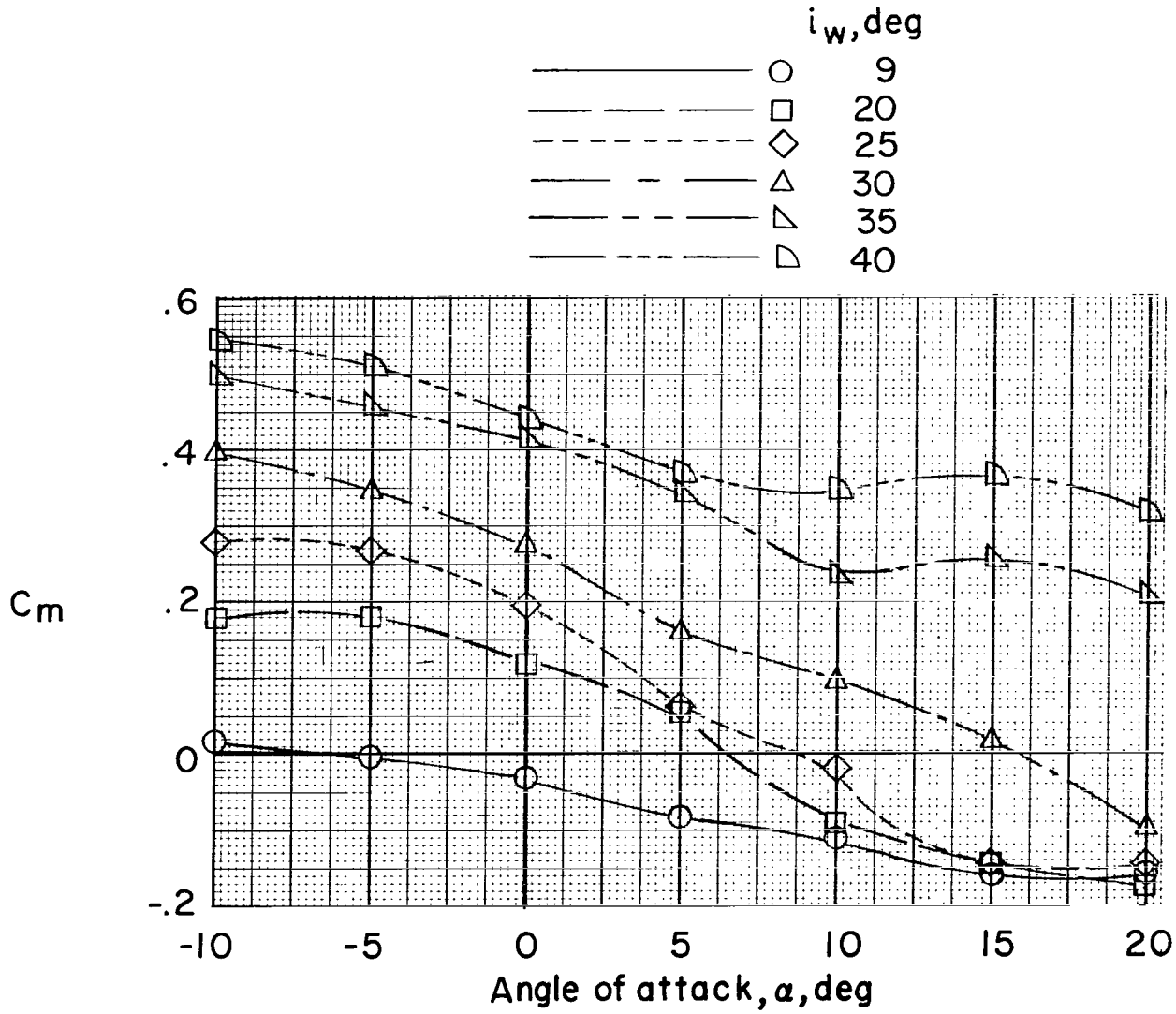

(a) Flap retracted.

Figure 7.- Variation of pitching-moment coefficient with angle of attack.

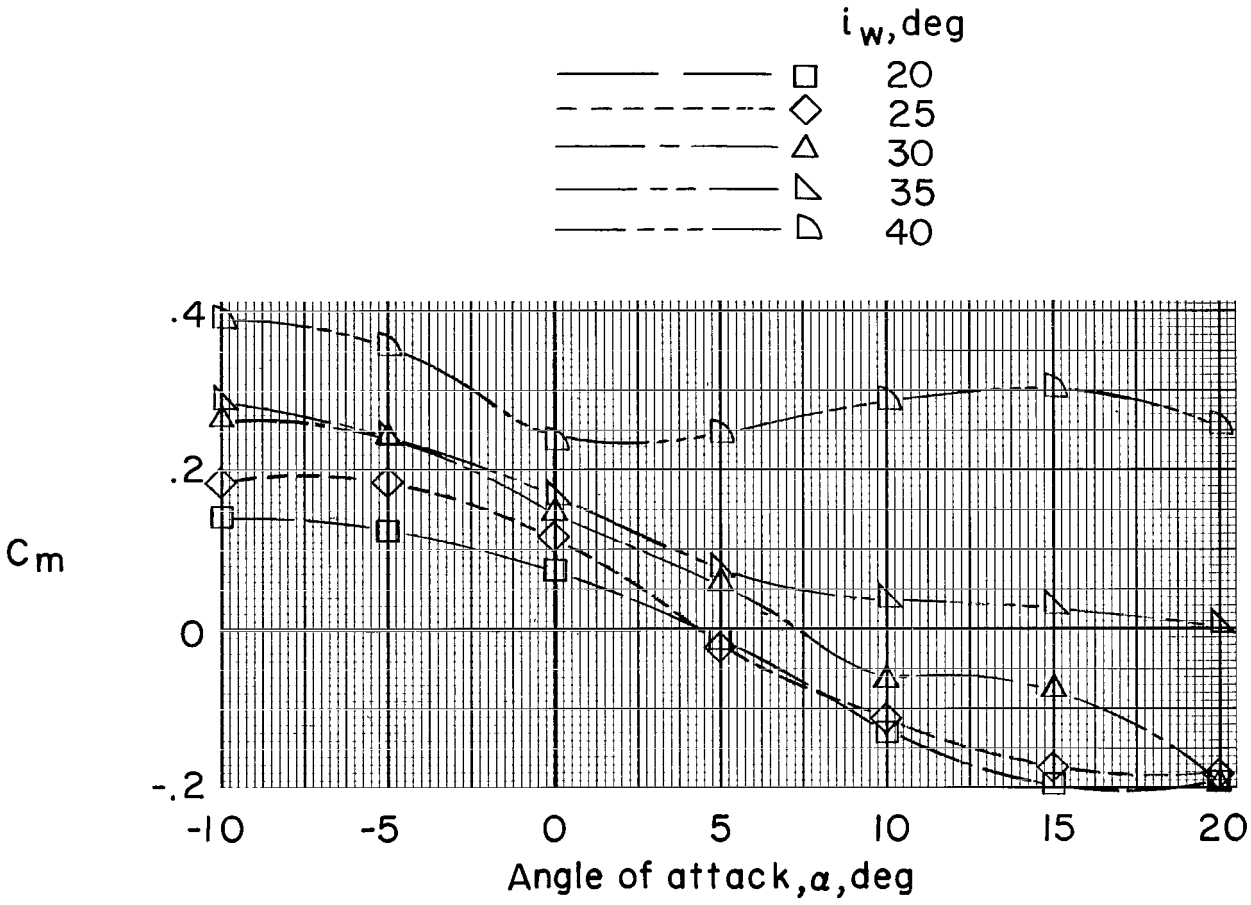

(b) $\delta_f = 0^o$ (flap extended).

Figure 7.- Continued.

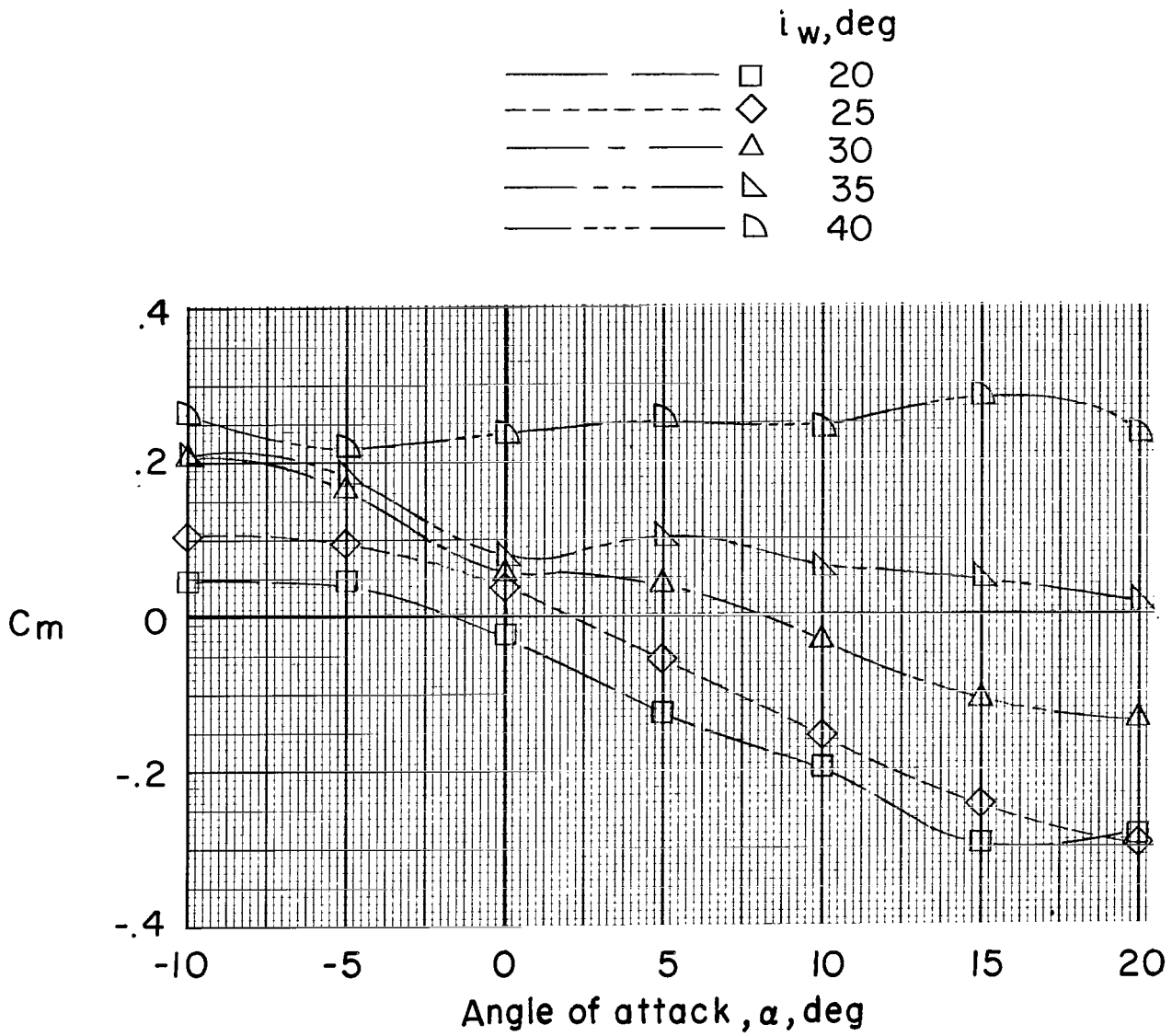

(c) $\delta_f = 10^\circ$.

Figure 7.- Continued.

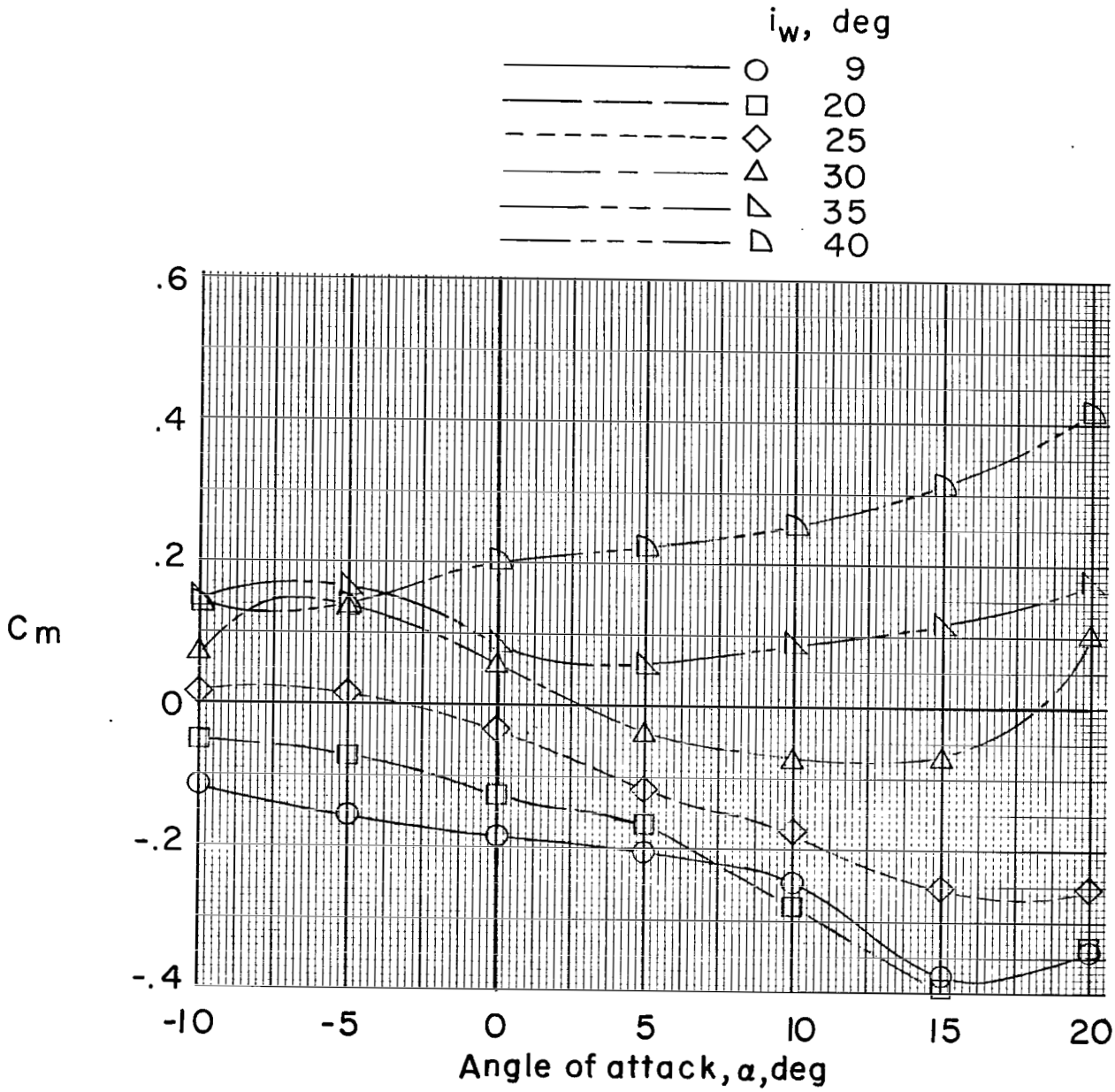

(d) $\delta_f = 20^\circ$.

Figure 7.- Continued.

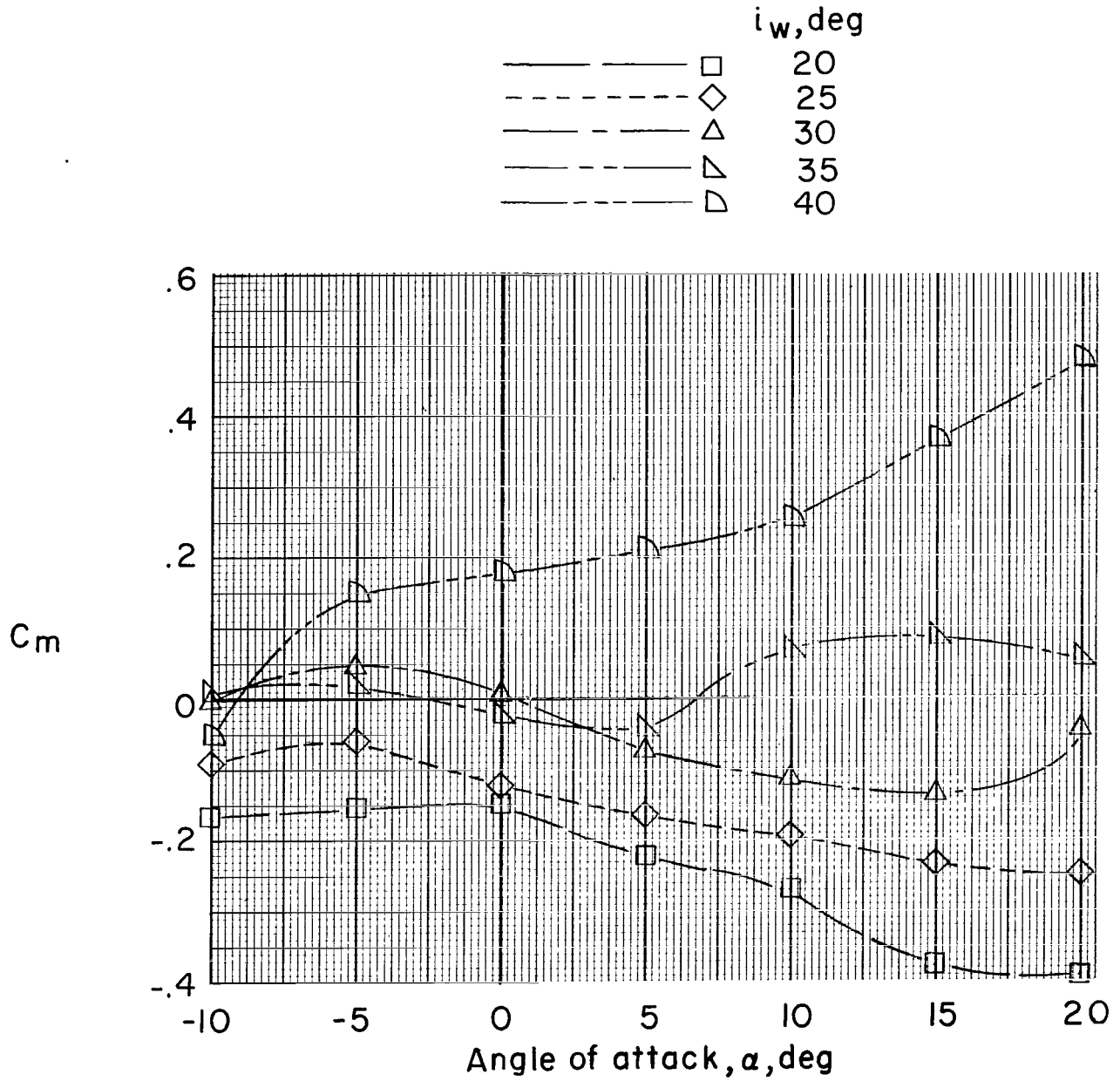

(e) $\delta_f = 30^\circ$.

Figure 7.- Continued.

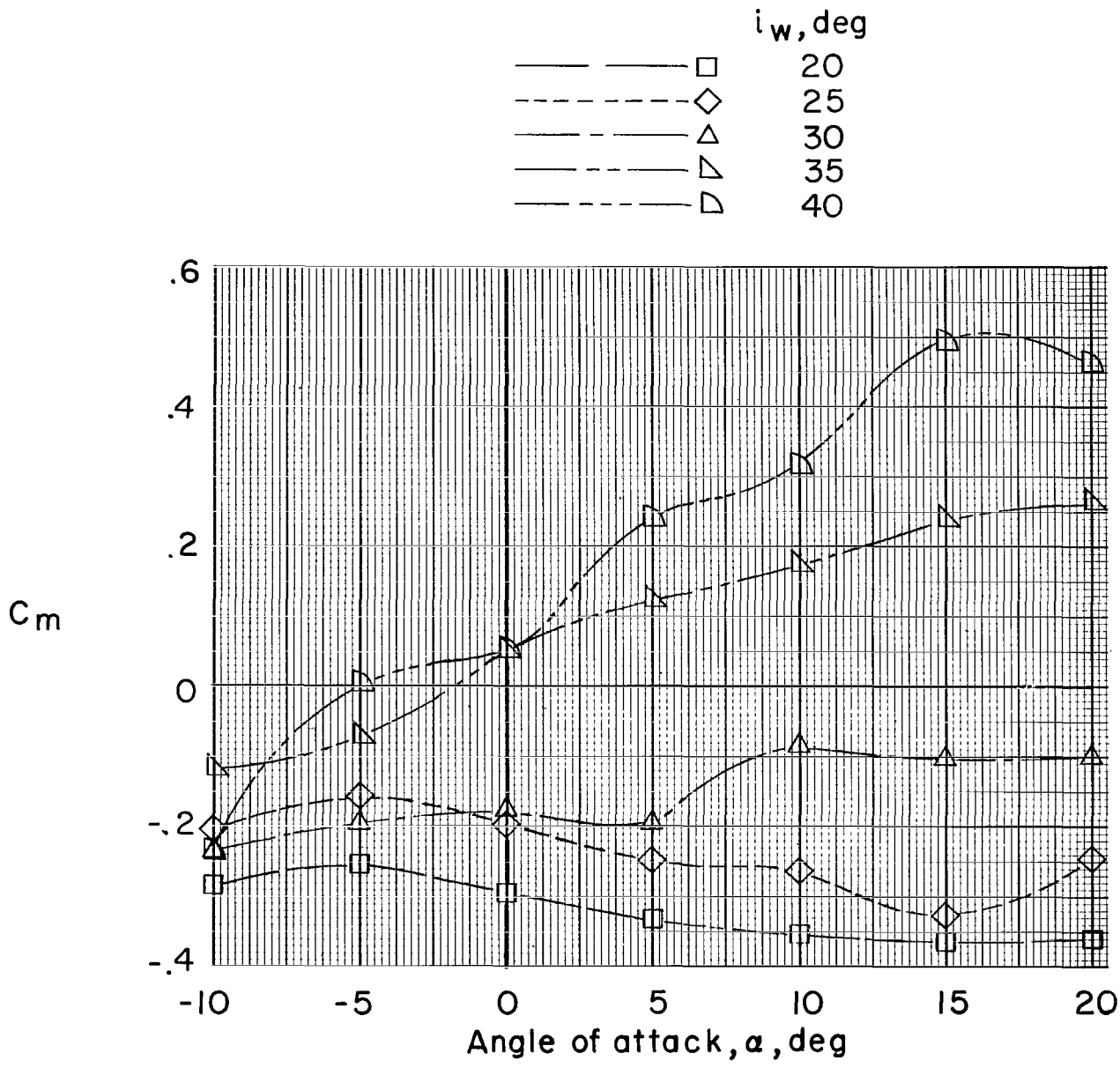

(f) $\delta_f = 40°$.

Figure 7.- Concluded.

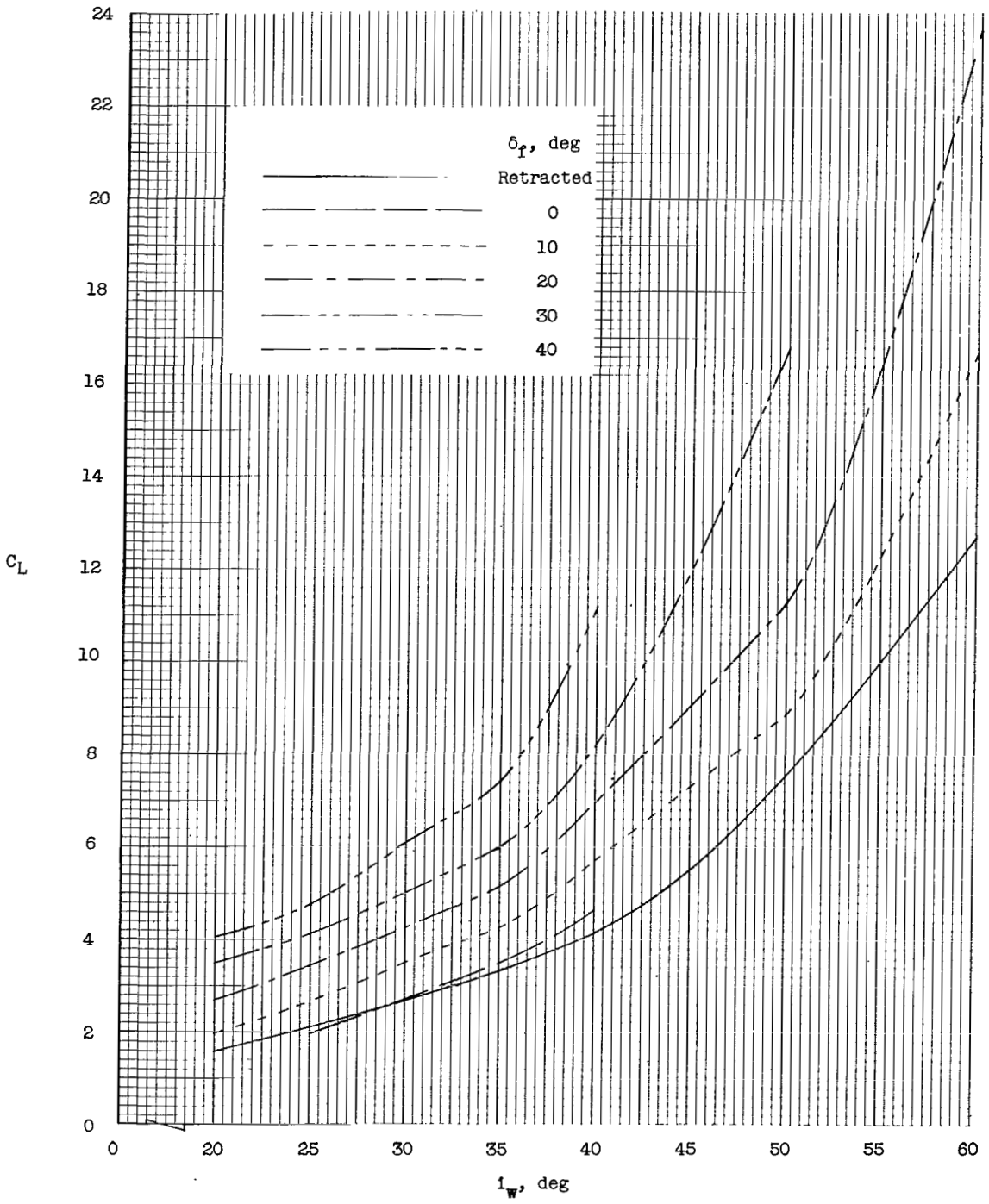

Figure 8.- Variation of lift coefficient with wing incidence at various flap deflections for $\alpha = 0^{\circ}$.

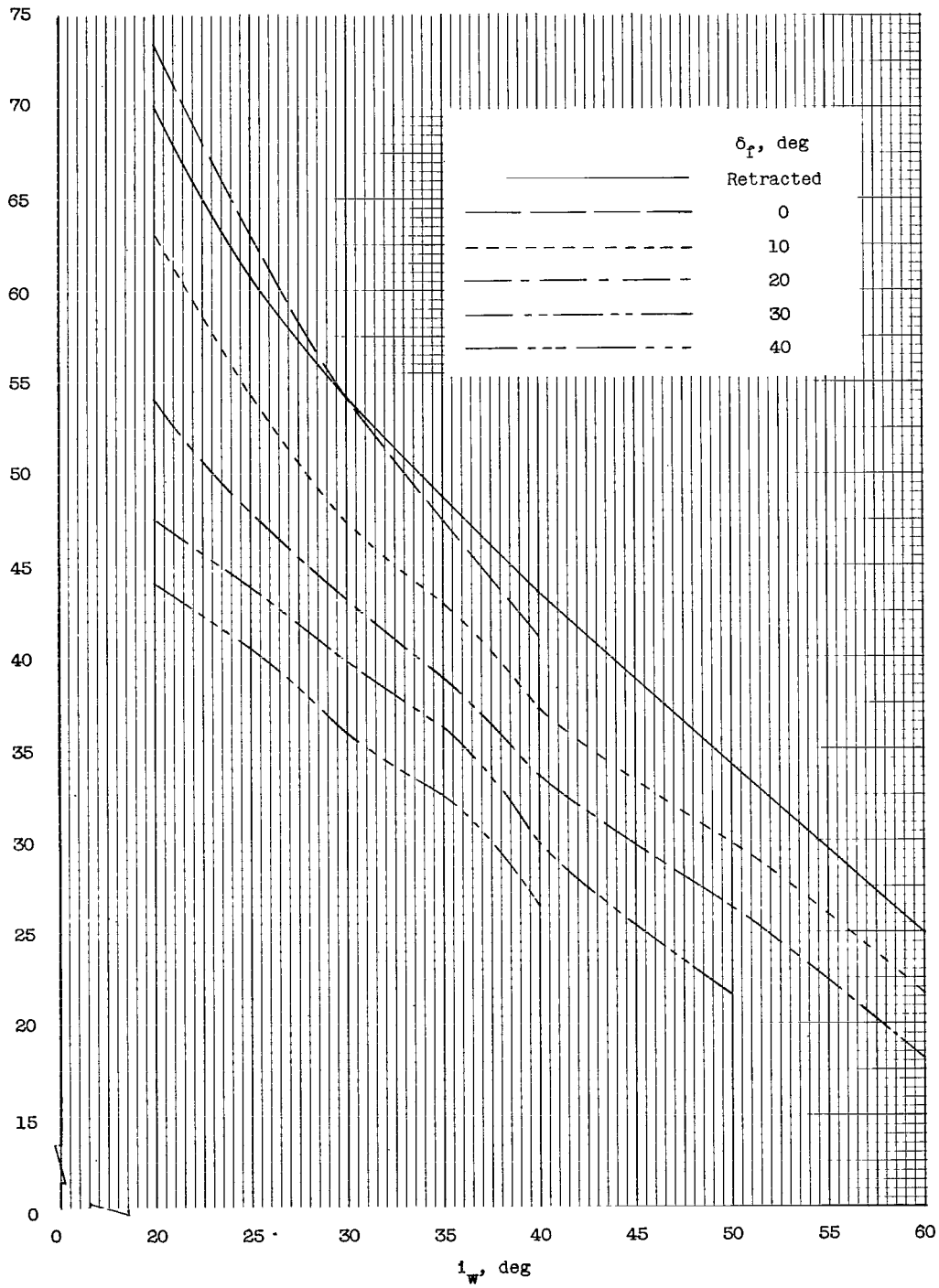

Figure 9.- Variation of forward speed with wing incidence at various flap deflections for $\alpha = 0^{\circ}$.

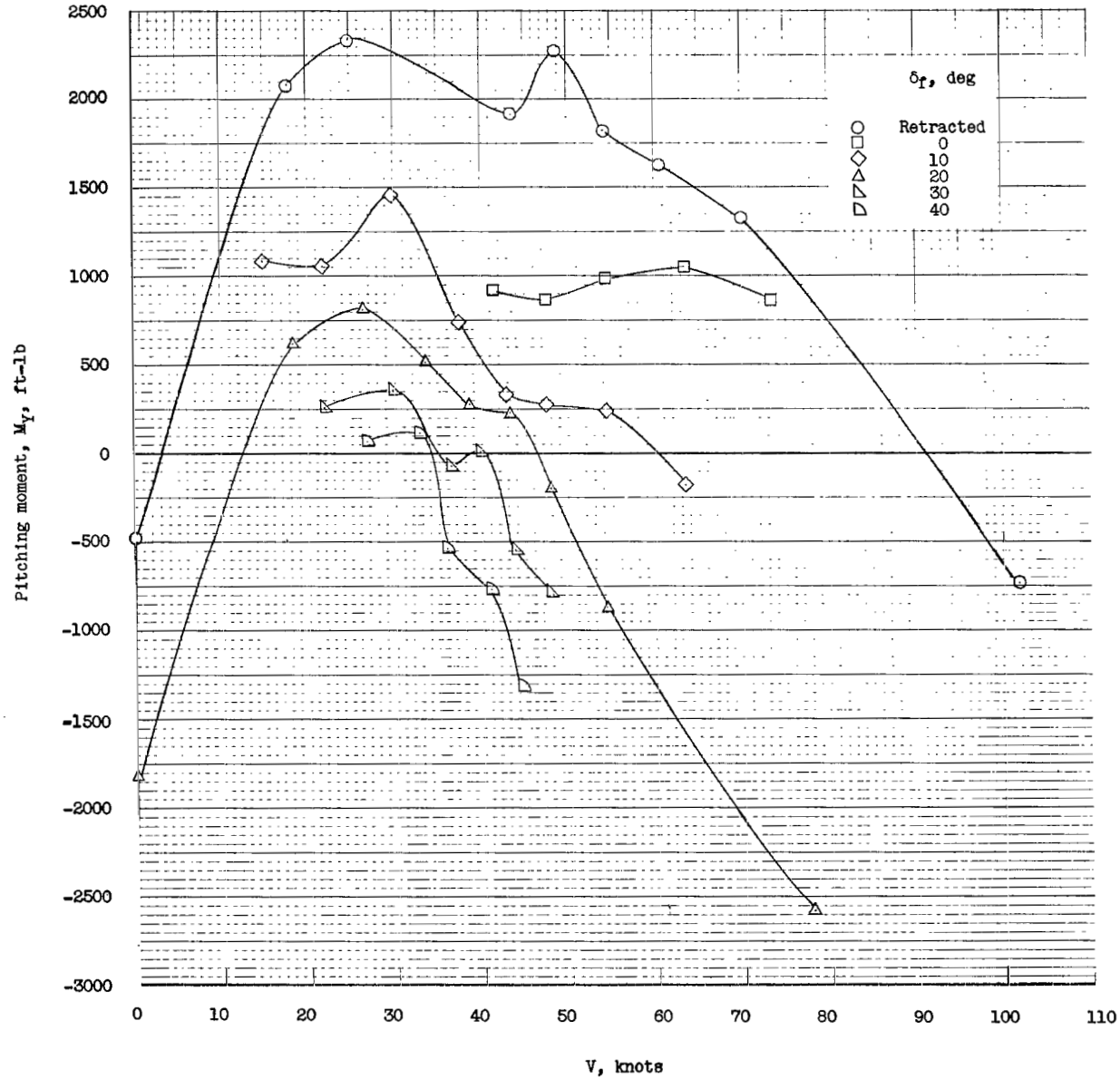

Figure 10.- Variation of pitching moment with speed for various wing incidences and flap deflections at $\alpha = 0^{\circ}$.

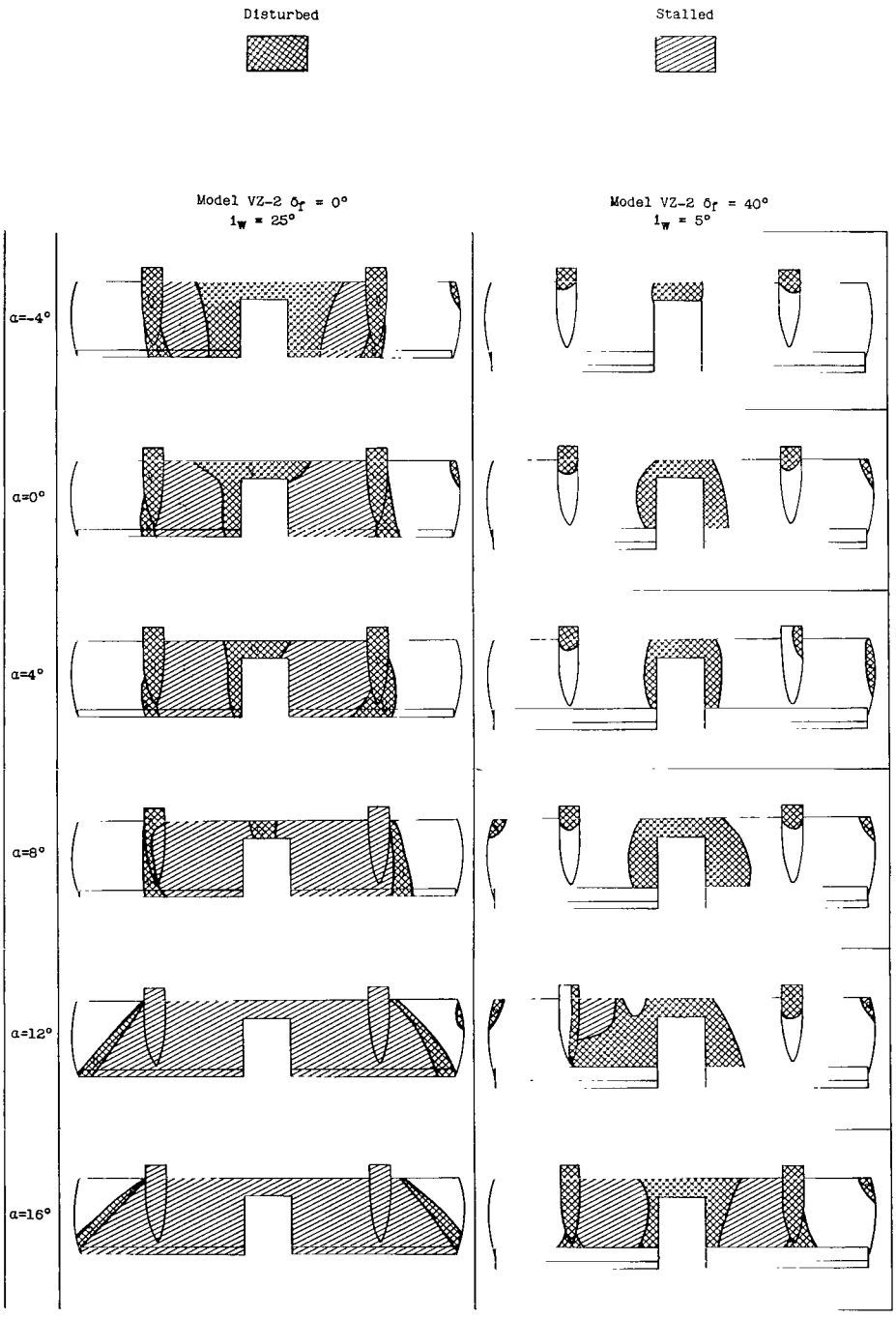

(a) V ≈ 61 knots.

Figure 11.- Effect of flap deflection on the wing flow patterns.

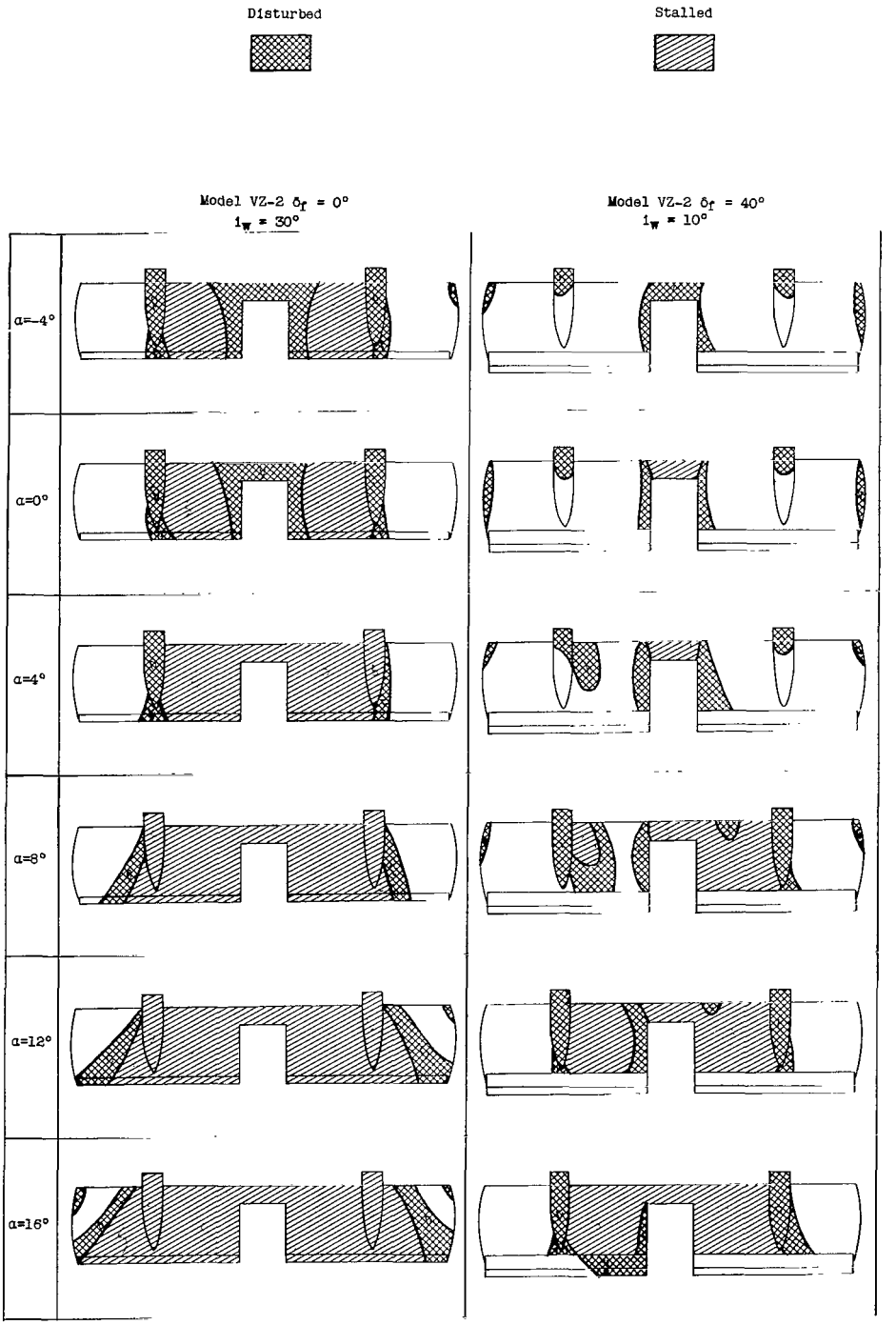

(b) V ≈ 54 knots.

Figure 11.- Continued.

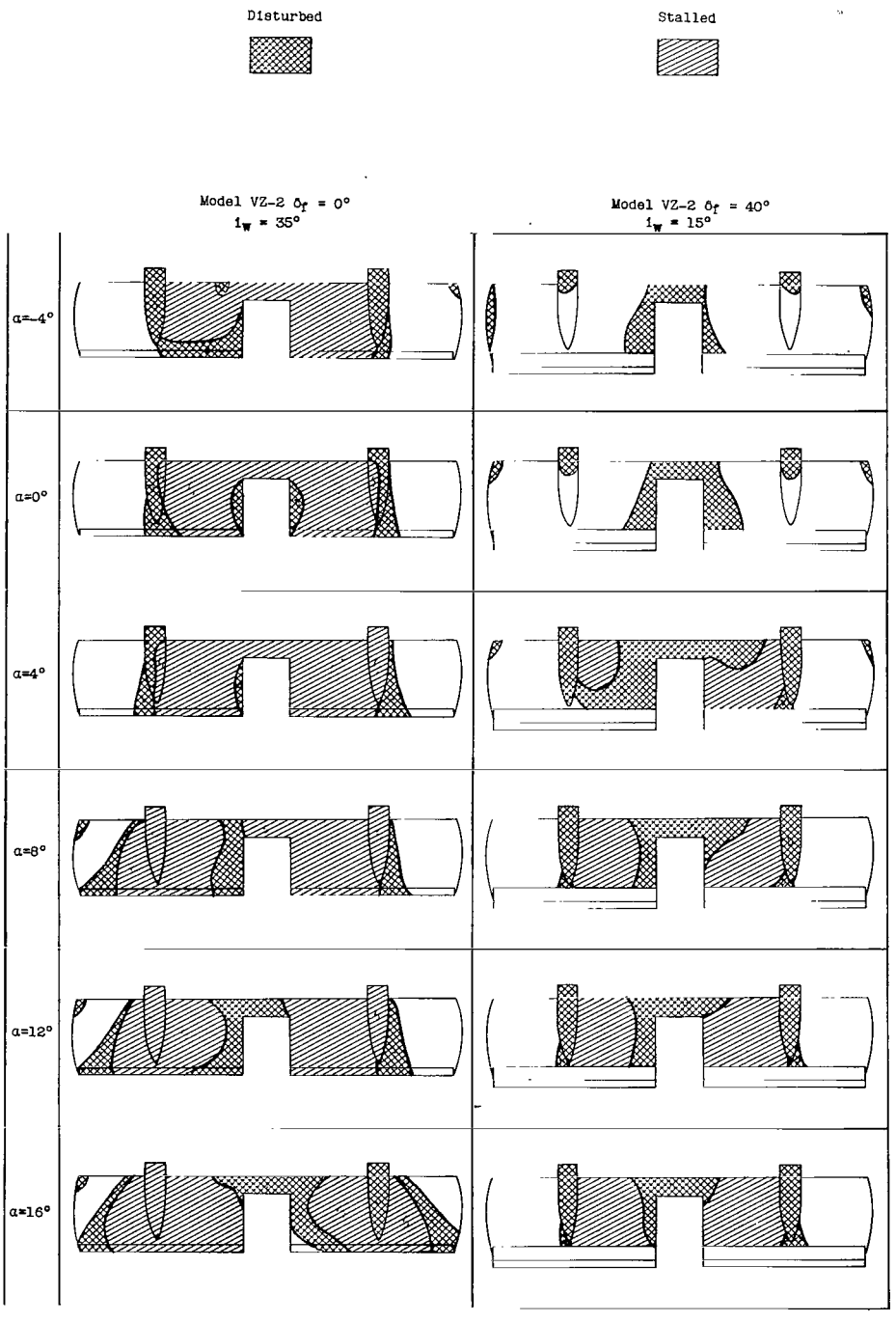

(c) V ≈ 49 knots.

Figure 11.- Continued.

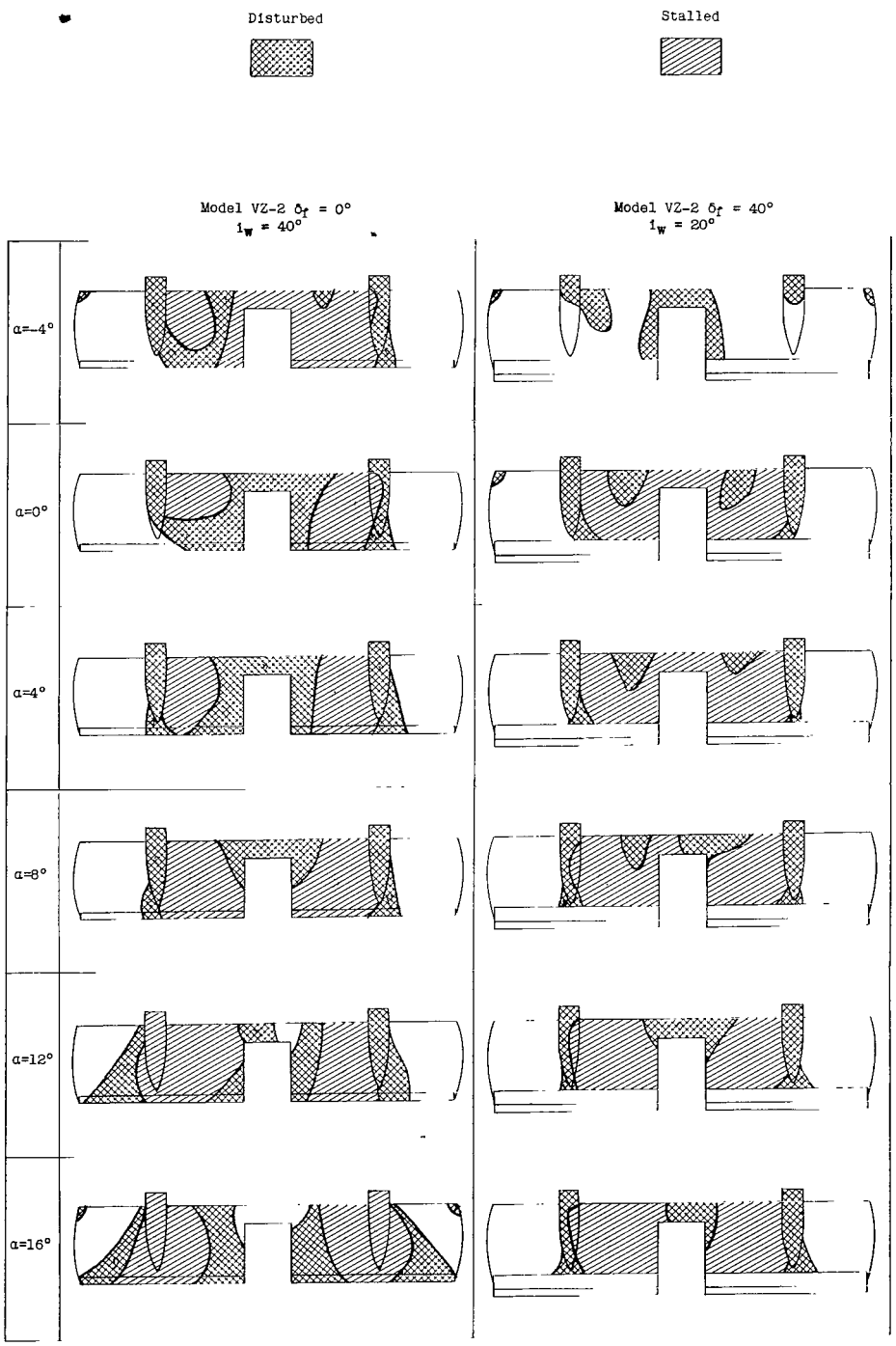

(d) V ≈ 44 knots.

Figure 11.- Continued.

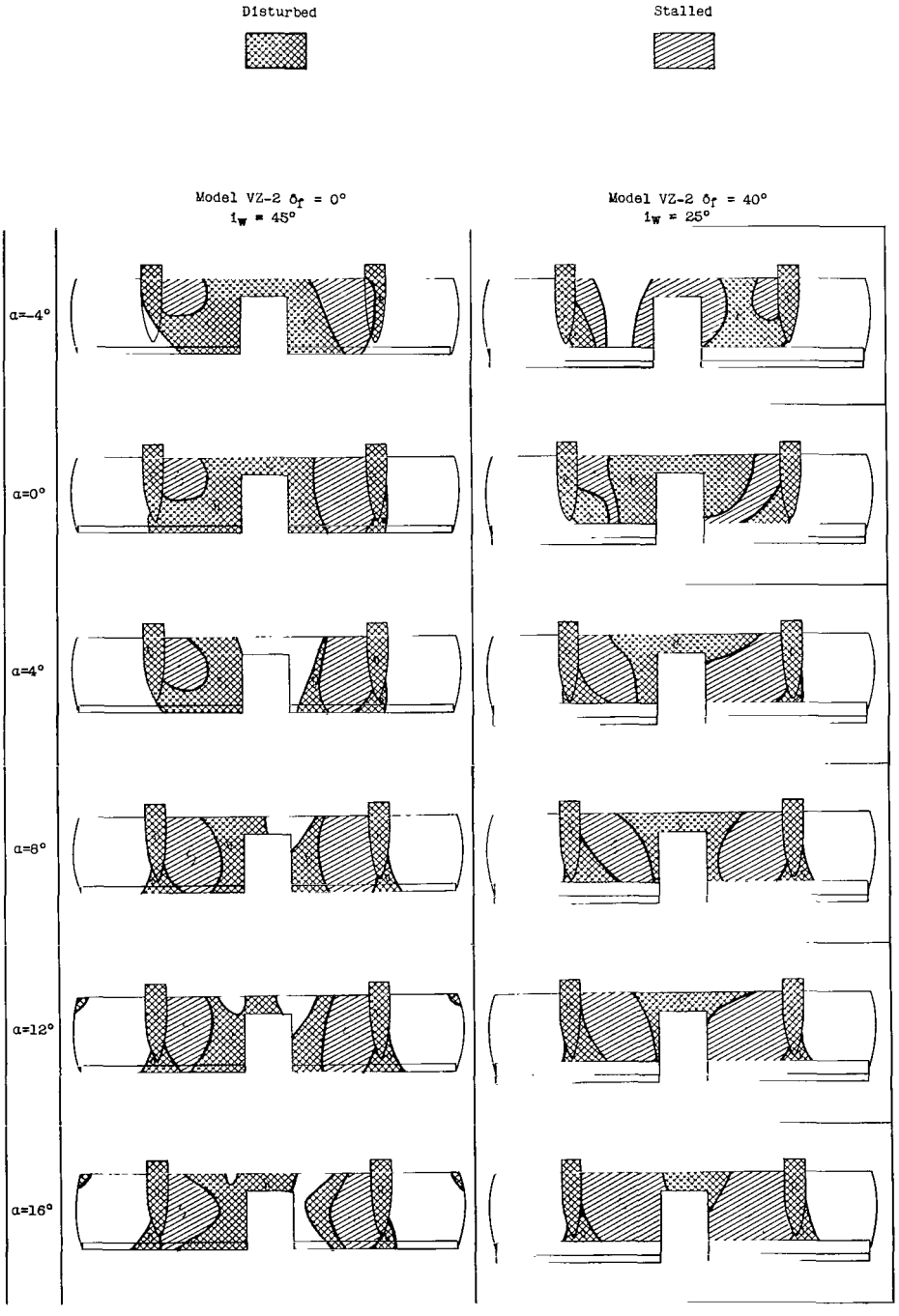

(e) V ≈ 39 knots.

Figure 11.- Concluded.

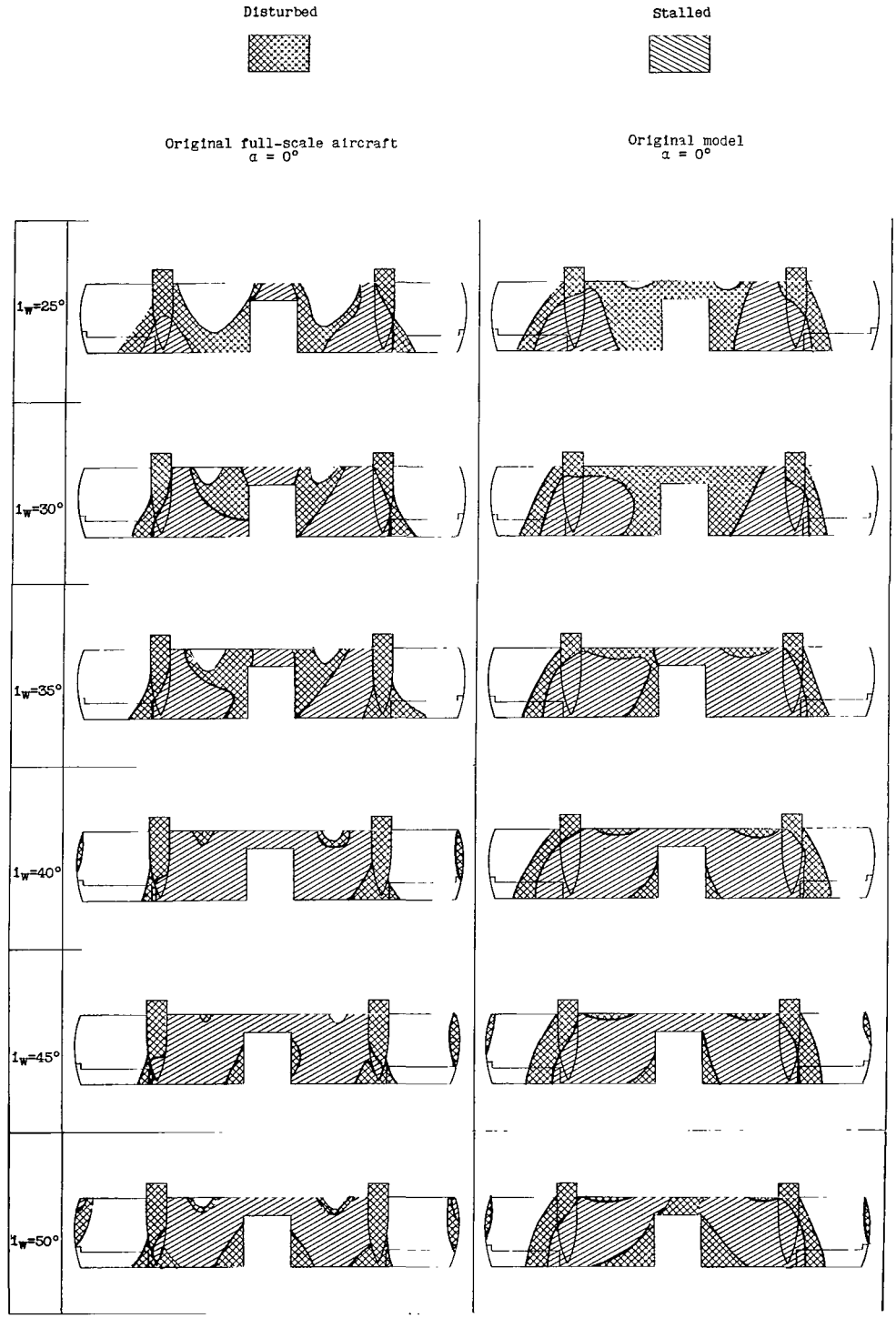

Figure 12.- Comparison of the wing flow patterns obtained from tuft tests on the original full-scale VZ-2 aircraft and the original small-scale VZ-2 model.

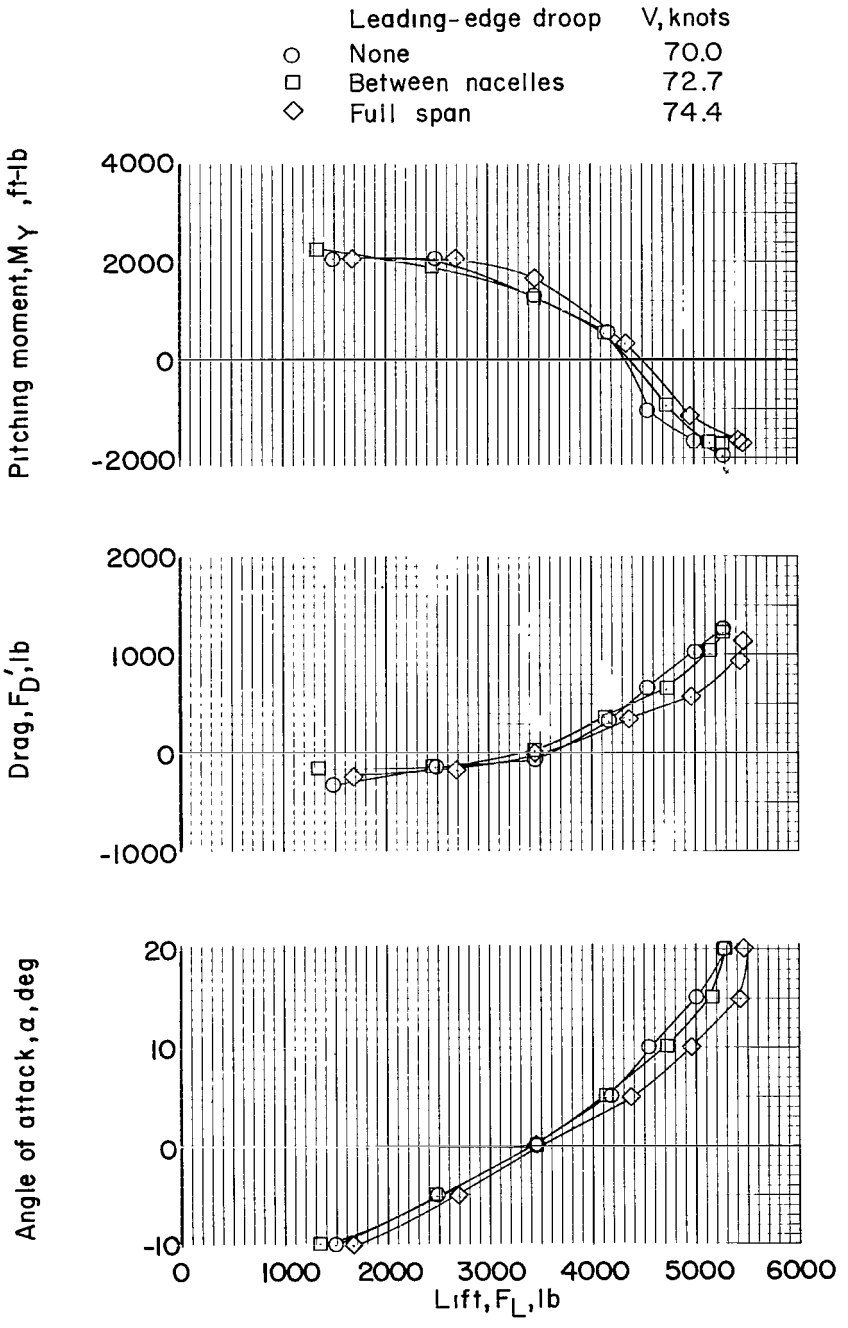

(a) $i_w = 20^\circ$.

Figure 13.- Effect of leading-edge droop on scaled-up longitudinal stability characteristics at wing incidences between 20° and 40°. Flap retracted.

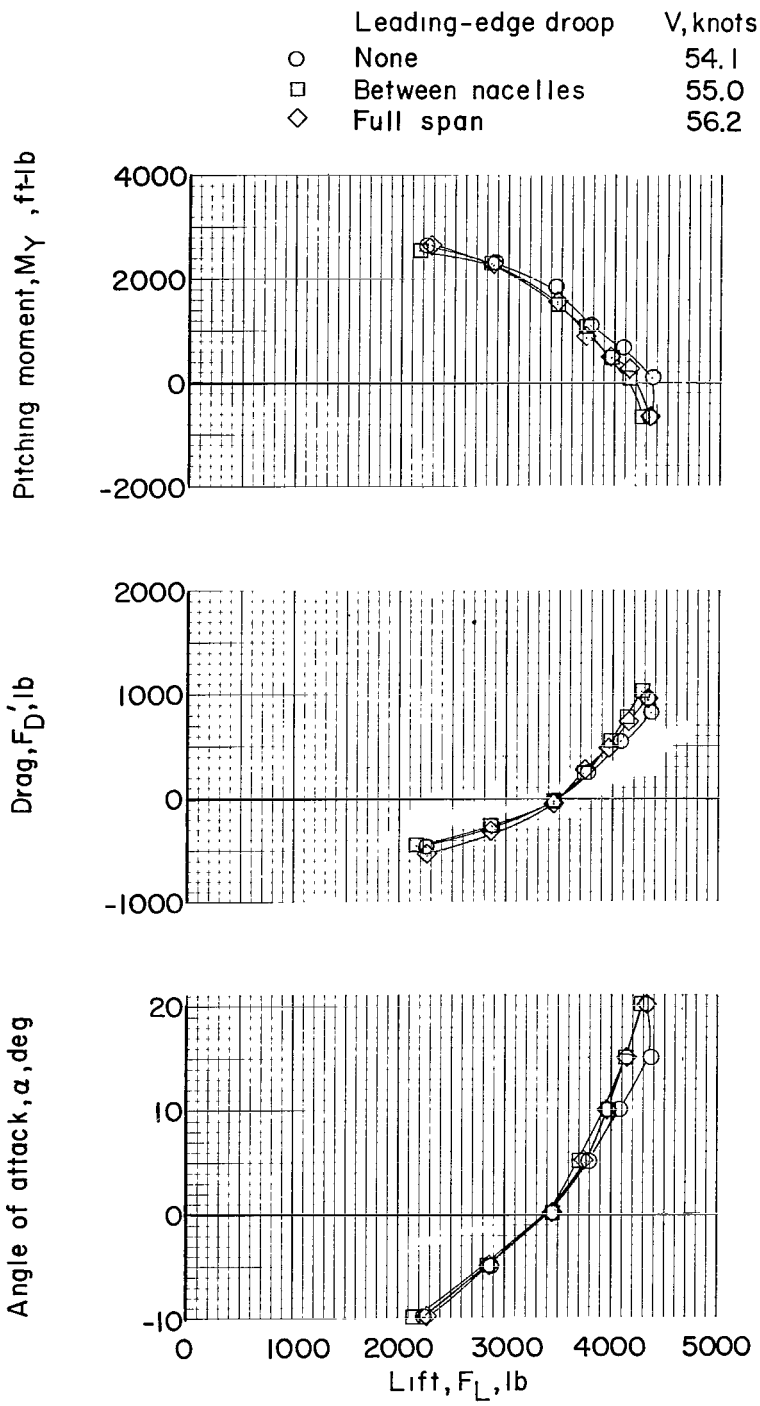

(b) $i_w = 30^\circ$.

Figure 13.- Continued.

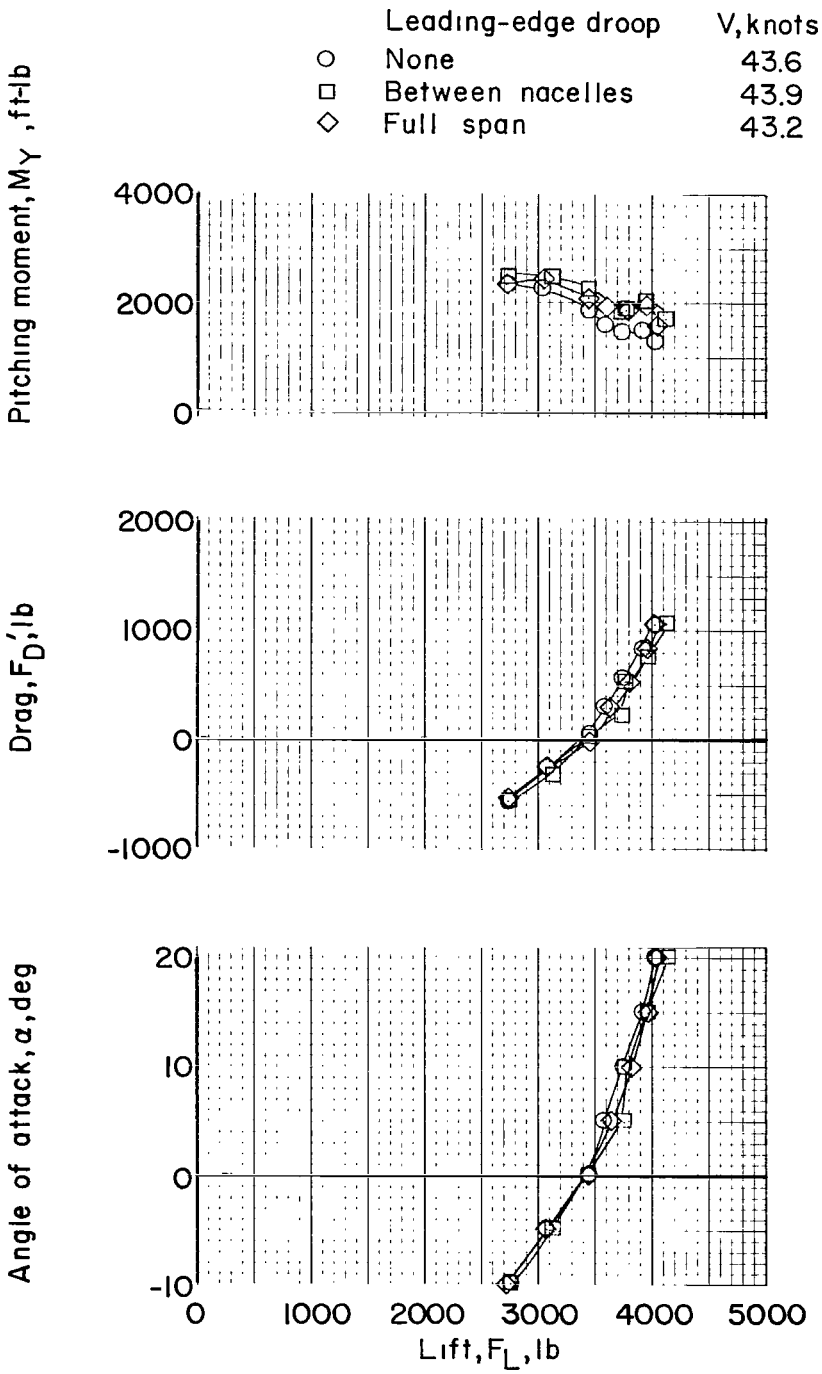

(c) $i_w = 40^\circ$.

Figure 13.- Concluded.

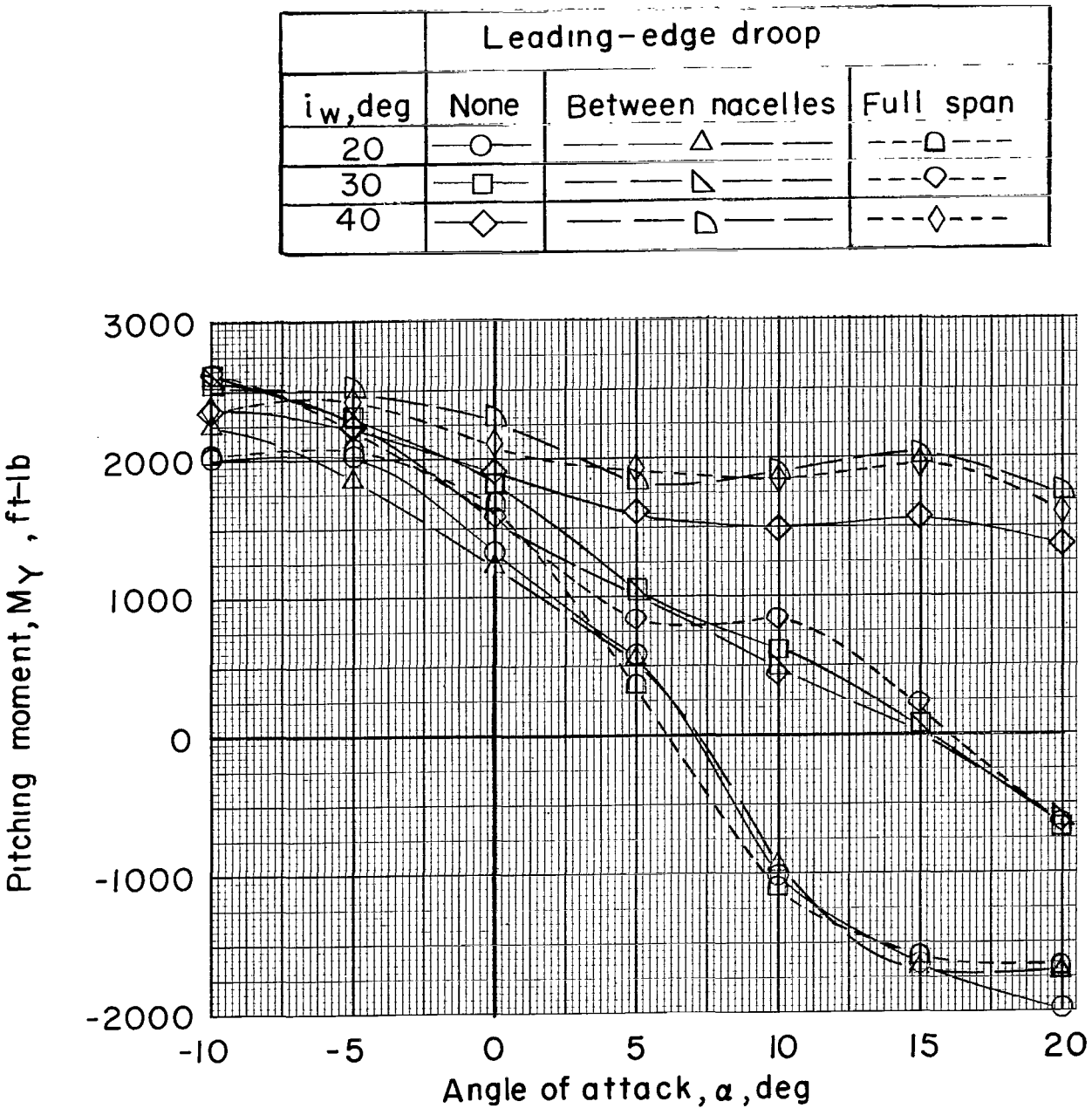

Figure 14.- Effect of leading-edge droop on the variation of scaled-up pitching moment with angle of attack for wing incidences between 20° and 40°. Flap retracted.

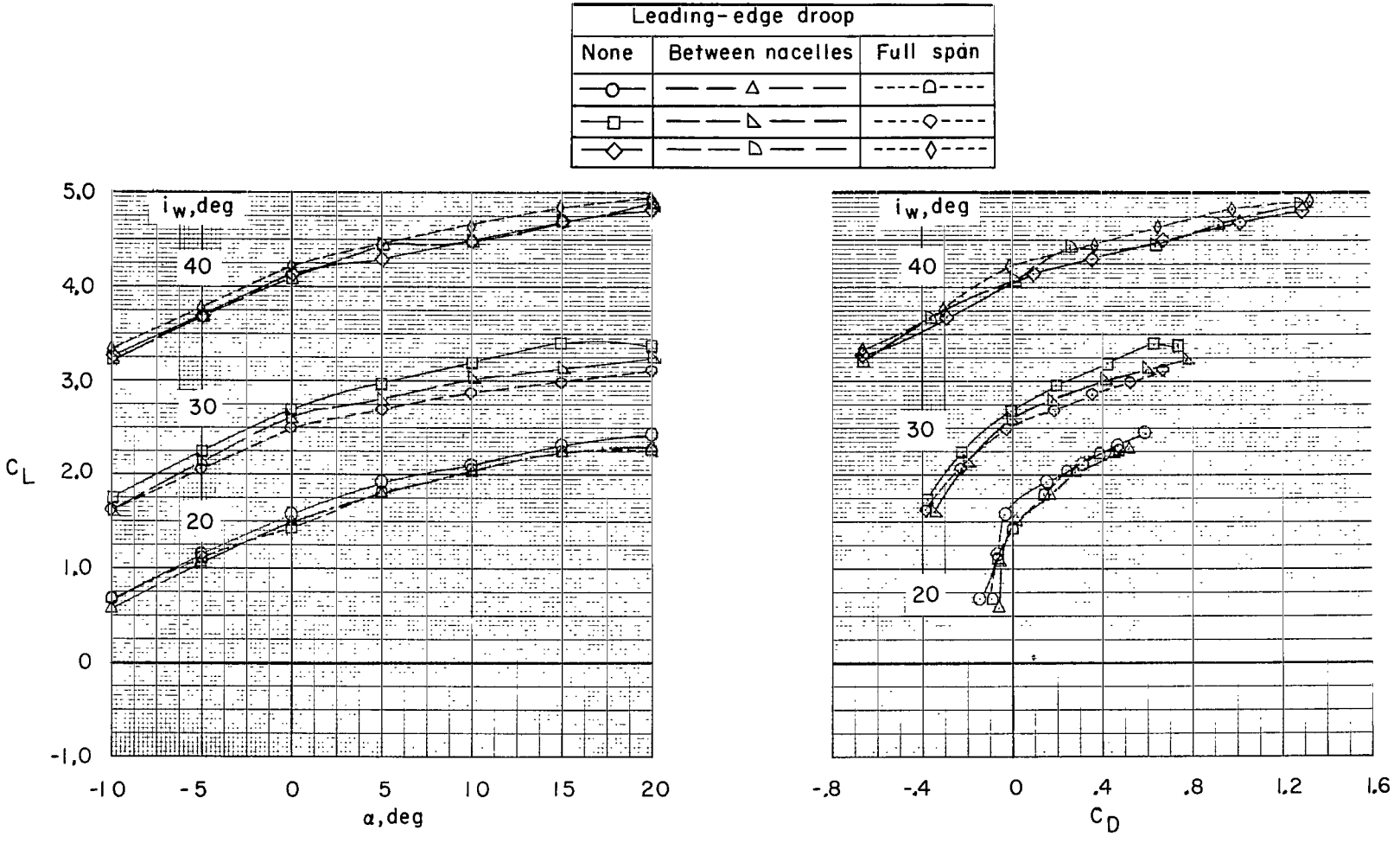

Figure 15.- Effect of leading-edge droop on the variation of lift coefficient with angle of attack and drag coefficient for wing incidences between 20° and 40°. Flap retracted.

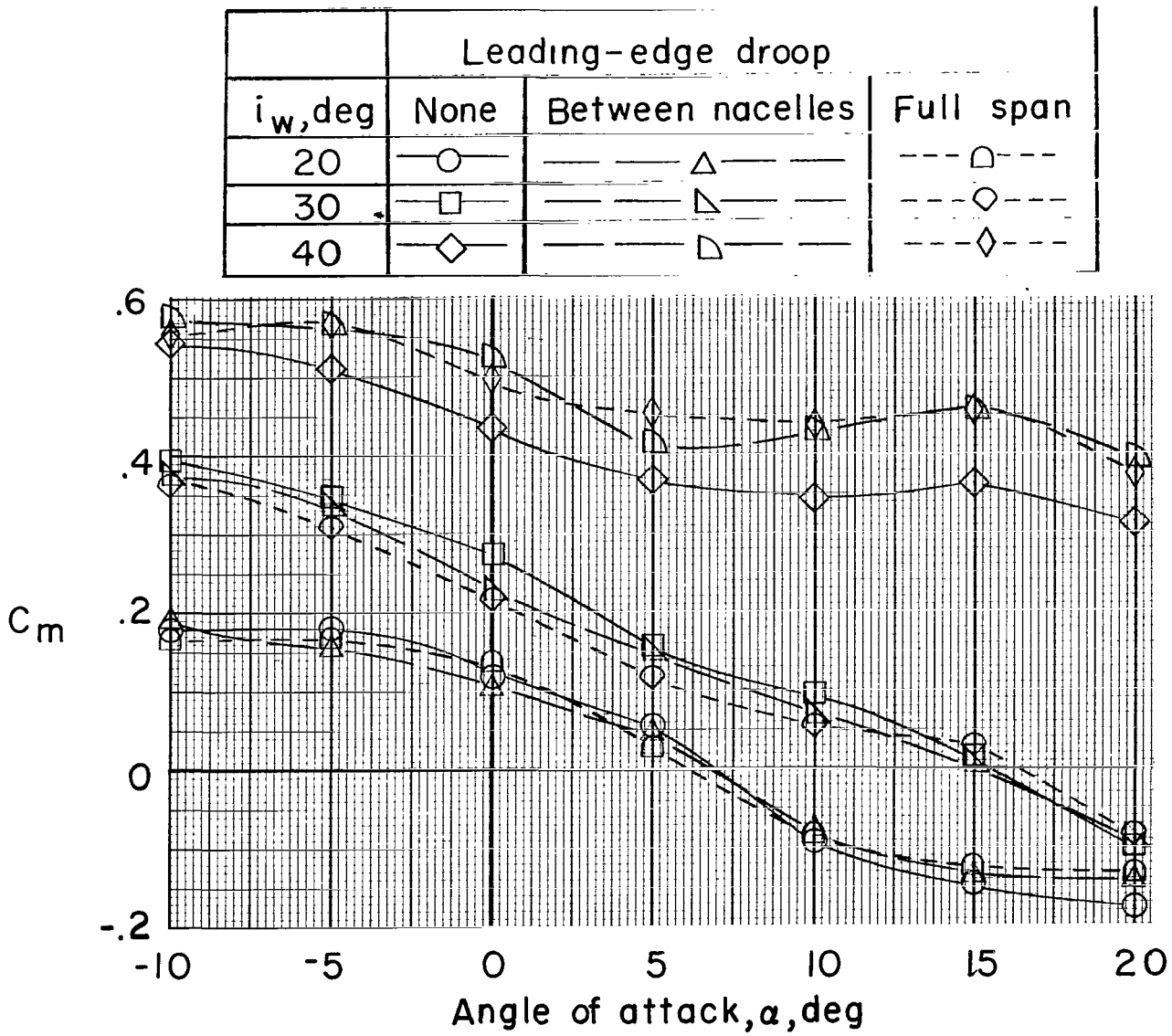

Figure 16.- Effect of leading-edge droop on the variation of pitching-moment coefficient with angle of attack for wing incidences between 20° and 40°. Flap retracted.

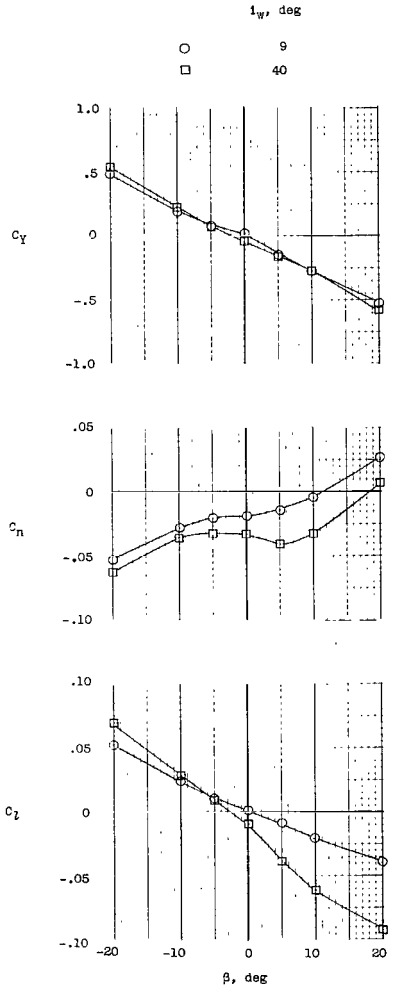

Figure 17.- Lateral stability characteristics in coefficient form for wing incidences of 9° and 40°. Flap retracted; α = 0°.

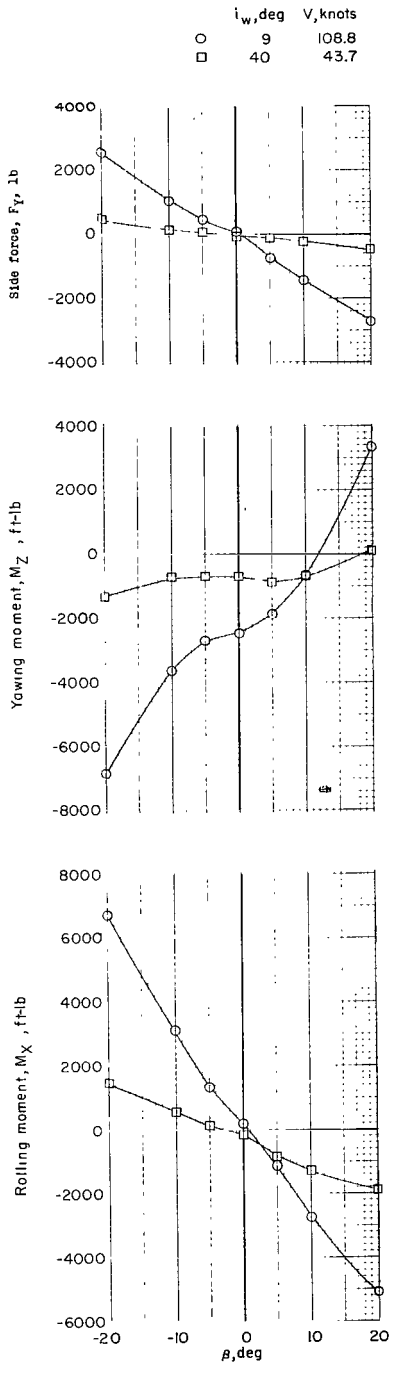

Figure 18.- Scaled-up lateral stability characteristics for wing incidences of 9° and 40°. Flap retracted; α = 0°.

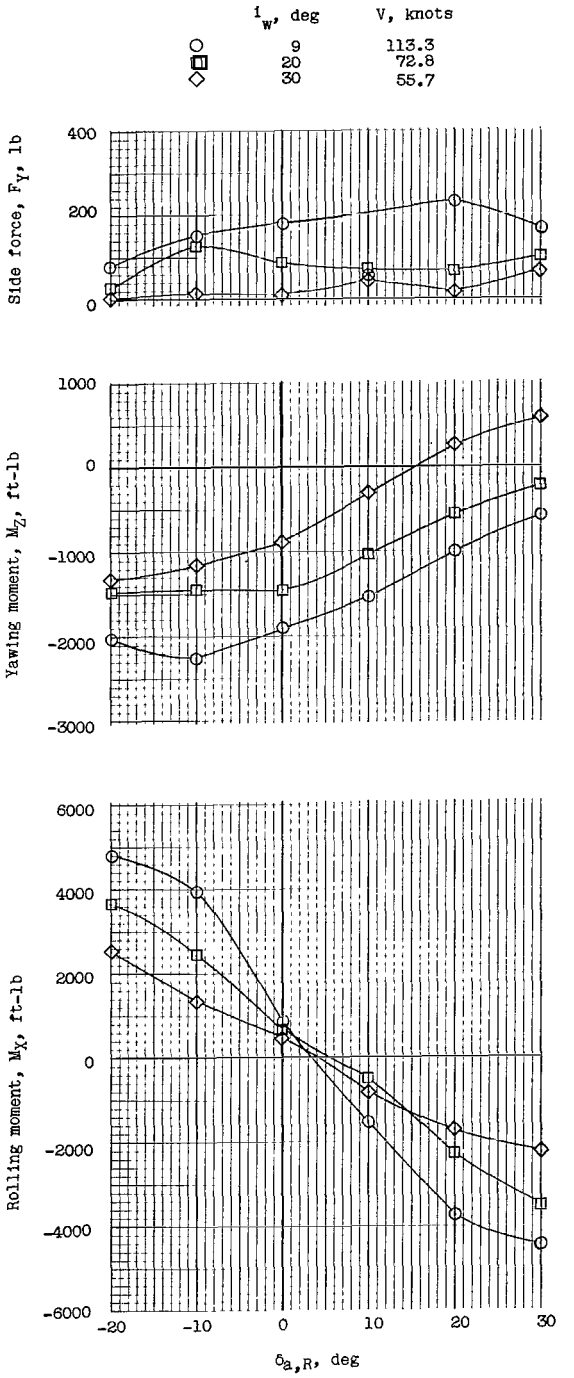

(a) $i_w = 9^\circ$, 20°, and 30°.

Figure 19.- Scaled-up aileron effectiveness at various wing incidences with the flap retracted. $\alpha = \beta = 0^\circ$.

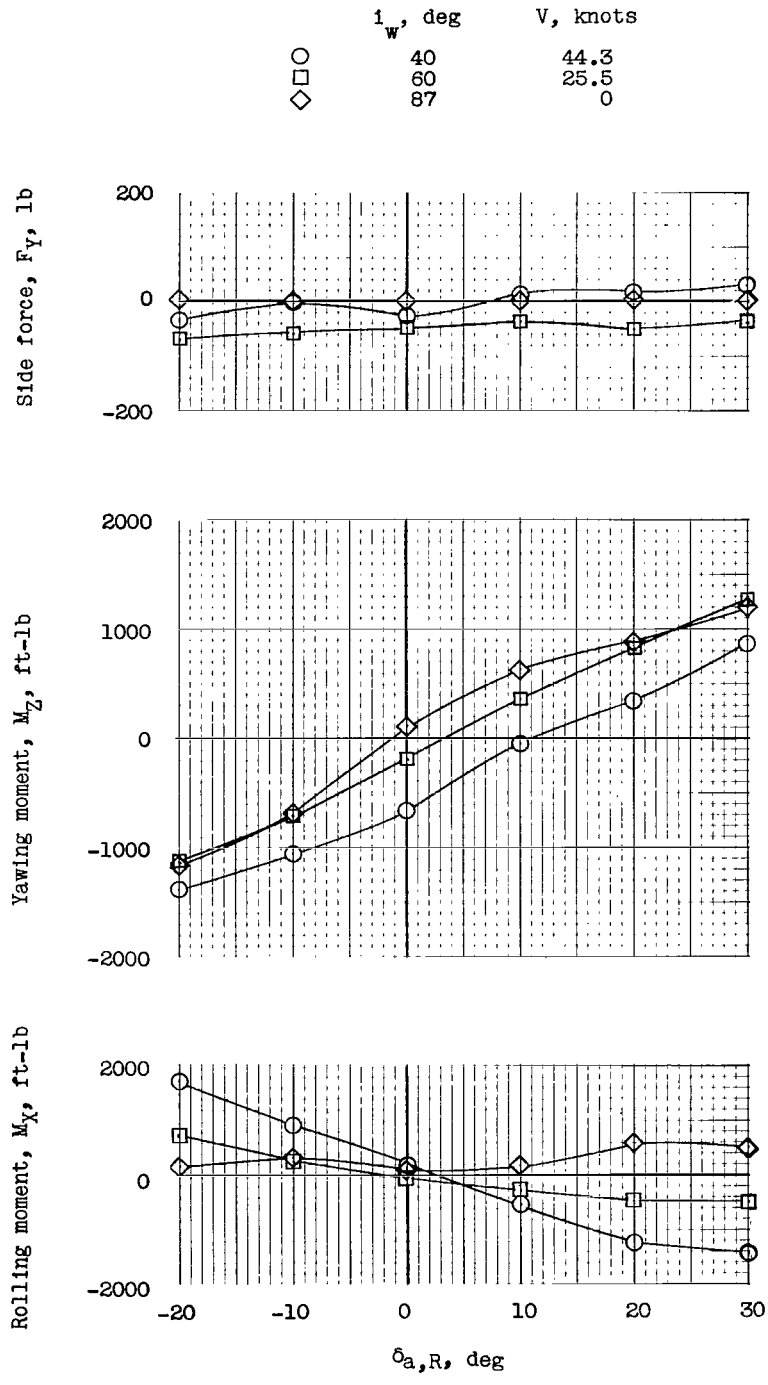

(b) $i_w = 40^\circ$, 60°, and 87°.

Figure 19.- Concluded.

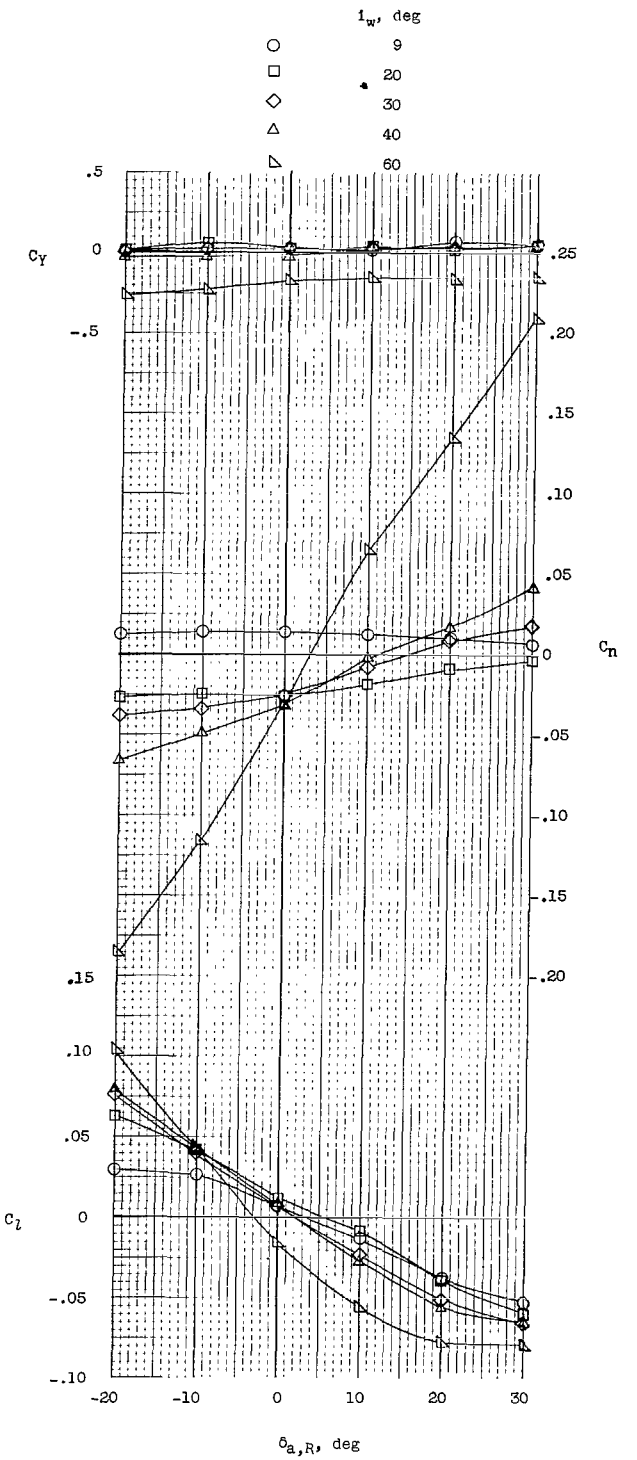

Figure 20.- Aileron effectiveness in coefficient form for wing incidences from 9° to 60°. Flap retracted; $\alpha = \beta = 0°$.

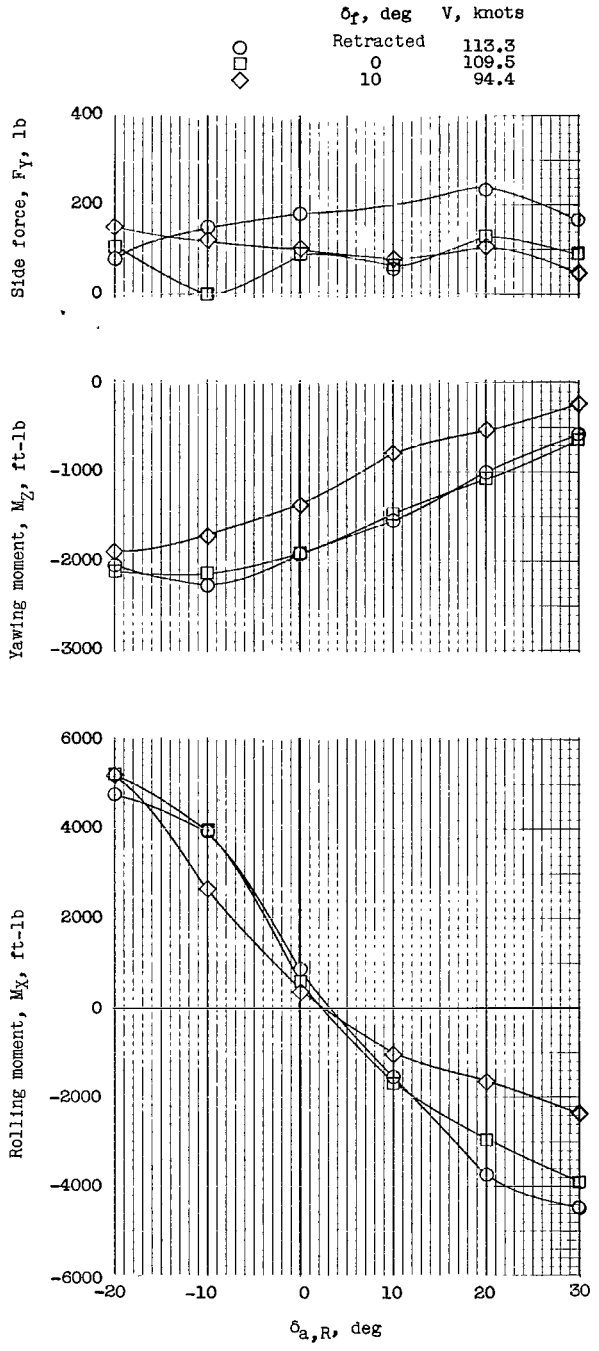

(a) $i_W = 9^\circ$.

Figure 21.- Scaled-up aileron effectiveness at various wing incidences and flap deflections. $\alpha = \beta = 0^\circ$.

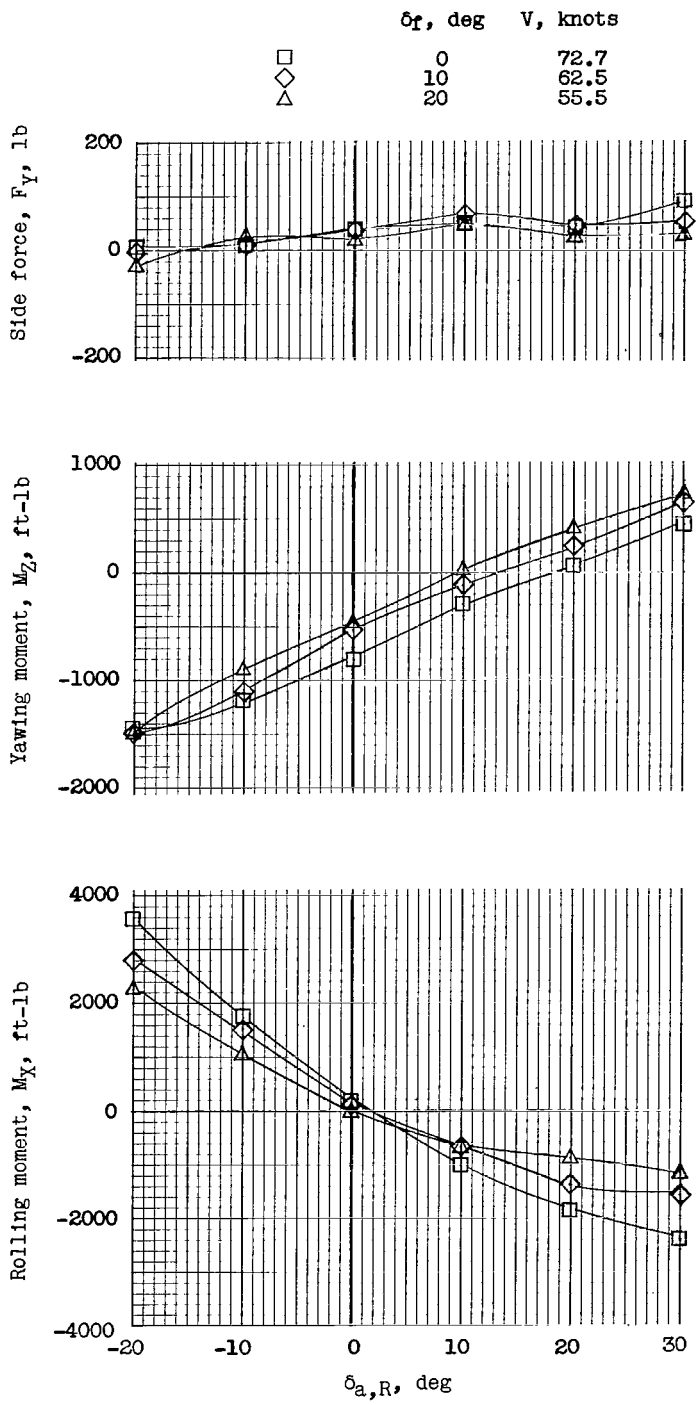

(b) $i_w = 20^\circ$.

Figure 21.- Continued.

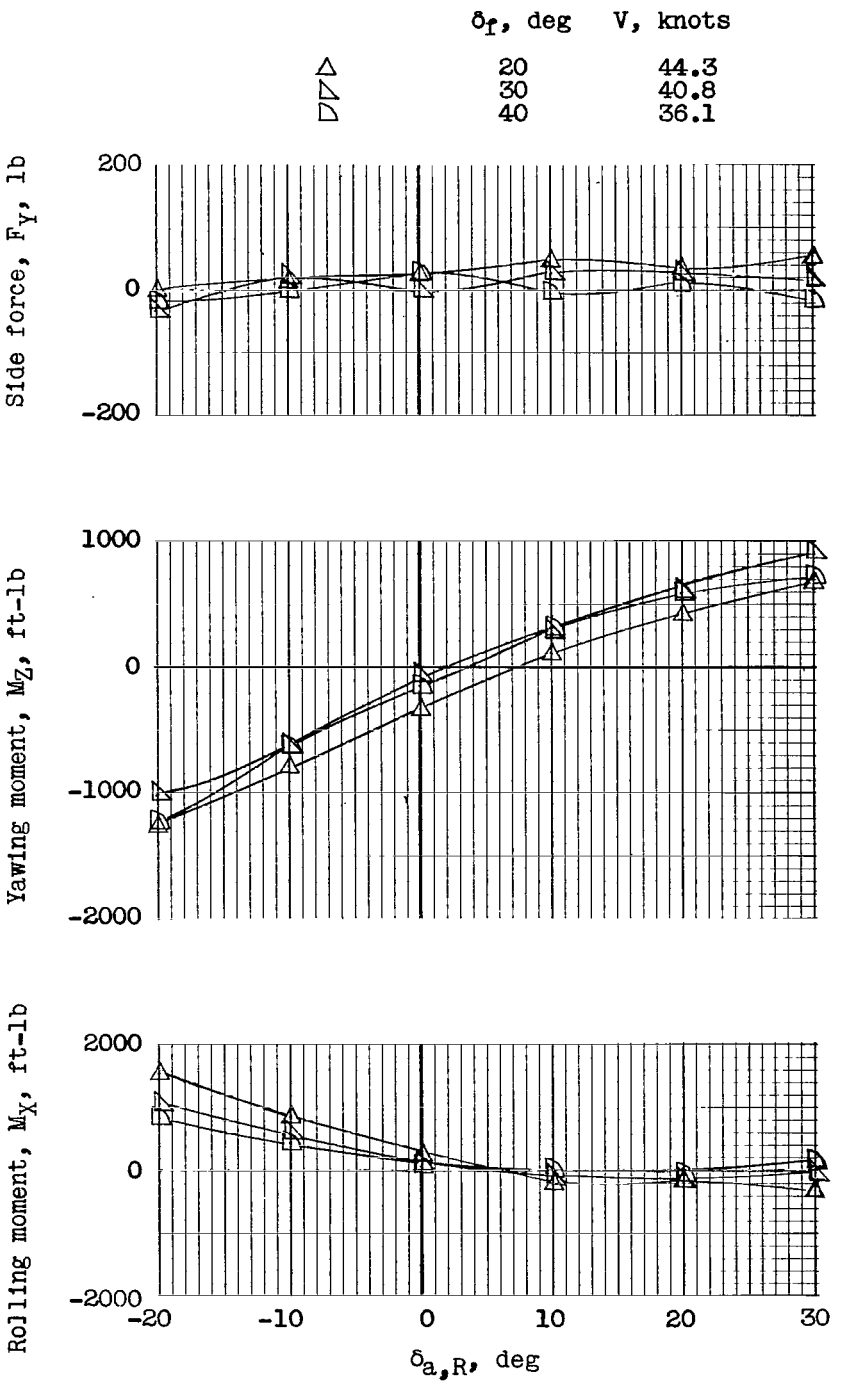

(c) $i_w = 30^\circ$.

Figure 21.- Continued.

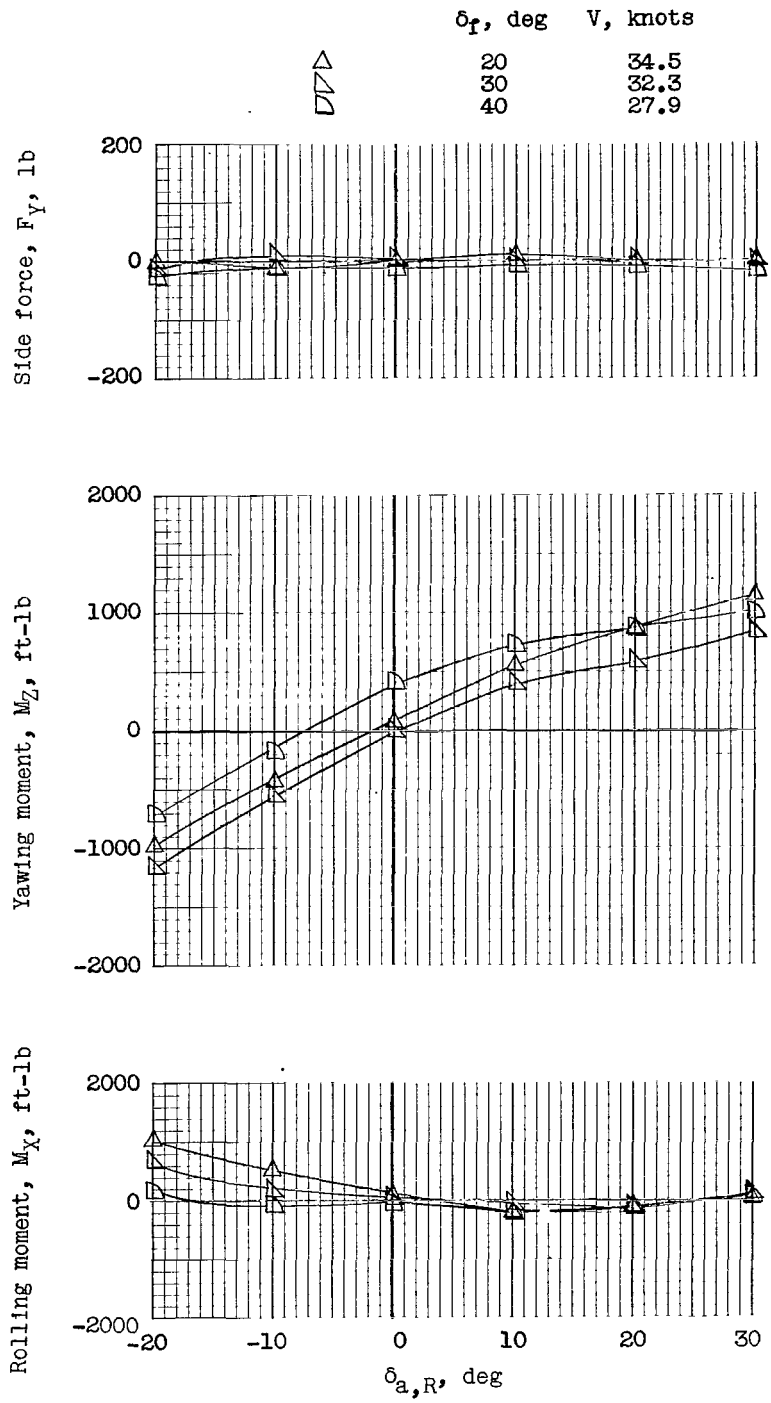

(d) $i_w = 40^\circ$.

Figure 21.- Continued.

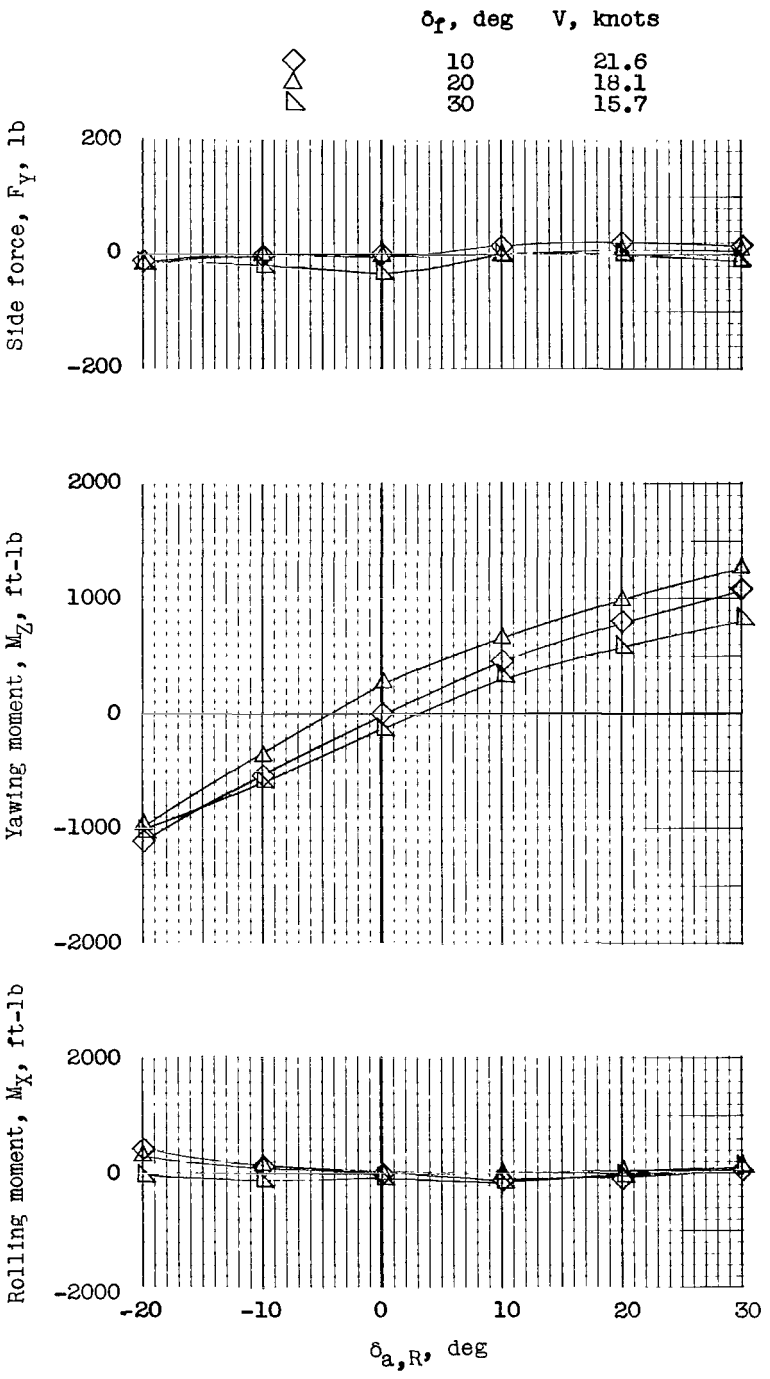

(e) $i_w = 60^\circ$.

Figure 21.- Continued.

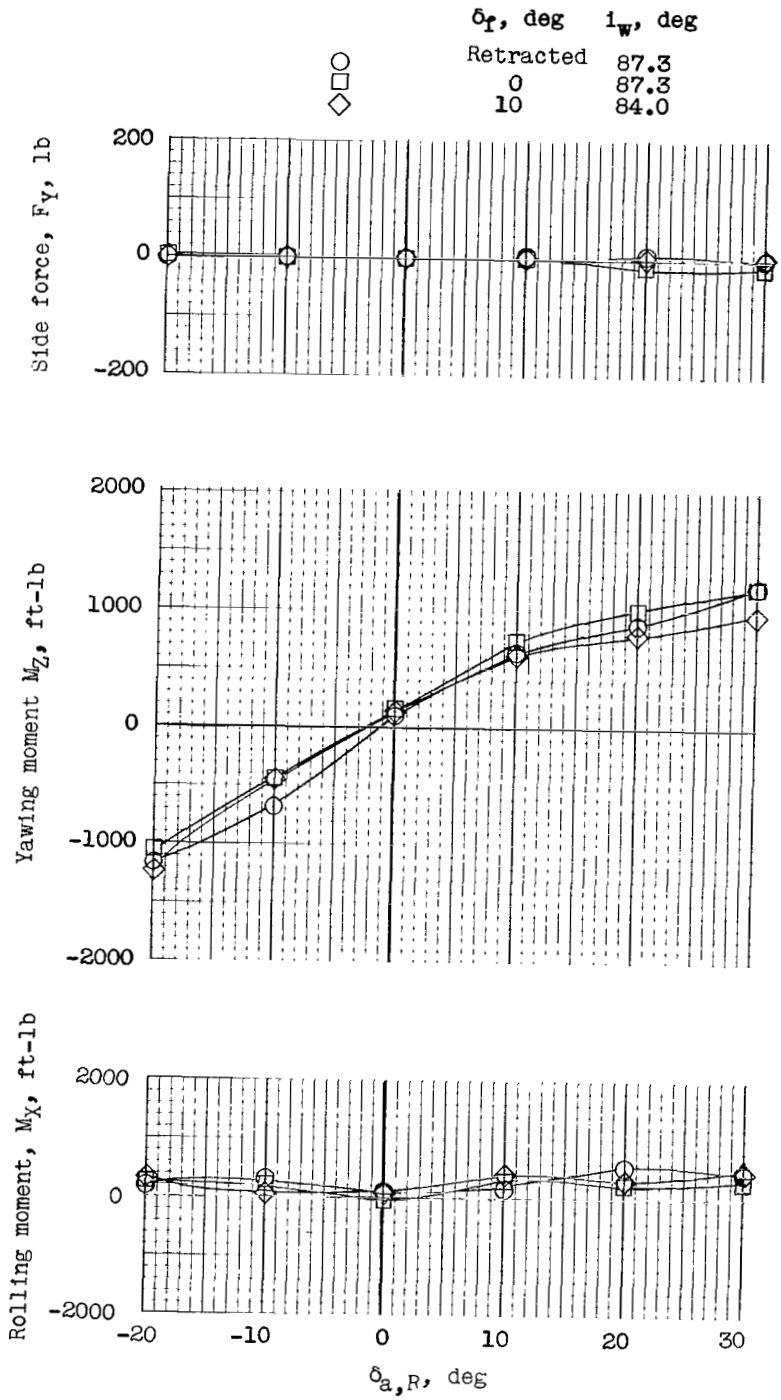

(f) $i_w = 84^\circ$ and 87.3°.

Figure 21.- Concluded.

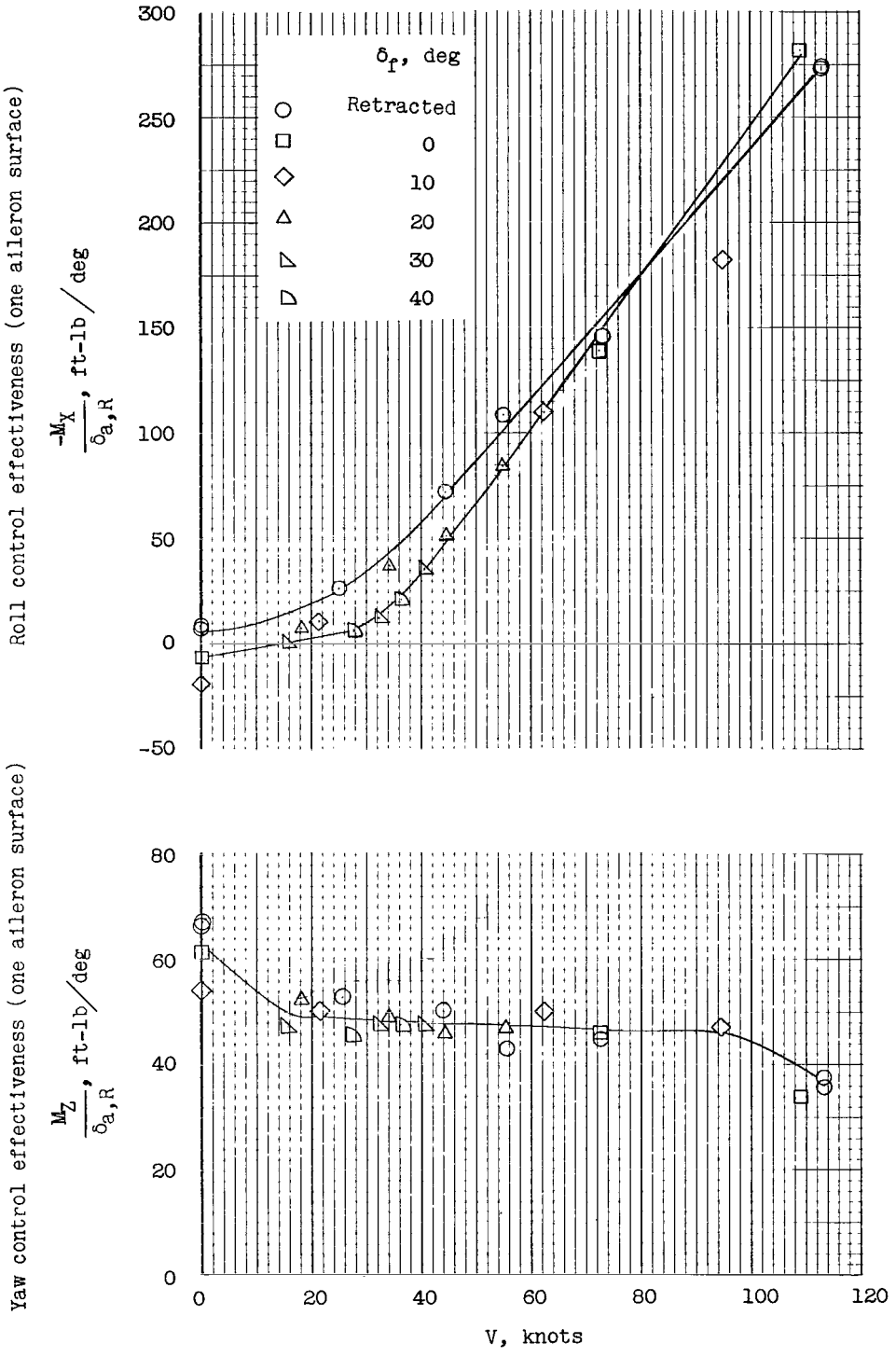

Figure 22.- Scaled-up full-span aileron control effectiveness in roll and yaw.

2 17 85

"The aeronautical and space activities of the United States shall be conducted so as to contribute . . . to the expansion of human knowledge of phenomena in the atmosphere and space. The Administration shall provide for the widest practicable and appropriate dissemination of information concerning its activities and the results thereof."

—NATIONAL AERONAUTICS AND SPACE ACT OF 1958

NASA SCIENTIFIC AND TECHNICAL PUBLICATIONS

TECHNICAL REPORTS: Scientific and technical information considered important, complete, and a lasting contribution to existing knowledge.

TECHNICAL NOTES: Information less broad in scope but nevertheless of importance as a contribution to existing knowledge.

TECHNICAL MEMORANDUMS: Information receiving limited distribution because of preliminary data, security classification, or other reasons.

CONTRACTOR REPORTS: Technical information generated in connection with a NASA contract or grant and released under NASA auspices.

TECHNICAL TRANSLATIONS: Information published in a foreign language considered to merit NASA distribution in English.

TECHNICAL REPRINTS: Information derived from NASA activities and initially published in the form of journal articles.

SPECIAL PUBLICATIONS: Information derived from or of value to NASA activities but not necessarily reporting the results of individual NASA-programmed scientific efforts. Publications include conference proceedings, monographs, data compilations, handbooks, sourcebooks, and special bibliographies.

Details on the availability of these publications may be obtained from:

SCIENTIFIC AND TECHNICAL INFORMATION DIVISION

NATIONAL AERONAUTICS AND SPACE ADMINISTRATION

Washington, D.C. 20546